Mechanism-based candidate inhibitors of galactopyranose mutase

by

Yasaman Mahdavi-Amiri

B.Sc., Sharif University of Technology, 2012

Thesis Submitted in Partial Fulfillment of the
Requirements for the Degree of
Master of Science

In the
Department of Chemistry
Faculty of Science

SIMON FRASER UNIVERSITY

Summer 2015

Approval

Name:	**Yasaman Mahdavi-Amiri**
Degree:	**Master of Science**
Title:	***Mechanism-based candidate inhibitors of galactopyranose mutase***

Examining Committee: **Chair:** Dr. David J. Vocadlo
Professor

Dr. Robert N. Young
Senior Supervisor
Professor
Department of Chemistry _____

Dr. B. Mario Pinto
Supervisor
Professor
Department of Chemistry _____

Dr. Erika Plettner
Supervisor
Professor
Department of Chemistry _____

Dr. Andrew J. Bennet
Internal Examiner
Professor
Department of Chemistry _____

_____

Date Defended/Approved: May 21, 2015

Abstract

The synthesis of candidate inhibitors of *Mycobacterium tuberculosis* cell-wall biosynthesis as potential therapeutic agents for the treatment of tuberculosis is presented.

A critical component of the cell wall of *M. tuberculosis* is a D-galactan polymer, a polysaccharide chain consisting of D-galactofuranose (Gal*f*) residues. Since Gal*f* residues are not found in mammalian systems, inhibition of the biosynthesis of this polymer constitutes a very attractive and accessible target for new anti-TB drugs. A critical enzyme required for the biosynthesis of the galactan polymer is uridine diphosphate galactopyranose mutase (UGM), which catalyzes the interconversion of UDP-galactopyranose (Gal*p*) and UDP-galactofuranose (Gal*f*).

The goal of the project was to synthesize compounds that inhibit growth of the cell wall by compromising the activity of the UGM enzyme. The compounds were intended to mimic not only the positive charge character of the galactopyranosyl cation (transition state in the UGM-catalyzed reaction) but also its shape (proposed $^{4}H_{3}$ conformation).

Keywords: Enzyme inhibitors, *Mycobacterium tuberculosis*, Synthesis, Transition-state analogues, UDP-Galactopyranose mutase.

To my parents and brother, for their endless love, support and encouragement.

Acknowledgements

I would like to thank Dr. B. Mario Pinto for his guidance and for giving me the opportunity to work in his group.

I would like to thank Dr. Robert N. Young and Dr. Erika Plettner for their valuable advice and feedback.

I am grateful to Dr. Sankar Mohan for his constant help and guidance throughout my MSc program.

I wish to thank my wonderful lab-mates for their help and company.

I would like to extend my thanks to Dr. Silvia Borrelli for help with HPLC, Dr. Andrew Lewis and Dr. Cinzia Colombo for the help with NMR spectroscopy, Mr. Hongwen Chen for the help with mass spectroscopy, and Mr. Gang Chen for helping me to purify compound **22**.

Finally, my deepest gratitude goes to my family for their unconditional love and support.

Table of Contents

List of Tables

List of Figures

List of Schemes

Abbreviations

AcOH	acetic acid
aq	aqueous
Ar	aromatic
BnBr	benzyl bromide
c	concentration
Calcd	calculated
COSY	correlation spectroscopy
d	doublet
DCM	dichloromethane
dd	doublet of doublet
ddd	doublet of doublet of doublet
DIAD	diisopropyl azodicarboxylate
DMF	*N*,*N*-Dimethylformamide
EtOAc	ethyl acetate
EtOH	ethanol
FAD	flavin adenine dinucleotide
Gal*f*	galactofuranose
Gal*p*	galactopyranose
h	hour
H	half chair
HCl	hydrochloric acid
HFIP	1,1,1,3,3,3-Hexafluoro-2-propanol
HMBC	heteronuclear multiple bond correlation
HRMS	high resolution mass spectrometry
HSQC	heteronuclear single quantum coherence
J	coupling constant
M	mycobacterium
m	multiplet
MeOH	methanol
NaH	sodium hydride
NaOMe	sodium methoxide

NMR	nuclear magnetic resonance
NOE	nuclear Overhauser effect
NOESY	nuclear Overhauser effect spectroscopy
Ph	phenyl
s	singlet
sat.	saturated
t	triplet
T	twist
TBAF	tetra-*n*-butylammonium fluoride
TBDMS	tert-butyldimethylsilyl
TBDMSCl	tert-butyldimethylsilyl chloride
THF	tetrahydrofuran
TsCl	4-methylbenzenesulfonyl chloride
UDP	uridine diphosphate

Chapter 1.
Introduction

1.1. Carbohydrates

Carbohydrates constitute a very important class of naturally occurring organic compounds. They are found in many foods such as cereals, potatoes, fruits, nuts and vegetables. Carbohydrates are one of the major nutrients which supply the body with energy. In Nature carbohydrates are produced by green plants through a process called photosynthesis, in which plants use sunlight energy to convert carbon dioxide and water into oxygen and carbohydrates. The overall chemical reaction in photosynthesis is $6CO_2 + 6H_2O$ (+ light energy) $\rightarrow C_6H_{12}O_6 + 6O_2$.

In the past carbohydrates were considered to be hydrates of carbons with the general formula $C_x(H_2O)_y$. However there are many compounds with this general formula that do not behave as carbohydrates. Also some of the derivatives of carbohydrates and nitrogen containing carbohydrates do not follow this general formula. A more accurate definition is to view carbohydrates as polyhydroxy aldehydes and polyhydroxy ketones.

Carbohydrates are divided into monosaccharides, disaccharides, oligosaccharides, and polysaccharides (the word saccharide is derived from the Greek word sakkharon, meaning sugar). Monosaccharides are the most basic units of carbohydrates which consist of a single polyhydroxy aldehyde or ketone unit. The most common monosaccharide in Nature is the 6-carbon sugar glucose (Figure 1.1) with the molecular formula $C_6H_{12}O_6$.

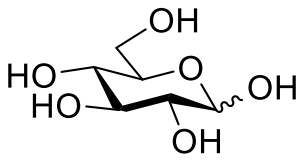

Figure 1-1: Monosaccharide glucose

Disaccharides consist of two monosaccharide units joined together by glycosidic linkages. They are formed when two sugars are joined together and one molecule of water is removed. Two common disaccharides are lactose, also called milk sugar, (Figure 1.2) and maltose (Figure 1.3).

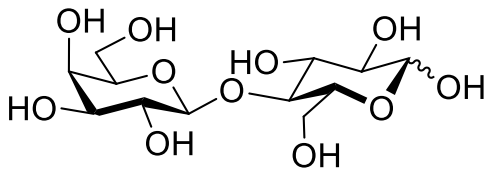

Figure 1-2: Disaccharide lactose (milk sugar)

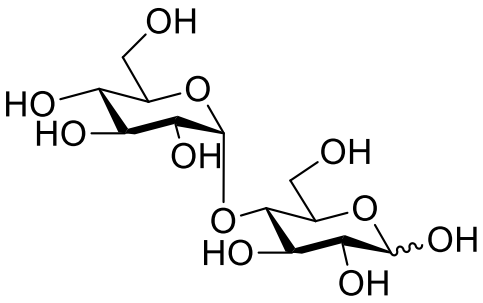

Figure 1-3: Disaccharide maltose

A disaccharide upon hydrolysis is cleaved into two monosaccharides. For example the disaccharide sucrose (table sugar) on hydrolysis yields one molecule of fructose and one molecule of glucose (Scheme 1.1).

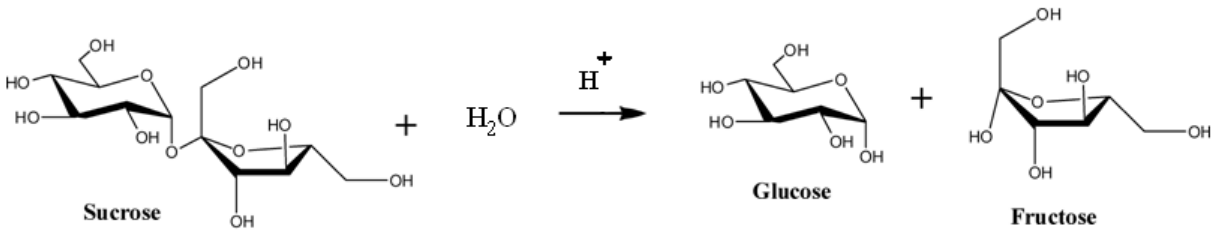

Scheme 1.1: Hydrolysis of disaccharide sucrose

Oligosaccharides (from the Greek word oligos, meaning a few) are saccharide polymers containing a small number of simple sugars units (3 to 10 monosaccharide units) joined together by glycosidic linkages. Polysaccharides also known as glycans are polymeric carbohydrate molecules composed of long chains of monosaccharide units joined together by glycosidic linkages. An example is cellulose, with the formula $(C_6H_{10}O_5)_n$ which consists of a chain of several hundred to many thousands of glucose units (Figure 1.4).

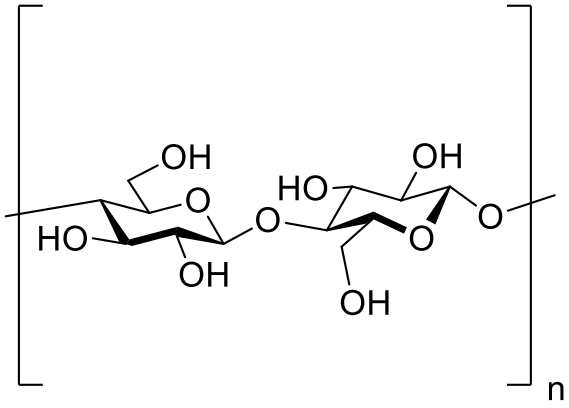

Figure 1-4: Polysaccharide cellulose

1.2. D-Galactofuranose and its importance in Tuberculosis disease

Galactose (from the Greek word galakt meaning milk), sometimes abbreviated Gal, is a monosaccharide. The polymer of this sugar is called Galactan. In Nature galactose is found in two forms, D-galactose and L-galactose. The most abundant and thermodynamically more stable form of D-galactose is the 6-membered ring form, galactopyranose (Gal*p*). The rare 5-membered ring form of D-galactose, galactofuranose (Gal*f*), is found in the lipopolysaccharide O-antigen of many Gram-negative bacteria such as *Klebsiella pneumoniae* and *Escherichia coli* [1]. Gal*f* residues are also found in the cell walls of fungi such as *Aspergillus fumigatus*, and in cell surface structures of protozoa, such as *Trypanosoma cruzi* and *Leishmania* species [2], and of relevance to the present thesis, in the cell walls of Mycobacteria [3] such as *Mycobacterium tuberculosis*.

Mycobacterium tuberculosis is the microorganism responsible for tuberculosis disease. Tuberculosis, also known as TB is one of the world's deadliest diseases. This disease mainly attacks the lungs but can also affect other parts of the body. About one-third of the world's population has latent TB, which means people have been infected by TB bacteria but are not (yet) ill with the disease and cannot transmit the disease. [4]

In 2013 about 9 million people around the world developed TB and 1.5 million died from this disease. People living with HIV are 26 to 31 times more likely to develop active TB disease than people without HIV. HIV and TB form a lethal combination, each speeding the other's progress. In 2013 about 360 000 people died of HIV-associated TB. Approximately 25% of deaths among HIV-positive people are due to TB [4].

TB occurs in every part of the world. In 2013 the largest number of new TB cases occurred in South-East Asia and Western Pacific Regions, accounting for 56% of new cases globally. However, Africa carried the greatest proportion of new cases per population with 280 cases per 100000 population [4].

Recently the impact of this disease on world health has been the source of increased interest. Traditional methods used to combat this infection are losing effectiveness owing to the appearance of multi-drug-resistant strains. Mycobacterial

diseases are difficult to treat with drugs, which is due in part to the particularly impermeable nature of the mycobacterium cell wall. In addition vaccines based on the Bacillus Calmette-Guerin (BCG) strain are only partially effective [4].

The unique cell wall of *Mycobacterium tuberculosis*, which is impenetrable to many antibiotics, is essential to the viability of the organism. Mycobacteria have a cell wall composed of mycolyl-arabinogalactan-peptidoglygan complex (MAPc). Arabinogalactan (AG) part of the cell wall is a polysaccharide containing D-arabinofuranosyl residues and D-galactan, a polysaccharide chain consisting of alternating 5- and 6-linked β-D-galactofuranose (β-D-Gal*f*) residues [5]. Part of the cell wall is shown in Figure 1.5.

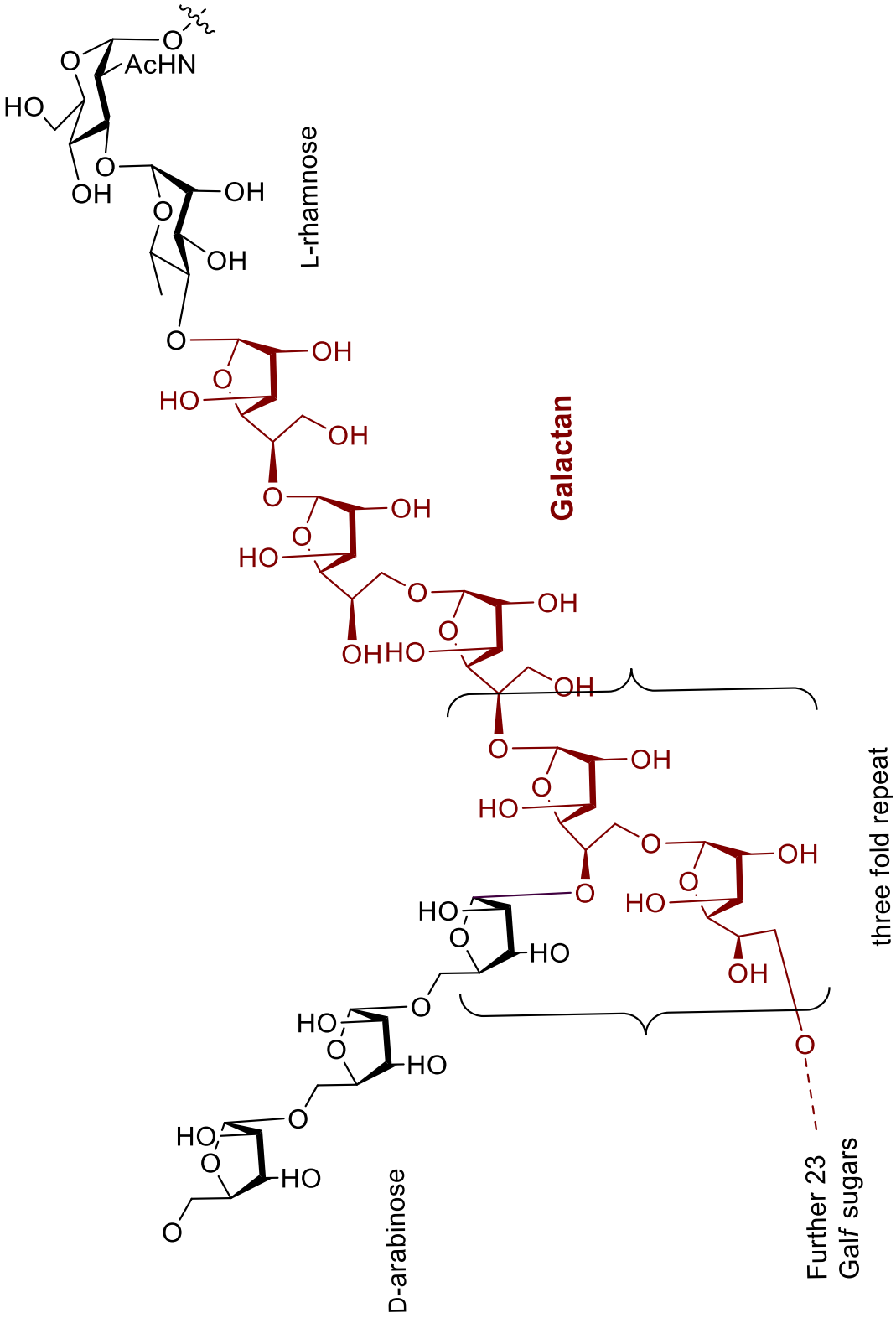

Figure 1-5: Part of the cell wall of *M. tuberculosis*

Arabinogalactan (AG) plays an important role in holding the lipid layer to peptidoglycan layer in the cell wall structure. An efficient drug in treatment of tuberculosis disease named Ethambutol (Figure 1.6) is known to inhibit the synthesis of cell wall arabinogalactan [6]. Therefore it is believed that a similar inhibition of the galactofuran formation might lead to the same result.

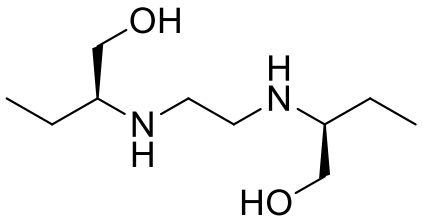

Figure 1-6: Structure of Ethambutol

In mammals galactose in only found in the 6-membered ring form as galactopyranose (Gal*p*). Since Gal*f* residues are not found in mammalian systems, inhibition of the biosynthesis of this galactofuran constitutes a very attractive target for new anti-TB drugs without deleterious side effects.

1.3. Enzymes involved in the cell-wall biosynthesis of *M. tuberculosis*

The biosynthesis of the galactan polymer involves two specific enzymes: UDP-galactopyranose mutase (UGM), which catalyzes the interconversion of UDP-galactopyranose (UDP-Gal*p*) to UDP-galactofuranose (UDP-Gal*f*) (Scheme 1.2), and UDP-Galactofuranosyl transferase (UDP-Gal*f* transferase), which catalyzes the transfer of UDP-Gal*f* onto a growing oligosaccharide chain (Scheme 1.3) [7].

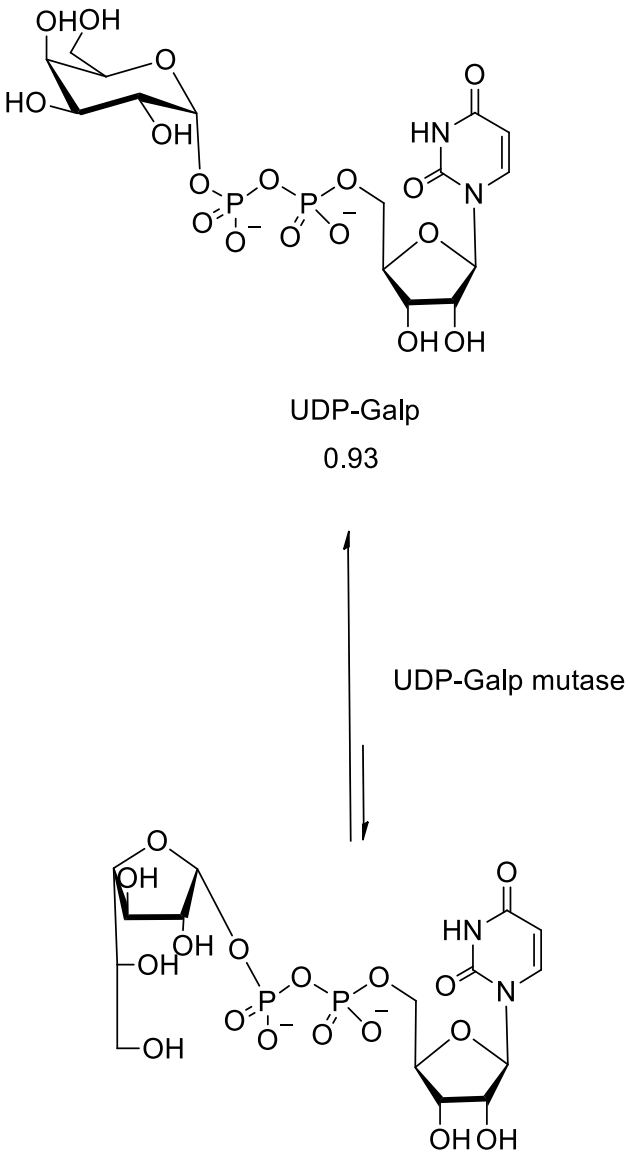

Scheme 1.2: UDP-Galactopyranose to UDP-Galactofuranose interconversion by the UGM enzyme

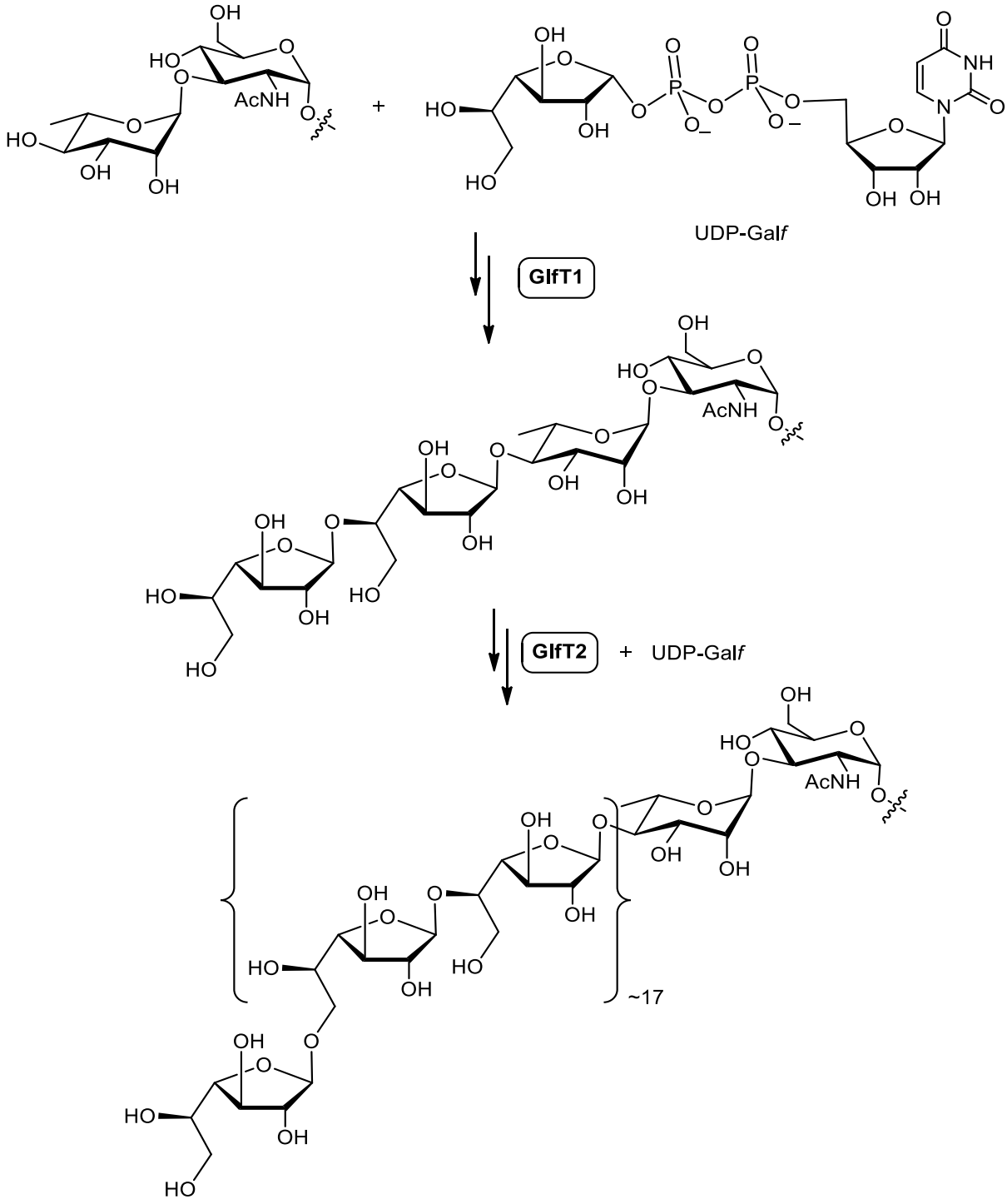

Scheme 1.3: Transfer of UDP-Galf onto a growing oligosaccharide chain by galactofuranosyltransferase enzymes

1.4. UDP-galactopyranose mutase (UGM)

The enzyme uridine 5'-diphosphate galactopyranose mutase (UGM) catalyzes the interconversion of UDP-Gal*p* and UDP-Gal*f* in numerous pathogens including *Mycobacterium tuberculosis*.

UGM is a flavoprotein, which incorporates flavin adenosine dinucleotide (FAD) coenzyme and is catalytically active only when the cofactor is in the reduced form [8]; the structure of the reduced cofactor ($FADH^-$) is shown below (Figure 1.7).

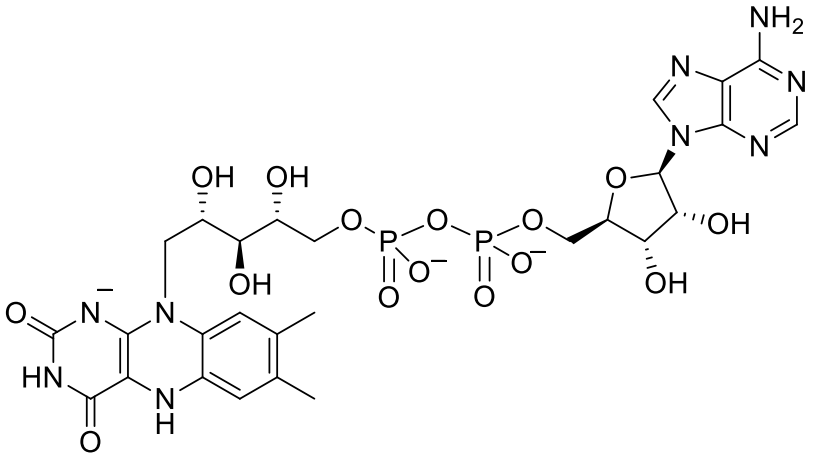

$FADH^-$

Figure 1-7: Reduced flavin adenosine dinucleotide cofactor

The first crystal structure of UGM (without substrate or inhibitor) from *Escherichia coli* (*ec*UGM) was solved in 2001 [8] (Figure 1.8).

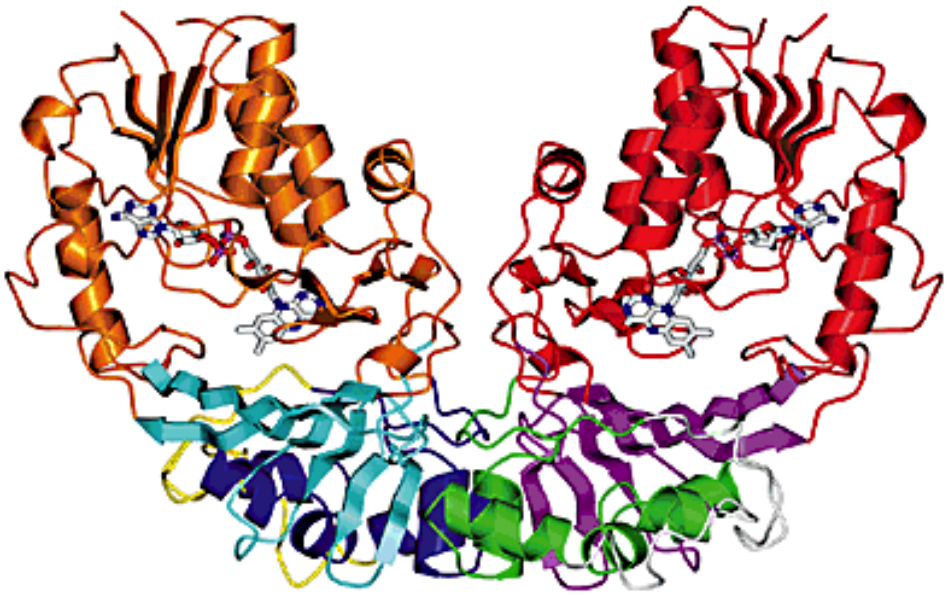

Figure 1-8: Dimer crystal structure of *E. coli* UGM [ref. 8]

Crystal structures of the enzyme from *Klebsiella pneumoniae* (kpUGM) and *M. tuberculosis* were also determined by the same team in 2005. Structures of the proteins from *M. tuberculosis* and *K. pneumoniae* are very similar to the *E. coli* homolog. The mutase enzyme is a mixed α/β class of protein, and functions as a homodimer with each monomer binding one molecule of FAD [9].

Knockout mutants of *Mycobacterium smegmatis* (a model for *M. tuberculosis*) show that the mutase gene is essential for cell viability [10]. Thus, the absence of both Gal*f* and UGM in humans makes UGM an attractive target for inhibition by new antimicrobial compounds.

1.5. Inhibitors of UDP-Galactopyranose mutase

Many inhibitors have been designed, synthesized and tested against UGM enzymes. These molecules are either substrate analogues (carbohydrates and

nucleotide-sugars) or compounds derived from inhibitor screenings for the discovery of novel antitubercular agents.

1.5.1. Substrate analogue inhibitors

Most efforts to design UGM inhibitors have focused on UDP-sugar substrate analogues. The first identified inhibitors of UGM were the galactofuranose mimics **1** and **2** (Figure 1.9). Both compounds caused inhibition of the biosynthesis of the mycobacterial cell wall (Table 1-1) [11].

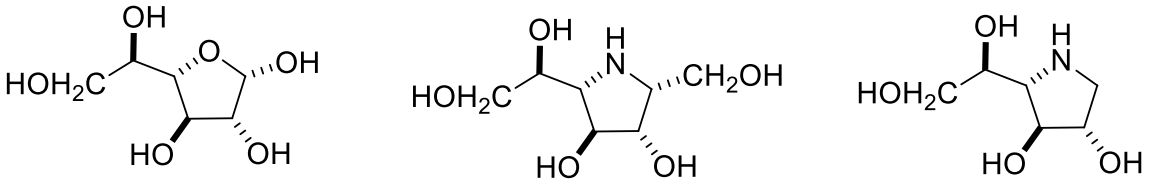

Figure 1-9: Galactofuranose and galactofuranose mimics 1 and 2

Table 1-1: Inhibition of iminosugars 1 and 2 against mycobacterial galactan biosynthesis and UGM

Compound 200 μg/ml	% inhibition of mycobacterial galactan biosynthesis	% inhibition of UDP-Gal*p* to UDP-Gal*f*	% inhibition of UDP-Gal*f* to UDP-Gal*p*
1	63	64	67
2	56	36	81

Later, based on the fact that compound **2** is an inhibitor of UGM, compounds **3-8** (Figure 1.10) were designed and synthesized as UGM inhibitors. However these compounds were shown to be poor inhibitors of UGM. Concentrations of 10 mM were required to begin to see inhibition (Table 1-2) [12].

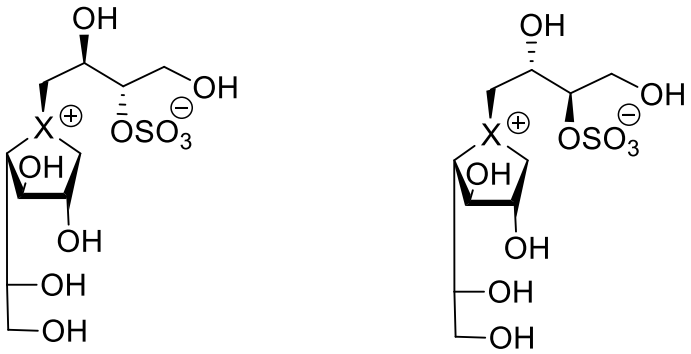

3 X=NH
5 X=Se
7 X=S

4 X=NH
6 X=Se
8 X=S

Figure 1-10: Sugar derivatives 3-8

Table 1-2: Inhibition of UGM by inhibitors 3-8

Inhibitor (10 mM final conc.)	% inhibition
3	40.7
4	16.7
5	None
6	18.5
7	43.7
8	None

Compounds **3-8** all lack the nucleotide moiety. However inhibitors with the uridine portion of the substrate bind better with affinities close to UDP-Gal*p.* For example, the substrate analogue **9** (Figure 1.11) designed by Liu and co-workers displayed K_d=46 μM and 54% inhibition at 2.5 mM [13].

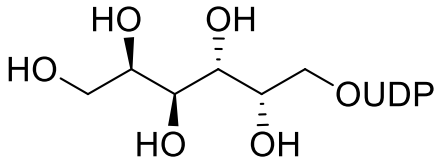

9

Figure 1-11: UGM inhibitor 9

However these approaches did not afford compounds that block mycobacterial growth.

1.5.2. Non substrate-based UGM inhibitors

Due to the lack of cell permeability of many identified inhibitors of UGM, Soltero-Higgin et al. examined a more structurally diverse set of compounds with favorable cell permeability properties to identify candidates for UGM inhibition. Using a high-throughput, fluorescence polarization (FP) screen they found compounds **10-12** (Figure 1.12) as inhibitors of UGM with IC_{50} values (IC_{50} is the concentration at which 50% of the enzymatic activity of the UGM enzyme is inhibited) in the µM range (Table 1-3) [14].

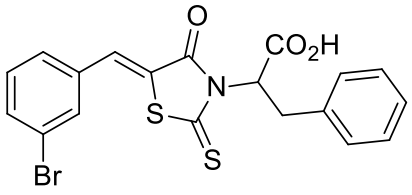

10

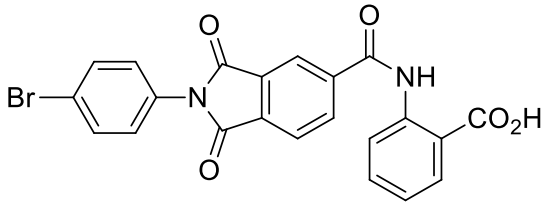

11

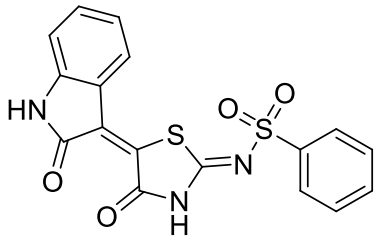

12

Figure 1-12: Compounds identified from the high-throughput screening that inhibit *K. pneumoniae* UGM

Table 1-3: IC_{50} values for compounds 10-12

Compound	IC_{50} (μM)
10	1.6
11	4.6
12	17

In 2006, identification of new antimycobacterial compounds was reported [15]. A 5-hydroxy-pyrazole compound with general structure **A** (Figure 1.13) was found as a hit candidate from virtual screening. Subsequent optimization of the hit and synthesis of a library of derivatives led to pyrazoles **13–15** (Figure 1.14) with MIC (Minimum inhibitory concentration) of 6.25 μg mL^{-1} for compounds **13** and **14** and MIC of 12.5 μg mL^{-1} for compound **15** against *M. tuberculosis* [15].

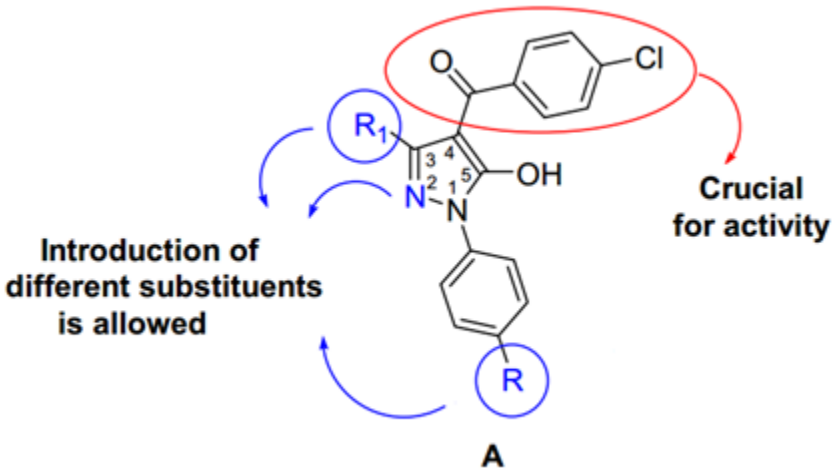

Figure 1-13: Hit compound A and structure-activity relationship considerations [ref. 16]

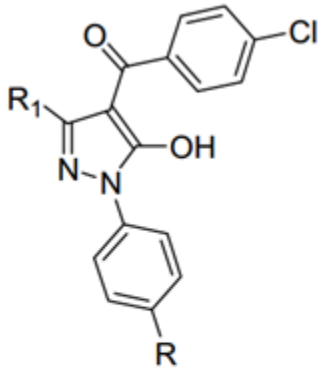

13 : R = Cl, R_1 = CH_3
14 : R = H, R_1 = CH_3
15 : R = F, R_1 = CH_3

Figure 1-14: Pyrazoles 13-15

The action of these compounds against UGM was not reported at that time. Later, in 2010, our group studied the *in vitro* properties of compound **13**. These studies showed that this compound was an inhibitor of UGM from *Mycobacterium tuberculosis* and *Klebsiella pneumoniae* with IC_{50}=62 µM against *tb*UGM and IC_{50}=44 µM against *kp*UGM. These data validate the choice of UGM enzyme as a target for antimycobacterial therapy [17].

This compound **13** however exhibited moderate cellular toxicity against mammalian cells [17]. There still remains a need for UGM inhibitors with antimicrobial activity and no toxicity against mammalian cells.

1.6. Mechanism of UDP-Galactopyranose Mutase

The mechanism of the reaction catalyzed by UGM has been the subject of much discussion. Previous studies have provided important insight into the chemical mechanism of the UGM-catalyzed reaction.

In 1999, Blanchard and co-workers using positional isotope exchange (PIX) studies, suggested that the anomeric C1-OP_β bond is broken and reformed during

turnover. Scrambling in the ^{18}O from the bridging position into the non-bridging phosphate positions during enzyme turnover provided proof for the reversible cleavage of the anomeric C-O bond with the departure of the nucleotide [18].

UGMs from *Escherichia coli* and *Klebsiella pneumoniae* are inactive upon full chemical oxidation; however, the addition of a strong reductant restores enzyme activity [8]. Also when the UGM enzyme was reduced by sodium dithionite its catalytic efficiency (k_{cat}/k_m) was increased by more than 2 orders of magnitude [19] Therefore mechanisms involving the reduced FAD cofactor had been proposed.

Formation of a FAD-substrate adduct in the UGM-catalyzed reaction is supported by experiments trapping the iminium ion **16** by chemical reduction and verification of the reduced product using mass spectroscopy. To trap this intermediate, UGM was treated with radiolabeled UDP-Gal*p* and sodium cyanoborohydride. Radiolabeled adduct **17** was obtained, which provides evidence for the intermediacy of the iminium ion **16** in the UGM-catalyzed reaction (Scheme 1.4) [20].

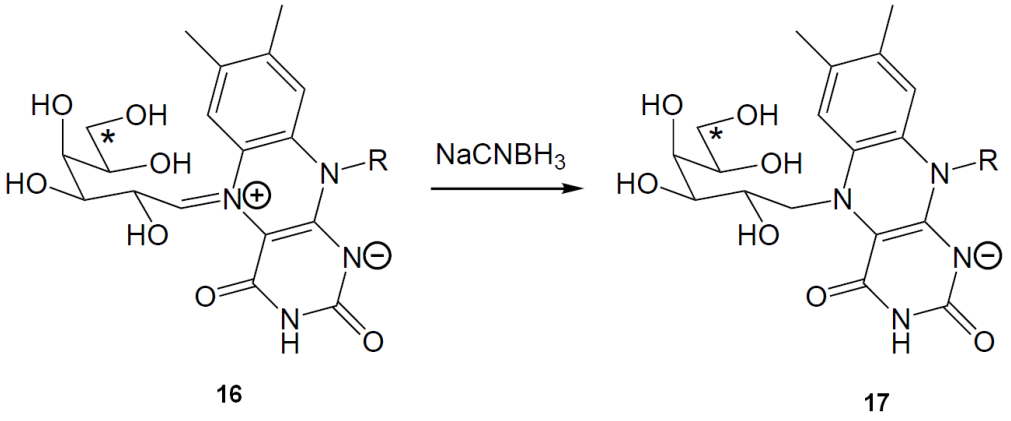

16 **17**

Scheme 1.4: Trapping the iminium ion 16 by sodium cyanoborohydride reduction

The intermediate **16** is likely derived from the FAD-substrate adducts in which the N-5 of the cofactor is covalently bound to the anomeric carbon of the substrate (Scheme 1.5).

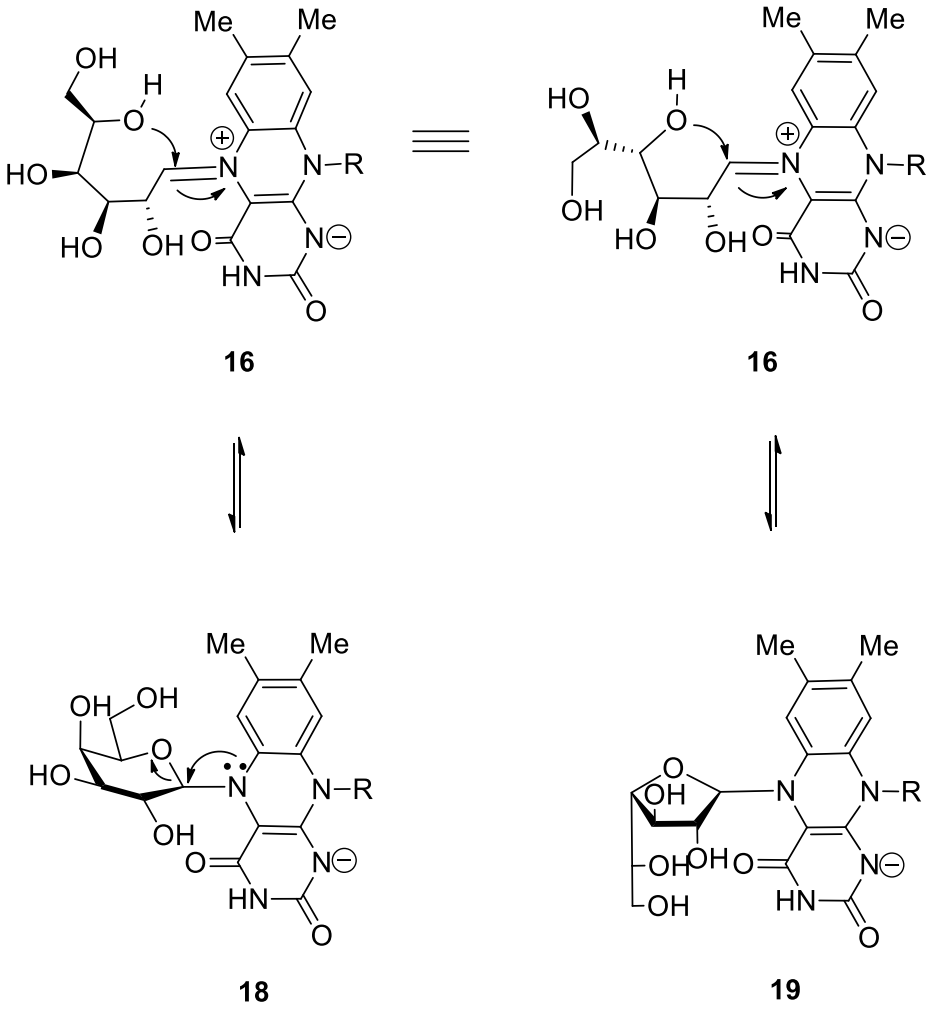

Scheme 1.5: Formation of the iminium ion 16 from FAD-substrate adducts

The X-ray crystal structure of the substrate-bound UGM enzyme revealed that the anomeric carbon of the substrate is in close proximity to the N-5 of the FAD_{red}. This orientation is consistent with participation of N-5 of the cofactor to form adducts **18** and **19** during catalytic turnover [21].

Three mechanisms involving reduced FAD cofactor have been proposed to explain the formation of FAD-substrate intermediates **18** and **19** (Scheme 1.6).

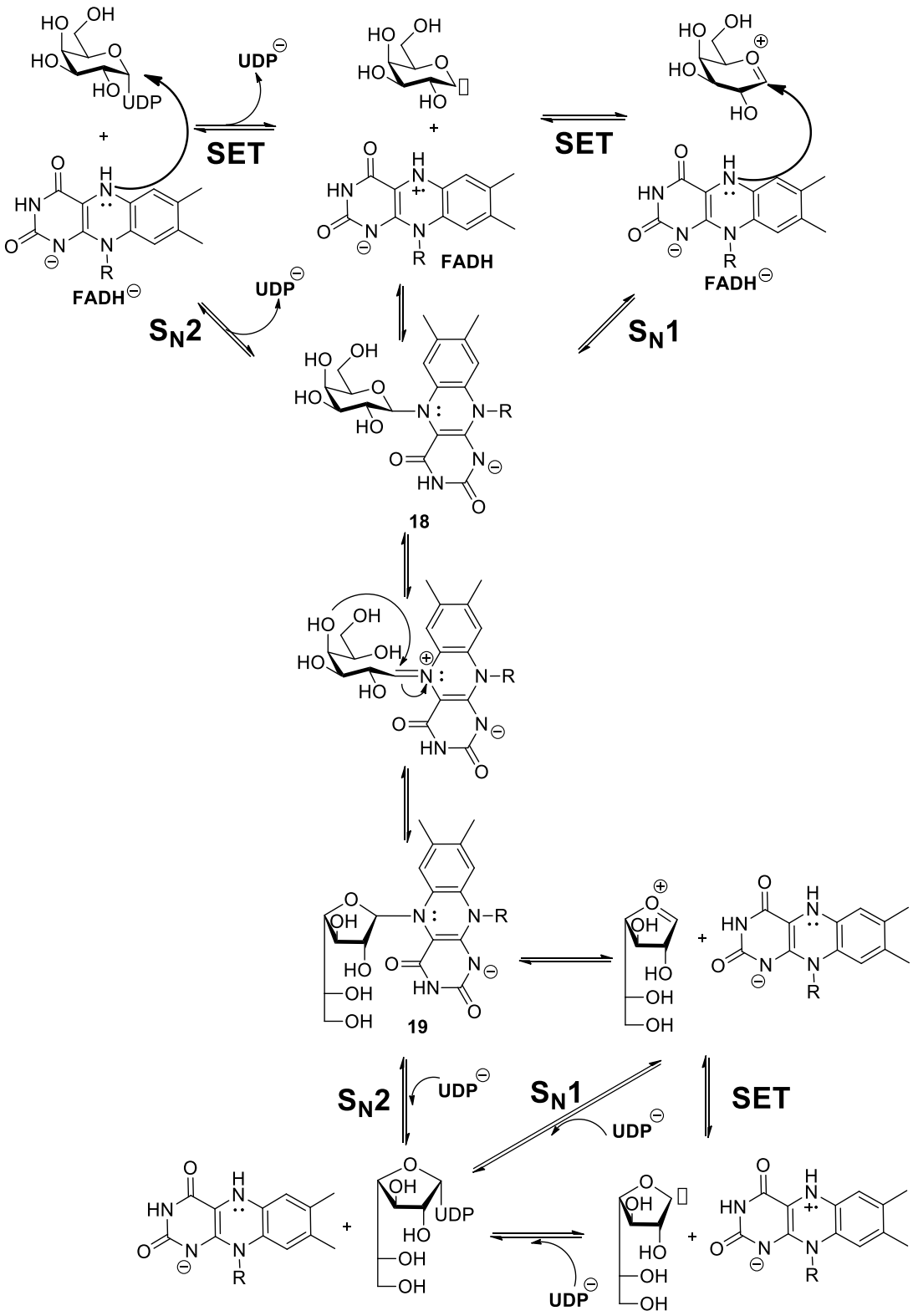

Scheme 1.6: Possible chemical mechanisms for the UGM-catalyzed reaction

The adduct formation may be initiated by homolytic cleavage of the glycosidic bond to form a glycosyl radical. The glycosyl radical is then oxidized to the oxacarbenium ion which, in turn, reacts with FADH anion and forms the adduct. Generation of the adduct may also occur via the nucleophilic attack of the N-5 of the cofactor at the anomeric carbon of the substrate in concert with cleavage of the glycosidic bond (S_N2-type substitution). Formation of the adduct may also take place in a stepwise fashion in which a oxacarbenium ion is generated after the cleavage of the UDP group, followed by a nucleophilic attack of the N-5 of the cofactor (S_N1-type substitution).

In a recent study, positional isotope exchange (PIX) and linear free energy relationships (LFERs) were employed to further investigate the role of N-5 of FAD_{red} in UGM catalysis. The observation that 5-deaza-FAD is unable to substitute for FAD_{red} in catalyzing PIX of the P_β oxygens implied that N-5 of FAD_{red} is necessary for the cleavage of the anomeric bond. To evaluate whether the cleavage of the anomeric bond goes through a S_N1, S_N2 or SET mechanism, the kinetic LFERs associated with changes in the nucleophilicity of the N-5 of FAD_{red} were examined. The observation that the rate of the steady-state turnover by UGM was sensitive to the nucleophilicity of N-5 was consistent with an S_N2-type mechanism, as the rate of the steady-state turnover is expected to be much less sensitive to the electron density at N-5 of FAD_{red} if adduct formation proceeds by a SET pathway or S_N1-type mechanism [22].

1.7. Transition state in S_N2-type UGM-catalyzed reaction

The proposed transition state for the UGM-catalyzed reaction could still have some oxacarbenium ion-like character. If bond cleavage is more advanced (leaving group departure) than bond making (nucleophilic attack by the cofactor) then the transition state will have substantial oxacarbenium-ion character (Scheme 1.7).

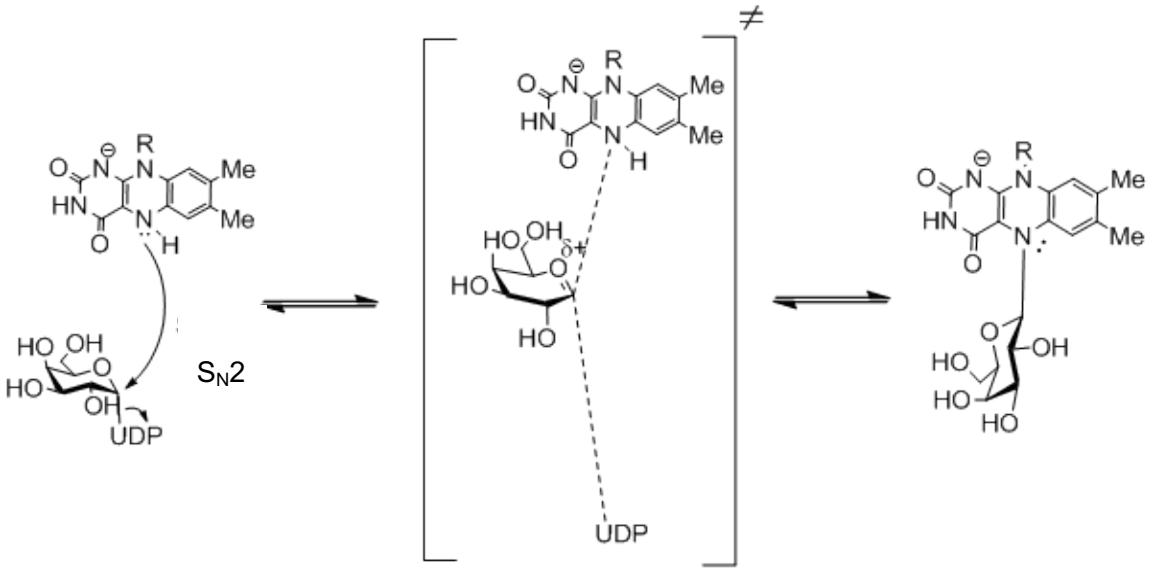

Scheme 1.7: Proposed transition state for the UGM-catalyzed reaction

1.8. Transition state analogues as enzyme inhibitors

Many drugs are enzyme inhibitors. An enzyme inhibitor is a molecule that binds to the enzyme and decreases its activity. One way of obtaining potent inhibition is to design inhibitors that resemble the transition state of an enzyme-catalyzed reaction.

Enzymes are biological molecules (proteins) which catalyze chemical reactions. They catalyze reactions by stabilizing the transition state via strong binding interactions which results in lowering the activation energy of the reaction as suggested by Linus Pauling [23]. (Figure 1.15 shows a free energy diagram for a simple reaction with and without enzyme catalysis). Transition state analogues are believed to be optimal candidates as enzyme inhibitors. As suggested by Richard Wolfenden, an ideal inhibitor which resembles the transition state of an enzyme catalyzed reaction should be bound much more tightly to the enzyme than the substrate [24].

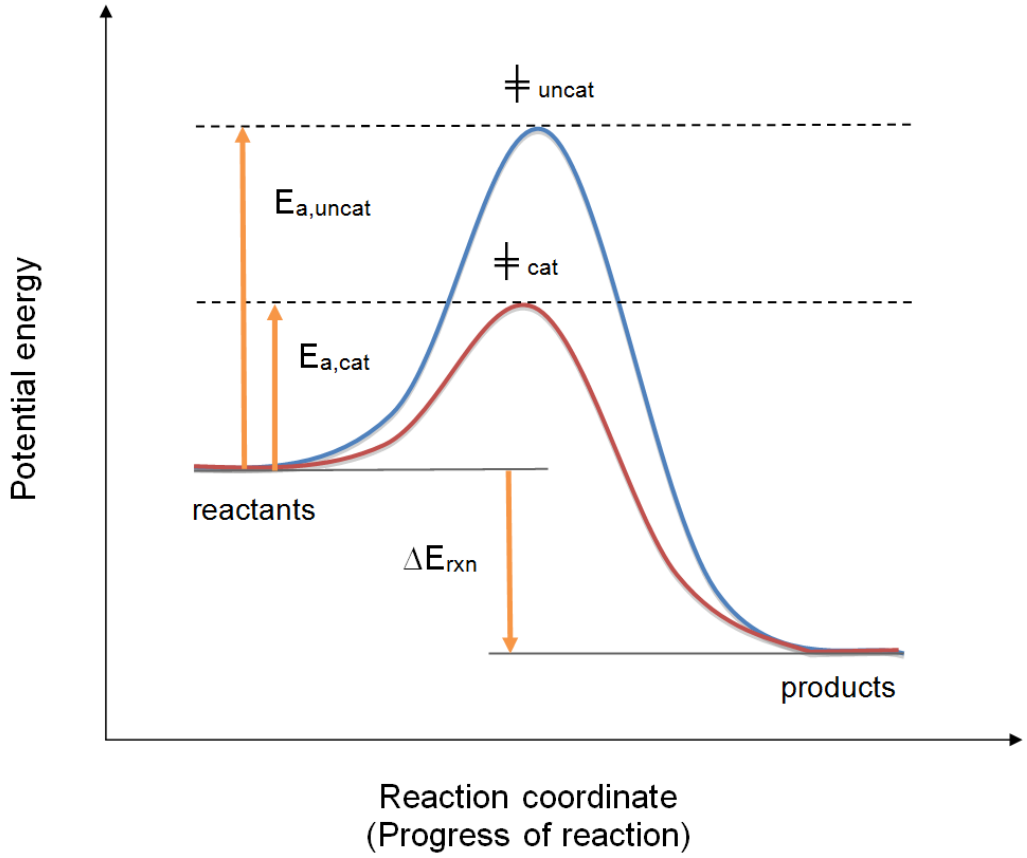

Figure 1-15: Free energy diagram for an enzyme-catalyzed reaction versus the uncatalyzed reaction

Vern L. Schramm has designed tight-binding transition state analogues for human purine nucleoside phosphorylase (hPNP) enzyme with K_d values in the picomolar range [25] [26], which validate the power of transition-state theory. hPNP enzyme is a molecular target in the treatment of leukemia and autoimmune disorders. The hPNP transition state and the structure of one of these potent inhibitors (compound **20**) are shown in Figure 1.16. Compound **20** indeed binds to hPNP 2400000 times tighter than substrate **21** (Figure 1.16) [25].

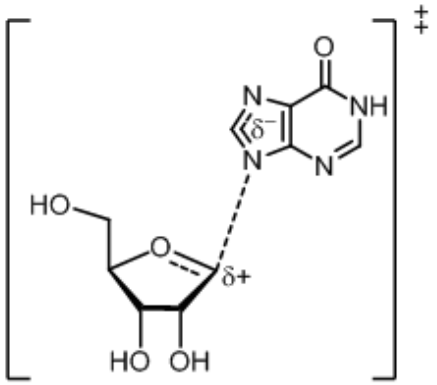

Transition state
for hPNP-catalyzed reaction

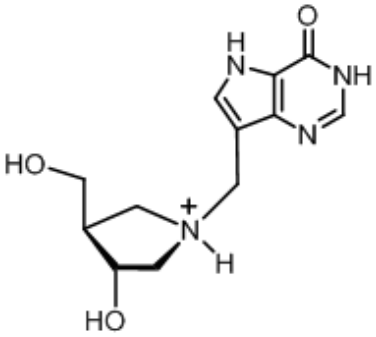

Transition state
analogue
20

K_d = 16 pM

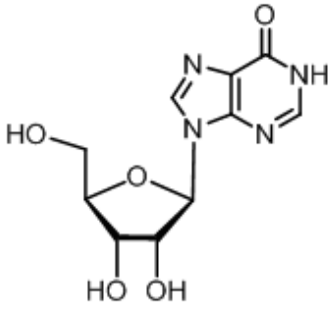

Substrate
21

Figure 1-16: Transition state, Transition state analogue and substrate for hPNP

1.9. Potential inhibitors of UGM and thesis overview

As proposed earlier, the reaction catalyzed by UGM could proceed through a transition state with some oxacarbenium-ion-like character. Therefore compounds that mimic both the shape and the charge of the oxacarbenium-ion-like transition state could be viable candidates as inhibitors of UGM.

The main goal of the work detailed in this thesis is to synthesize stable compounds with a permanent positive charge at the ring hetero atom as potential transition state (galactopyranosylium ion) analogue inhibitors of the UGM enzyme, to interfere with cell wall biosynthesis of *Mycobacterium tuberculosis*.

Our design strategy is based on the well accepted premise that a transition state analogue would be the optimal candidate as an enzyme inhibitor (for the reason elaborated previously). Sulfonium and selenonium ion-containing inhibitors may be suitable for this purpose. A special feature of these inhibitors is the permanent positive charge carried by the sulfur or selenium, which may mimic closely the charge of the oxacarbenium ion-like transition state.

An ideal inhibitor for UGM would be a stable compound that contains moieties that mimic both galactofuranose and uridine diphosphate domains, and possesses a permanent positive charge to mimic the oxacarbenium ion-like transition state, such as compound **A** which is potentially a transition state analogue (permanent positive charge on sulfur) with a diphosphate linkage and uridine moiety, or compound **B** with a polyhydroxylated side chain and a uracil moiety attached to it (Figure 1.17). The polyhydroxylated side chain can be used as a mimic for the pyrophosphate portion. Inhibitors should be able to penetrate membranes of cells and high polarity and the charge on pyrophosphate are unacceptable properties for cell permeability; therefore replacement of the pyrophosphate moiety with a polyhydroxylated side chain may increase the bioavailability of the inhibitors. This concept was first advanced to derive non-ionic mimics of the sugar-nucleoside donor of the human blood group B galactosyltransferase [27], [28].

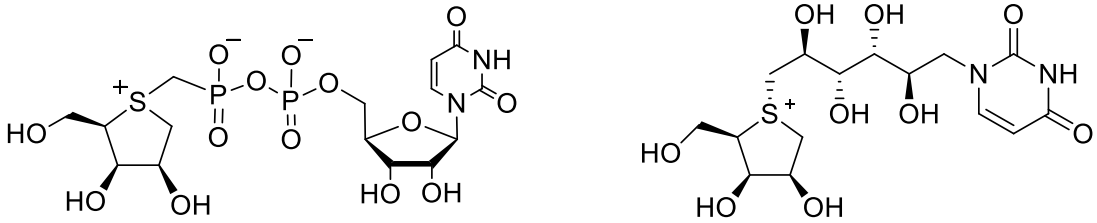

Figure 1-17: Potential inhibitors of UGM

For the purpose of this M.Sc. thesis, however, simpler compounds **22** and **23** (Figure 1.18) were chosen initially as potential UGM inhibitors to test the hypothesis that the permanent positive charge as well as the shape of the molecules could mimic the oxacarbenium ion-like transition state of the UGM-catalyzed reaction. In this thesis the synthesis and biological evaluation of the two candidates are presented. Further justification for the choice of these particular compounds is presented in Chapter 2 of this thesis.

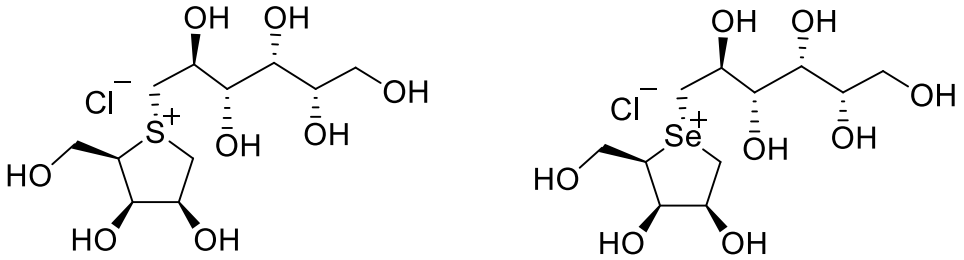

Figure 1-18: Proposed UGM inhibitors

Chapter 2.
Novel Sulfonium ion as a potential UGM inhibitor

2.1. Abstract

In this chapter the synthesis of compound **22** as a potential inhibitor of UGM is described. The synthesis of compound **46**, which was used as a simpler model to confirm the stability and structure elucidation of compound **22**, is also described.

2.2. Introduction

Yoshikawa *et al.* discovered two naturally occurring sulfonium ions salacinol [29] and kotalanol [30] (Figure 2.1) as glycosidase inhibitors in 1997 and 1998 respectively. These compounds were isolated from the plant *Salacia reticulata* which is a large woody, climbing plant widespread in Sri Lanka and India.

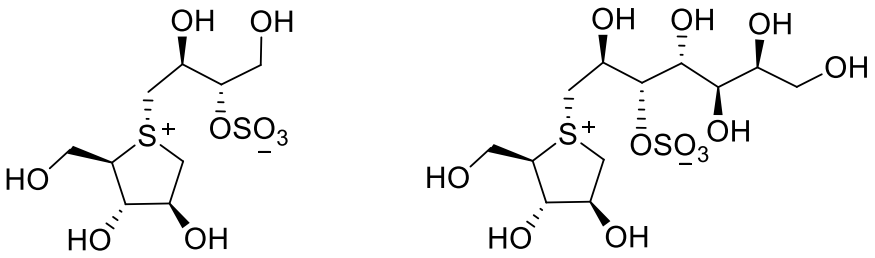

Figure 2-1: Salacinol and Kotalanol, compounds isolated from the *Salacia reticulata* plant

Since then, an increasing amount of research on cyclic sulfonium compounds has been carried out. Ponkoranol and Salaprinol (Figure 2.2) were also later obtained from the *Salacia prinoides* plant [31].

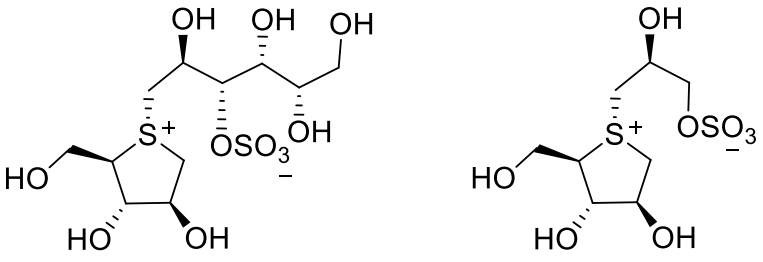

Ponkoranol Salaprinol

Figure 2-2: Ponkoranol and Salaprinol, compounds isolated from the *Salacia prinoides* plant

De-*O*-sulfonated salacinol [32], [33], de-*O*-sulfonated kotalanol [34], [35], [36], de-*O*-sulfonated ponkoranol [37], [38] and de-*O*-sulfonated salaprinol [38] (Figure 2.3) were also isolated from *Salacia* genus.

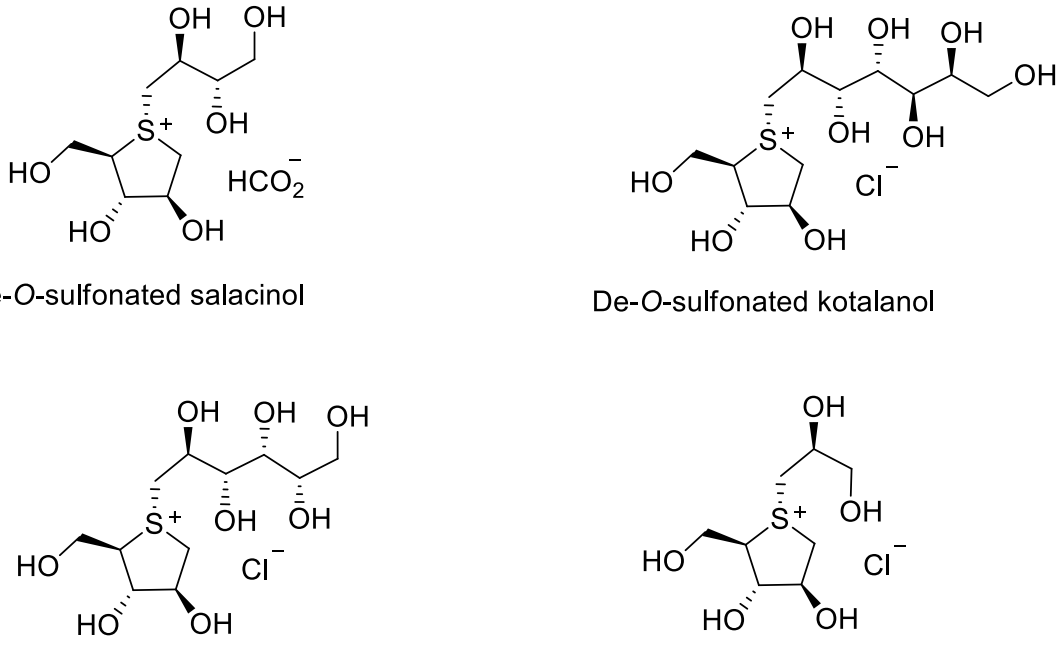

De-*O*-sulfonated salacinol

De-*O*-sulfonated kotalanol

De-*O*-sulfonated ponkoranol

De-*O*-sulfonated salaprinol

Figure 2-3: De-*O*-sulfonated derivatives isolated from *Salacia* genus

For most of the above mentioned compounds the absolute stereostructures were not known at the time of their isolation. Synthetic studies by our group and others have led to the establishment of the stereostructures shown above [39], [40], [41]. One way to prove the stereostructure of a natural product is by total synthesis of reasonable candidates. For example the absolute stereostructure of the acyclic side chain in kotalanol was not determined for many years after its isolation. In 2010 our group established the absolute stereostructure for kotalanol (Figure 2.4) by first narrowing down the possible stereostructures for kotalanol (based on the structure-activity-relationship studies directed towards salacinol and related analogues) and then synthesizing several candidates and comparing their NMR data with those reported for kotalanol and de-*O*-sulfonated kotalanol [40].

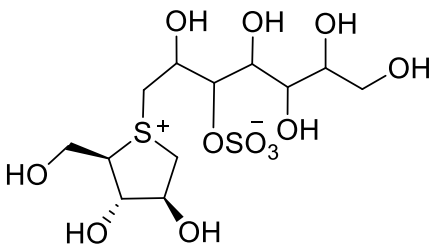

reported tructure of kotalanol at the time of isolation [30]

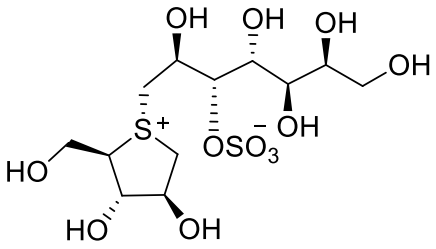

absolute stereostructure of kotalanol [40]

Figure 2-4: Structure of kotalanol at the time of isolation from *Salacia* species and its absolute stereostructure

Through structure-activity-relationship (SAR) studies our group have modified the natural compounds to derive more potent inhibitors of human intestinal glucosidases namely maltase glucoamylase (MGAM) and sucrase-isomaltase (SI) which are known targets in the treatment of type 2 diabetes. MGAM and SI are anchored to the small intestinal brush-border epithelial cells, and each contains a catalytic N- and C-terminal subunit, namely ntMGAM, ctMGAM, ntSI and ctSI. This structure refinement yielded the most potent inhibitors known to date for each subunit, some of which are shown in figure 2.5 [42].

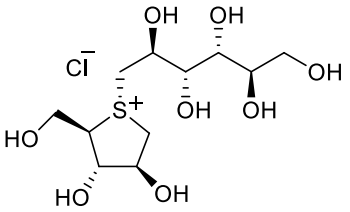

K_i = 132 nM for ctSI
K_i = 138 nM for ntSI
K_i = 15 nM for ntMGAM
K_i = 138 nM for ctMGAM-N20

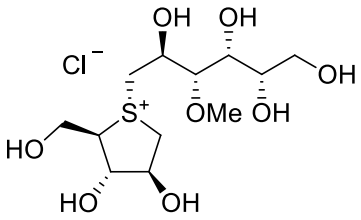

K_i = 7 nM for ctSI
K_i = 35 nM for ntSI
K_i = 500 nM for ntMGAM
K_i = 60 nM for ctMGAM-N2
K_i = 55 nM for ctMGAM-N20
Best inhibitor of ctSI

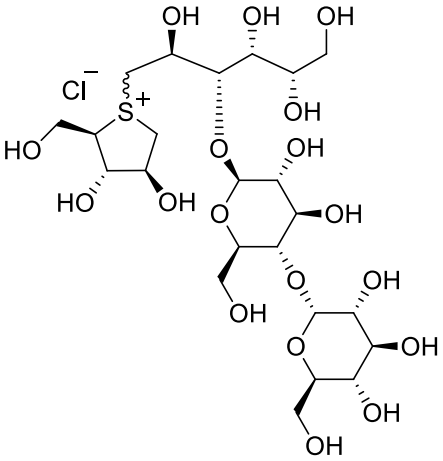

K_i = 62 nM for ctSI
K_i = 46 nM for ntSI
K_i = 39 nM for ntMGAM
K_i = 655 nM for ctMGAM-N20

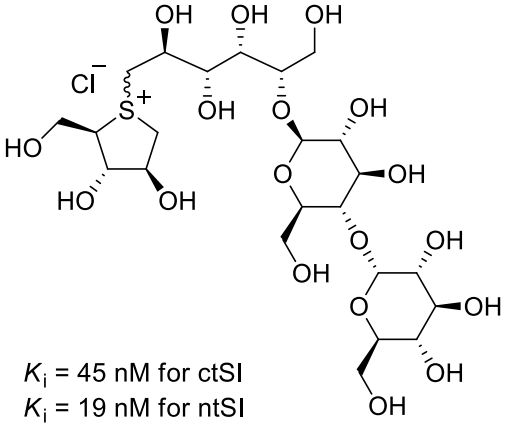

K_i = 45 nM for ctSI
K_i = 19 nM for ntSI
K_i = 8 nM for ntMGAM
K_i = 77 nM for ctMGAM-N2
K_i = 67 nM for ctMGAM-N20
Best inhibitor of ntMGAM

Figure 2-5: Potent synthetic inhibitors of ntMGAM, ctMGAM, ntSI and ctSI [ref. 42]

It has been proposed that the $^{3}T_{2}$ bound conformation of salacinol-based compounds in the active site of intestinal glucosidases superimpose well on the $^{4}H_{3}$

conformation of the proposed oxacarbenium ion intermediate (glucopyranosylium cation) (Figure 2.6) in the glucosidase-catalyzed reaction [43].

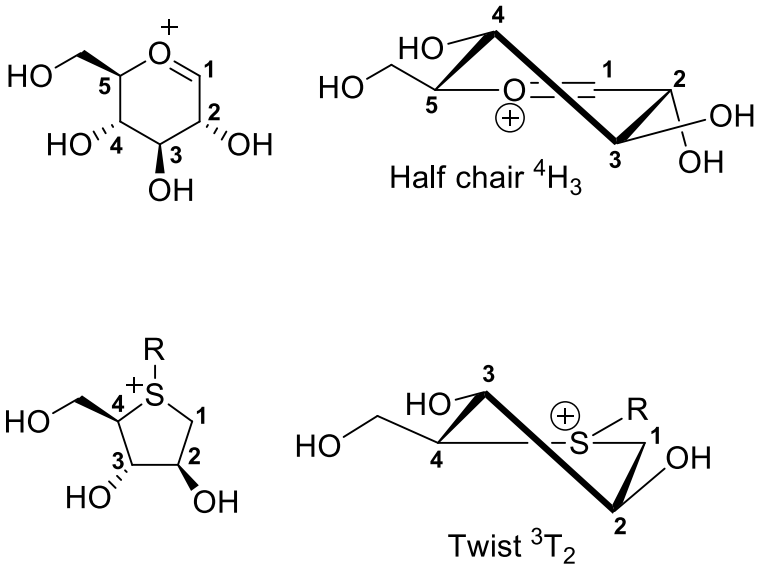

Figure 2-6: Correspondence of the glucopyranosylium cation intermediate in the glucosidase-catalyzed reaction and the sulfonium ion glucosidase inhibitors

Since the proposed transition state for the UGM-catalyzed reaction may contain oxacarbenium ion character similar to the proposed transition state in the glucosidase-catalyzed reaction we reasoned that a similar strategy could be used for the design of UGM inhibitors. The design of compound **22** as a potential UGM inhibitor is based on the hypothesis that if we invert the configuration at C3 in the salacinol based compounds then the resulting conformation may superimpose well on the proposed $^4H_3$ conformation of the galactopyranosyl cation in the UGM-catalyzed reaction (Figure 2.7).

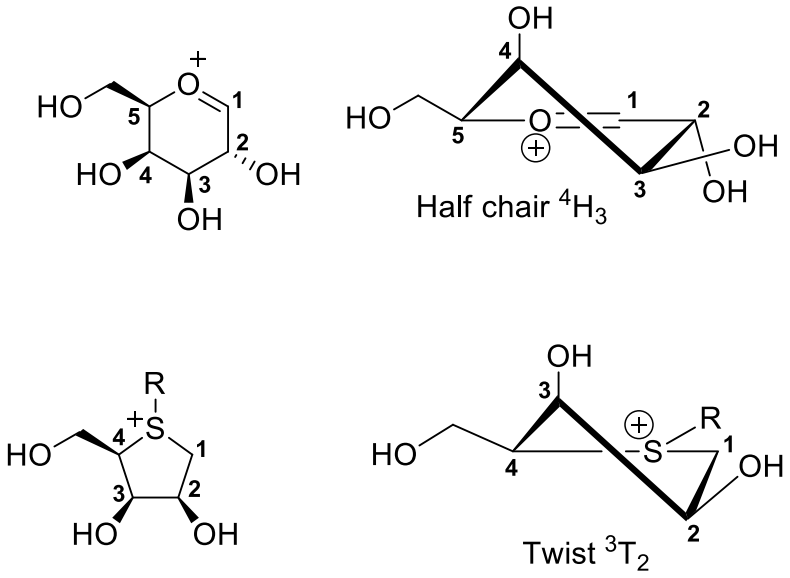

Figure 2-7: Correspondence of the galactopyranosylium cation intermediate in the UGM-catalyzed reaction and the proposed sulfonium ion inhibitors

We also note that long chain S-alkylated sulfonium ions with gluco configuration which were synthesized as glucosidase inhibitors [44], showed some activity against *tb*UGM [45] (Figure 2.8).

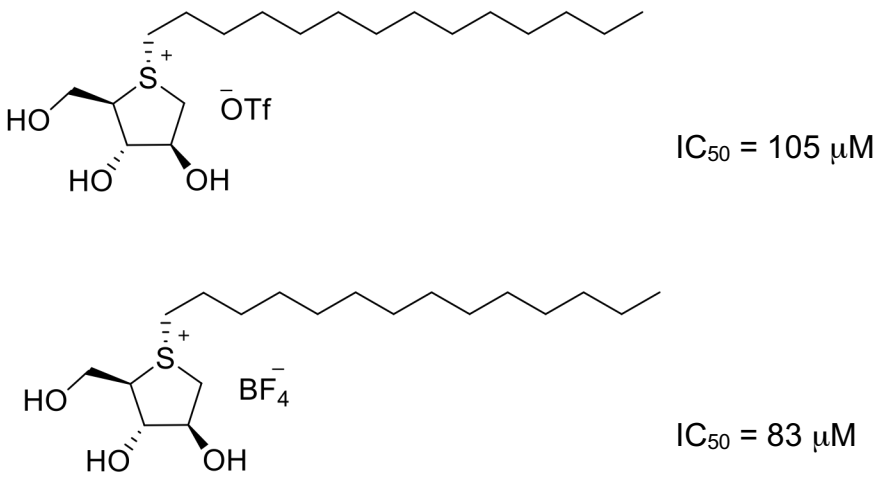

Figure 2-8: S-alkylated sulfonium ions and their inhibitory activity against *tb*UGM

Therefore, synthesis of compounds with galacto configuration may yield more potent inhibitors.

2.3. Result and discussion

Retrosynthetic analysis indicated that compound **22** could be synthesized by the coupling reaction between a protected thio-D-arabinitol **X** and agent **Y** (Scheme 2.1).

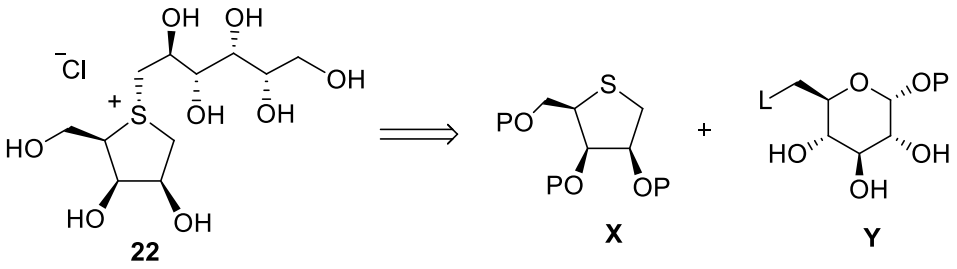

L = leaving group P = protecting group

Scheme 2.1: Retrosynthetic analysis for compound 22

The protected thio D-arabinitol **24** was synthesized following a reported procedure [46], starting from the commercially available D-lyxose (Scheme 2.2).

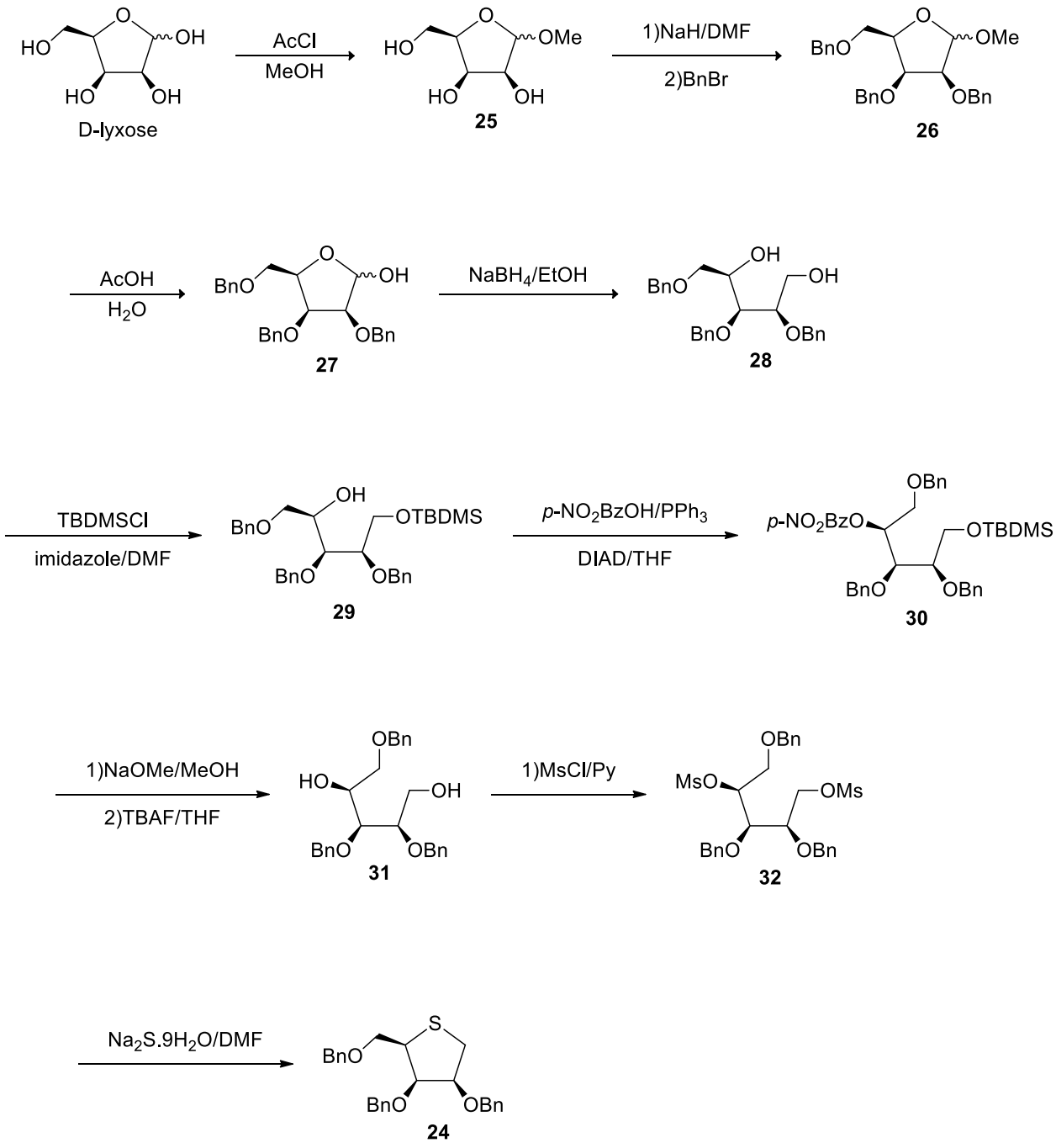

Scheme 2.2: Synthesis of compound 24

2,3,5-Tri-*O*-benzyl-D-lyxofuranoside (**27**) was prepared in 3 steps starting from D-Lyxose. Glycosylation using acetyl chloride and methanol gave methyl glycoside **25**. Then benzylation using sodium hydride and benzyl bromide followed by hydrolysis using acetic acid and water gave compound **27**. Reduction of **27** with sodium borohydride gave the diol **28**. Selective protection of the primary hydroxyl group using *tert*-butyldimethylsilylchloride gave compound **29**, which was then converted to compound **30** using Mitsunobu conditions. Deprotection of the *p*-nitrobenzoyl and *tert*-butyldimethylsilyl groups using sodium methoxide and tetrabutylammonium fluoride, respectively, gave the diol **31**. Diol **31** was then converted to the dimesylate using methanesulfonyl chloride in pyridine, and the dimesylate was then treated with sodium sulfide to give the desired product **24**.

The tosylate **33** was synthesized from penta-*O*-acetyl glucopyranose (**34**) in 3 steps. Using benzyl alcohol and boron trifluoride diethyl etherate, compound **34** was converted to the benzyl glucoside **35** [47]. Acetyl groups were removed using sodium methoxide and methanol. Compound **36** was then treated with tosyl chloride and pyridine to get the desired primary tosylate **33** (Scheme 2.3).

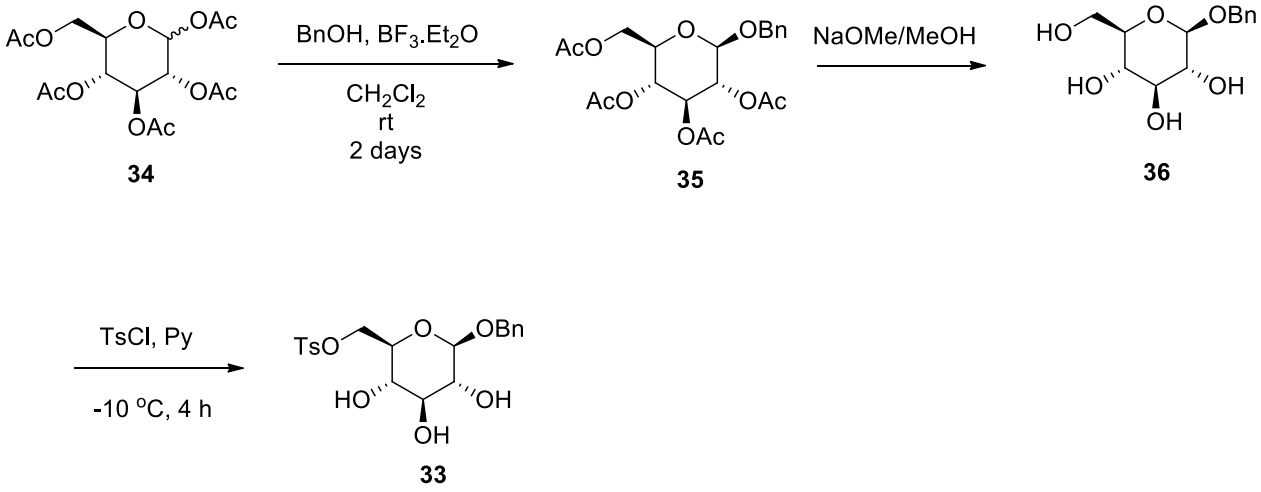

Scheme 2.3: Synthesis of tosylate 33

Initially the coupling reaction between protected thio D-arabinitol **24** and *p*-toluenesulfonyl ester **33** in HFIP at 70 °C was examined based on the procedure that has been reported [37] (Scheme 2.4) but the reaction was not successful and we were not able to isolate appreciable amounts of the desired product.

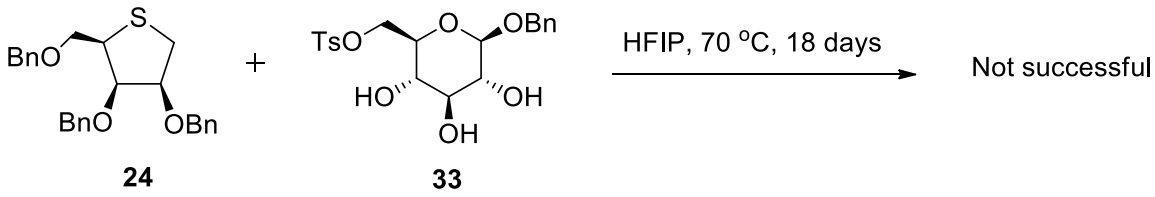

Scheme 2.4: First attempted synthesis of compound 22

It had been shown that the coupling yields between acetyl protected triflates and D-glucose and D-mannose-derived cyclic thioethers were substantially increased with no need for high temperatures [48]. Following that strategy, we synthesized triflate **37** to try the coupling reaction between the protected thio D-arabinitol **24** and triflate **37**. D-glucose was converted to the trityl derivative **38** using triphenylmethyl chloride and pyridine. Compound **38** was then converted to the tetra acetate **39** by treatment with acetic anhydride and pyridine. The trityl protecting group was removed using 33% hydrogen bromide to give compound **40** [49], which was then treated with triflic anhydride and lutidine to provide the desired triflate **37** [48] (Scheme 2.5).

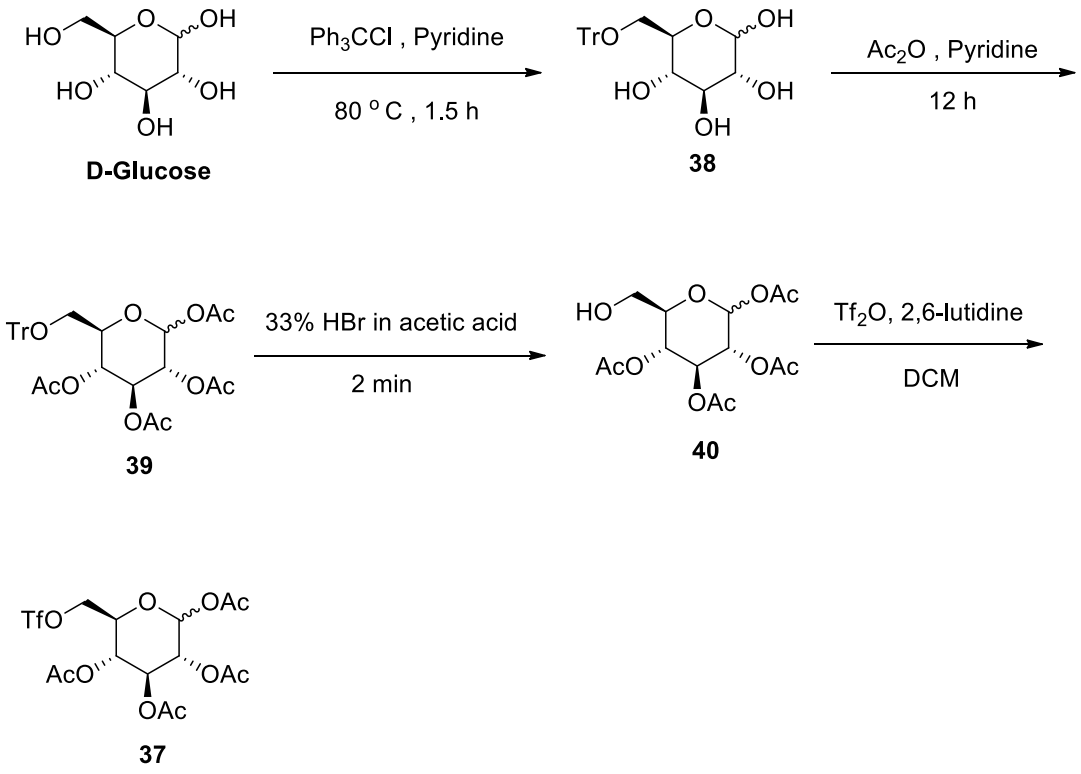

Scheme 2.5: Synthesis of the triflated coupling partner 37

The coupling reaction between compound **24** and triflate **37** in THF at room temperature proceeded smoothly and yielded the sulfonium ion **41** in 48% yield (Scheme 2.6).

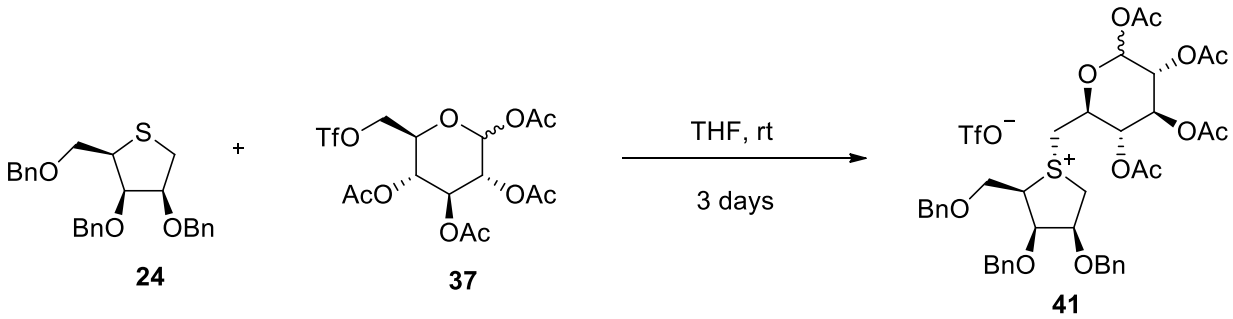

Scheme 2.6: synthesis of coupled product 41

The acetyl groups were removed by treatment with 4N aqueous hydrochloric acid at 50 °C. To remove the benzyl groups we tried both boron trichloride and hydrogenolysis. The route involving hydrogenolysis resulted in a cleaner product, which was subsequently treated with Amberlyst A-26 resin (chloride form) to completely exchange the *p*-toluenesulfonate counter ion with chloride ion. Finally, the crude product was reduced with sodium borohydride to provide the desired compound **22** (Scheme 2.7).

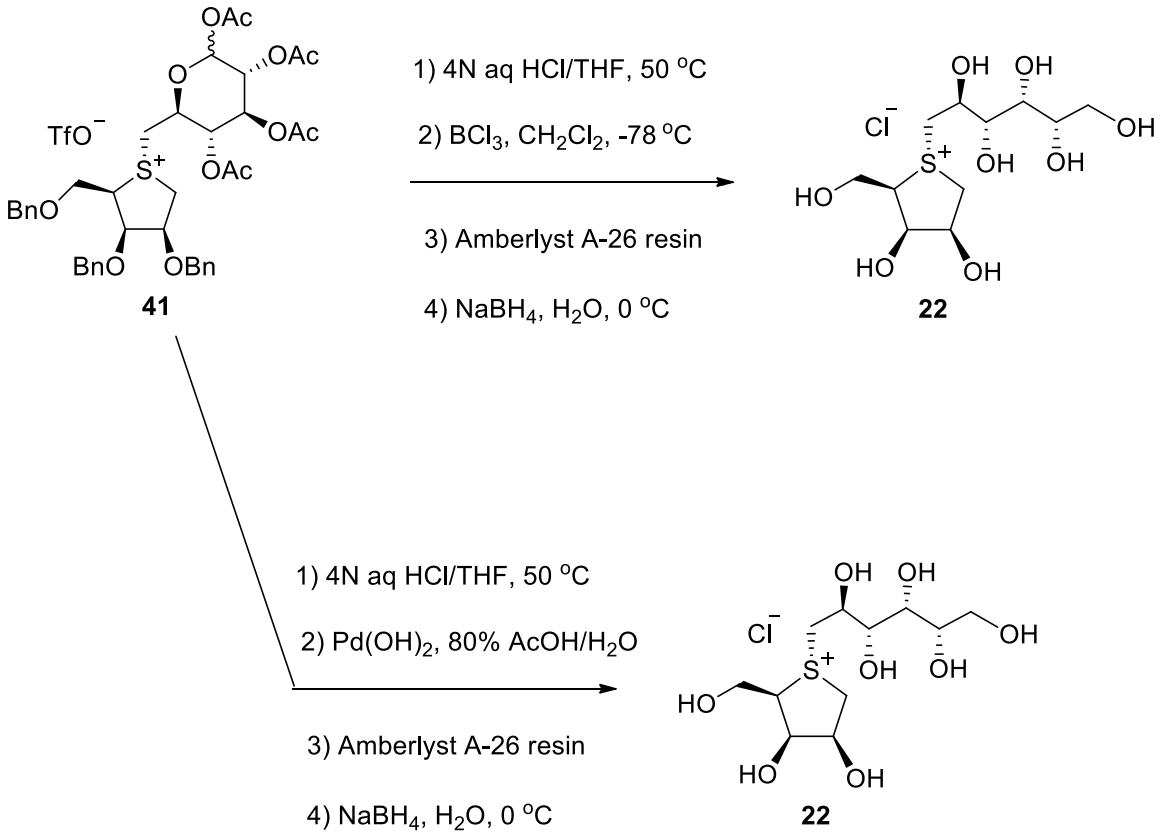

Scheme 2.7: Synthesis of the target compound 22

To reduce the number of steps involved in the synthesis of thioether coupling partner, we also considered alternative synthetic strategy by following a recent literature report. Gunasundari et al. developed an efficient synthetic route for thio-D-arabinitol starting from D-ribonolactone in three steps as shown in Scheme 2.8 [50].

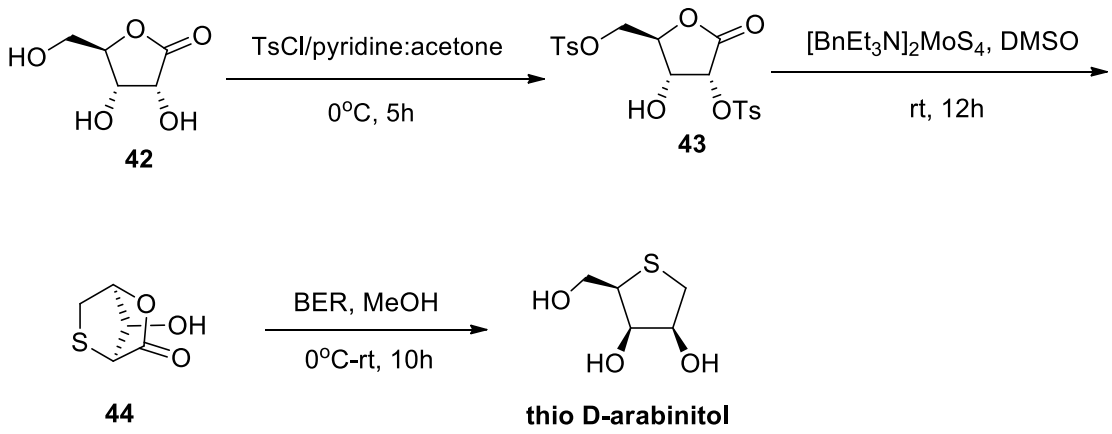

Scheme 2.8: recent reported short synthetic pathway for thioether coupling partner [ref. 50]

At first, D-ribose was converted to the ribonolactone **42** by treatment with sodium bicarbonate and bromine (Scheme 2.9) [51]. Treatment of **42** with tosyl chloride and pyridine in acetone gave tosylate **43**. The reported procedure requires benzyltriethylammonium tetrathiomolybdate for the cyclization of the ditosylate into lactone **44**. However, several attempts to prepare this reagent from ammonium tetrathiomolybdate and benzyltriethylammonium chloride resulted in thick black slurry which was not soluble in any solvent. Finally, we optimized this step by making this reagent *in situ*. Thus, benzyltriethylammonium chloride and ammonium tetrathiomolybdate were mixed in acetonitrile and stirred under nitrogen atmosphere for one hour followed by the addition of ditosylate to get the desired lactone **44**. Considering the cost of the ammonium tetrathiomolybdate and the difficulties in handling it, we also attempted to do this cyclization with sodium sulfide and we are pleased to report that this reaction proceeds smoothly by reacting the ditosylate with sodium sulfide in acetonitrile. Further, reduction of the compound **44** will provide an easy access to the desired thio D-arabinitol by following the literature procedure using the sodium borohydride exchange resin (Scheme 2.9).

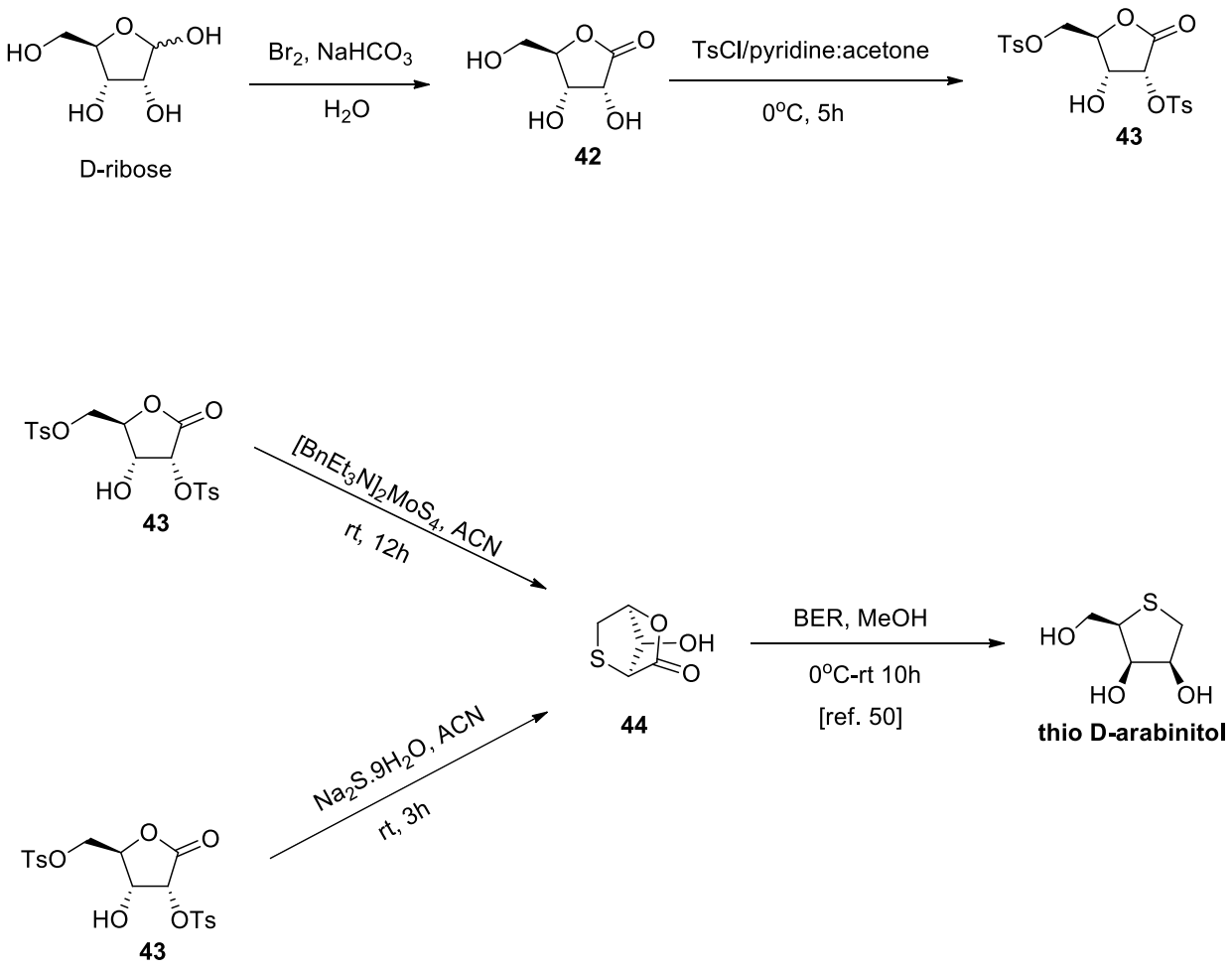

Scheme 2.9: Shorter route for small scale synthesis of thioether coupling partner

To confirm the stability of the target compound **22**, and also for structure elucidation, the simpler methylsulfonium compound **46** was also synthesized by the coupling reaction between methyl iodide and the protected thio-arabinitol **24**. Benzyl groups were then removed by treatment with boron trichloride (Scheme 2.10).

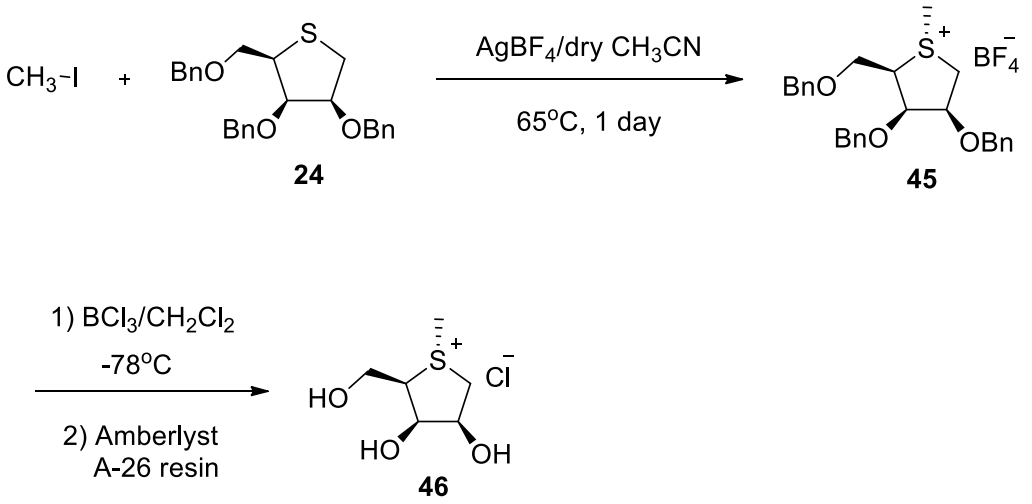

Scheme 2.10: Synthesis of methylsulfonium 46

Analysis by ^{1}H NMR spectroscopy indicated that compound **46** was a mixture of diastereomers (2.3:1 ratio) at the sulfur centre. The major component of the mixture was assigned to be the diastereomer with a trans relationship between C-methyl and C-5 on the basis of NOE observations. Irradiation of the methyl protons of the major isomer at δ= 2.97 ppm enhanced the H-1, H-2, H-3, H-4 signals whereas Irradiation of the methyl protons of the minor isomer at δ= 3.02 ppm enhanced the H-1b and H-5a signals (Figure 2.9).

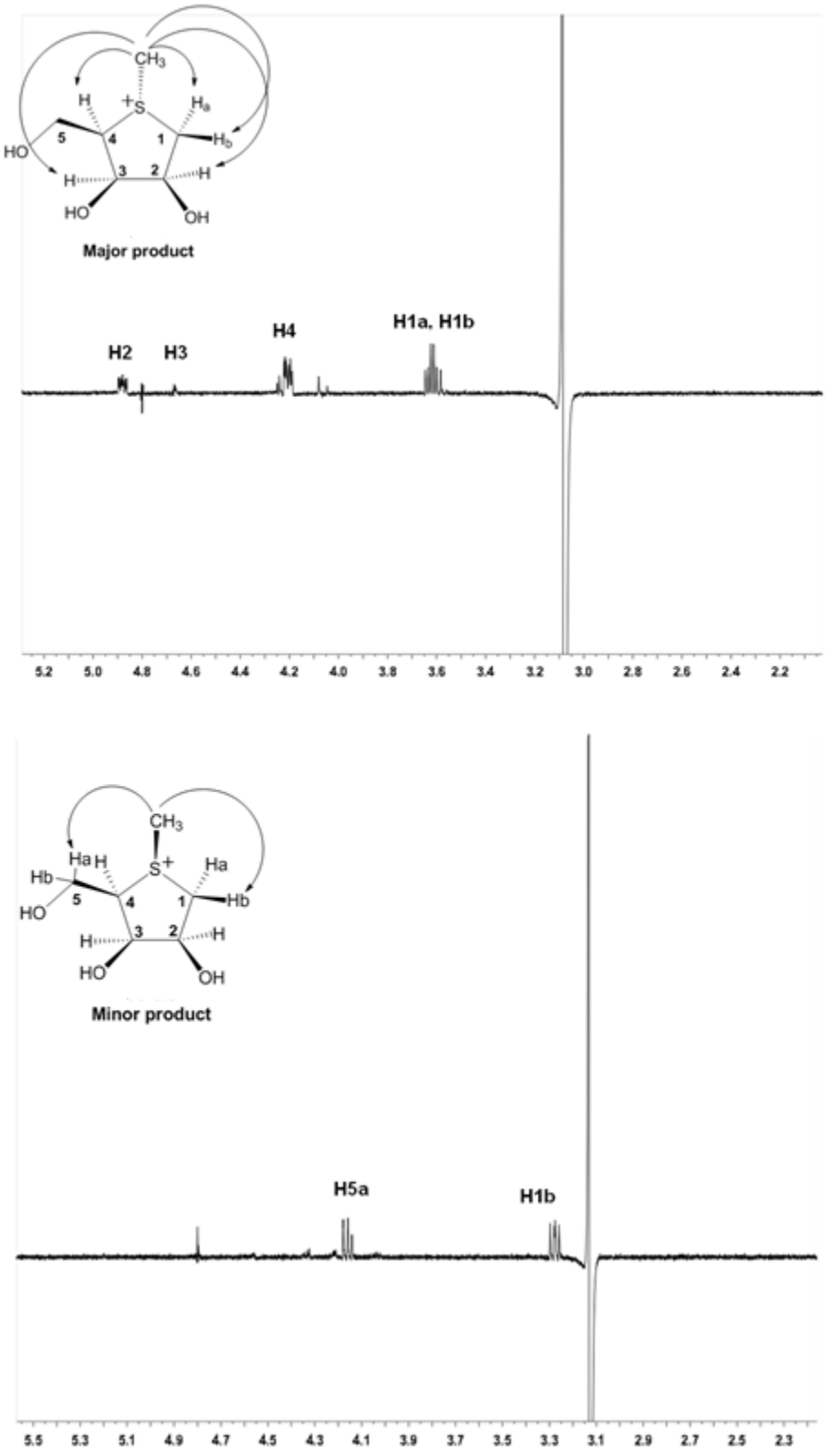

Figure 2-9: NOE spectra for compound 46

2.4. Experimental

2.4.1. General methods

Optical rotations were measured at 23 °C. ^{1}H NMR spectra were recorded at 600 and 500 MHz. ^{13}C NMR spectra were recorded at 150 and 126 MHz. Assignments were confirmed with the aid of attached proton test (^{13}C-APT) and two-dimensional ^{1}H-^{1}H (COSY), ^{1}H-^{13}C (HSQC) and ^{1}H-^{13}C (HMBC) experiments using standard pulse programs. Processing of the spectra was performed with MestReNova software. Analytical thin-layer chromatography (TLC) was performed on aluminum plates pre-coated with silica gel 60F-254 as the adsorbent. The developed plates were air-dried, exposed to UV light and/or sprayed with a solution containing 1% ceric sulfate and 1.5% molybdic acid in 10% aqueous sulfuric acid, and heated. Column chromatography was performed with an automated flash chromatography system. High resolution mass spectra were obtained by the electrospray ionization method, using a TOF LC/MS high resolution magnetic sector mass spectrometer.

2.4.2. Compound synthesis and characterization

Methyl-2,3,5-tri-*O*-benzyl-D-lyxofuranoside (26)

To a stirred solution of D-lyxose (1 g, 6.7mmol) in MeOH (15 mL) at 0 °C under N_2, AcCl (0.05 mL) was added dropwise. The mixture was stirred at 0° C under N_2 for 7 h, then at room temperature for overnight. The mixture was neutralized with 2 N NaOMe/MeOH solution and concentrated. The residue was diluted in DMF (5 mL) and then added dropwise to a suspension of NaH (60% in oil, 1 g, 25 mmol) in DMF (12.5 mL) at 0 °C under N_2. The mixture was stirred at room temperature for 30 min and then cooled to 0 °C. BnBr (2.6 mL, 22.1 mmol) was added dropwise and the mixture was stirred at room temperature for 2 h. The mixture was cooled to 0 °C and quenched with ice (1.5 mL) and extracted with ethyl acetate (3 × 20 mL). The organic phase was washed with H_2O (2 × 7.5 mL), dried over anhydrous sodium sulfate and concentrated to give a yellow oil. The crude product was used in the next step without purification.

^{1}H NMR (500 MHz, $CDCl_3$): δ 7.38 – 7.10 (m, 15H, Ar), 4.94 (d, $J_{1,2}$ = 2.5 Hz, 1H, H-1), 4.63 – 4.41 (m, 6H, C*H2*Ph), 4.31 – 4.22 (m, 1H, H-4), 4.12 (t, J = 5.0 Hz, 1H, H-3), 3.81 (dd, $J_{2,3}$ = 4.6 Hz, $J_{2,1}$ = 2.5 Hz, 1H, H-2), 3.76 – 3.63 (m, 2H, H-5a, H-5b), 3.30 (s, 3H, C*H3*).

2,3,5-Tri-*O*-benzyl-D-lyxofuranose (27)

Crude compound **26** (1.47 g) was dissolved in 70% AcOH/H_2O (20 mL) and the mixture was heated to reflux. The stirring was continued at 100 °C for 15 h and concentrated. The residue was dissolved with H_2O (100 mL) and extracted with DCM (150 mL). The organic phase was washed with sat. sodium bicarbonate, dried over anhydrous sodium sulfate and concentrated. The crude product (1.53 g) was used in the next step without purification.

1,3,4-Tri-*O*-benzyl-D-arabinitol (28)

To a stirred solution of compound **27** (1.53 g, 3.64 mmol) in EtOH (15 mL) at 0°C was added sodium borohydride (110 mg, 2.9 mmol) in small portions. The mixture was stirred in an ice bath for 40 min, then it was quenched with AcOH (pH = 7). The mixture was concentrated and then diluted with EtOAc (100 mL). The organic phase was washed with H_2O (2 × 100 mL) and brine (100 mL), dried and concentrated. The crude product (1.38 g) was used in the next step without purification.

1,3,4-Tri-*O*-benzyl-5-*O*- *tert*- butyldimethylsilyl-D-arabinitol (29)

A mixture of compound **28** (1.38 g, 3.27mmol), imidazole (0.41 g, 6.072 mmol) and TBDMSCl (0.5 g, 3.59 mmol) in DMF (15 mL) was stirred at 0 °C under N_2 for 1.5 h. Then it was quenched with ice (2 mL). The mixture was diluted with H_2O (100 mL) and extracted with ether (3 × 50 mL). The organic phase was washed with H_2O (2 × 50 mL), brine (50 mL), dried over anhydrous sodium sulfate and concentrated. The crude product was purified via flash chromatography (EtOAc/Hexane 0-100%) to give a pale yellow oil (1.5 g).

^{1}H NMR (500 MHz, $CDCl_3$): δ 7.42 – 7.11 (m, 15H, Ar), 4.65-4.35 (m, 6H, C*H2*Ph), 4.01 (m, 1H, H4), 3.83 (dd, J = 10.9, 4.1 Hz, 1H, H1a), 3.79 – 3.63 (m, 3H, H1b, H3, H2),

3.52 – 3.42 (m, 2H, H5a, H5b), 2.96 (d, 1H, OH), 0.85 (s, 9H, (CH_3)$_3$CSi), 0.02 (s, 6H,(CH_3)$_2$Si).

2,3,5-Tri-*O*-benzyl-1-*O*- *tert*- butyldimethylsilyl-4-*O*-*p*-nitrobenzoyl-D-ribitol (30)

To a stirred solution of compound **29** (1.2 g, 2.24 mmol), *p*-nitrobenzoic acid (1.02 g, 6.14 mmol) and triphenylphosphine (1.62 g, 6.18 mmol) in THF (10 mL) at 0 °C under N_2 was added a solution of DIAD (1.22 mL, 6.16 mmol) in THF (10 mL), dropwise over 15 min. The mixture was stirred at room temperature for 15 h and partitioned between ether (75 mL) and H_2O (150 mL). The organic phase was washed with sat. sodium bicarbonate (3 × 50 mL), brine (50 mL), dried over anhydrous sodium sulfate and concentrated. The crude product was purified via flash chromatography (EtOAc/Hexane 0-30%) to give a yellow oil (0.8 g, 52%).

2,3,5-Tri-*O*-benzyl-D-ribitol (31)

To a stirred solution of compound **30** (0.63 g, 0.91 mmol) in MeOH (8 mL) was added 2 M NaOMe/MeOH (18 μL). The mixture was stirred at room temperature for 1.5 h and concentrated. The residue was partitioned between ether (75 mL) and H_2O (100 mL). The organic layer was washed with brine (100 mL), dried over anhydrous sodium sulfate and concentrated. The residue was dissolved in THF (8 mL) and a solution of tetra-*n*-butylammonium fluoride (1 M in THF, 1 mL) was added. The mixture was stirred at room temperature for 1.5 h and then it was partitioned between ether (75 mL) and H_2O (100 mL). The organic layer was washed with brine (100 mL), dried over anhydrous sodium sulfate and concentrated to give a pale yellow oil. The crude product was purified via flash chromatography (EtOAc/Hexane 0-100%) to give a colorless oil (0.22g, 57%). HRMS Calcd for $C_{26}H_{30}NaO_5$ (M+Na): 445.1985 Found: 445.2001.

2,5-Anhydro-1,3,4-tri-*O*-benzyl-2-deoxy-2-thio-D-arabinitol (24)

To a stirred solution of compound **31** (0.22 g, 0.52 mmol) in pyridine (4 mL) at 0 °C under N_2 was added methanesulfonyl chloride (0.12 mL, 3 eq) dropwise. The mixture was stirred at at 0 °C for 1.5 h and then quenched with ice (5-6 pieces). The mixture was partitioned between H_2O (30 mL) and DCM (2 × 50 mL). The organic phase was dried over anhydrous sodium sulfate and concentrated. The residue was dissolved in DMF (5

mL) along with $Na_2S.9H_2O$ (0.21 g, 0.83 mmol). The mixture was stirred at 110 °C for 1.5 h. After cooling to room temperature, the mixture was diluted with ether (100 mL) and washed with H_2O (50 mL), brine (50 mL) and dried over anhydrous sodium sulfate and concentrated. The crude product was purified via flash chromatography (EtOAc/Hexane 0-80%) to give a colorless oil (0.21 g, 96%). $[\alpha]_D$= +60 (*c* 0.01, $CHCl_3$). ^{1}H NMR (600 MHz, $CDCl_3$): δ 7.50 – 7.16 (m, 15H, Ar), 4.86 (d, $J_{a,b}$ = 11.7 Hz, 1H, C*H*$_2$Ph), 4.68 (d, $J_{b,a}$ = 11.7 Hz, 1H, C*H*$_2$Ph), 4.58 (s, 2H, C*H*$_2$Ph), 4.49 (s, 2H, C*H*$_2$Ph), 4.2 (m, 1H, H-3), 4.05 (ddd, J= 9.0, 6.2, 2.9 Hz, 1H, H-2), 3.90 (t, J = 8.2 Hz, 1H, H-5a), 3.59 (m, 1H, H-4), 3.54 (dd, J = 9.0, 6.5 Hz, 1H, H-5b), 3.06 (m, 1H, H-1b), 2.91 (m, 1H, H-1a). ^{13}C NMR (150 MHz, $CDCl_3$) δ 138.12, 137.64, 137.55 (3 C*ipso*), 128.04 – 126.81 (15C, Ar), 83.04 (C2), 78.37 (C3), 73.11, 72.85, 71.69 (3*C*H$_2$Ph), 69.76 (C5), 45.21 (C4), 29.85 (C1). HRMS Calcd for $C_{26}H_{29}O_3S$ (M+H): 421.1832 Found: 421.1814, Calcd for $C_{26}H_{28}NaO_3S$ (M+Na): 443.1651 Found: 443.1630, Calcd for $C_{26}H_{28}KO_3S$ (M+K): 459.1391 Found: 459.1393.

Benzyl 2,3,4,6-Tetra-*O*-acetyl-β-D-glucopyranoside (35)

Boron trifluoride diethyl etherate (3.16 mL) was added slowly to a mixture of penta-*O*-acetyl glucopyranose (10 g, 25.6 mmol), Benzyl alcohol (2.65 mL) and DCM (50 mL). The reaction was stirred at room temperature for 2 days and then poured into 100 mL of 5% sodium bicarbonate. 100 mL of DCM was added and the organic layer was separated and washed successively with 5% sodium bicarbonate (2 × 120 mL) and concentrated. The crude product was recrystallized from ethanol then purified using column chromatography (EtOAc/Hexane 0-100%) to give a white solid (6.8 g, 60%). ^{1}H NMR (600 MHz, $CDCl_3$): δ 7.48 – 7.31 (m, 5H,Ar), 5.20– 5.06 (m, 3H, H3, H-4,H-2), 4.93 (d, $J_{a,b}$ = 12.3 Hz, 1H, C*H*$_2$Ph), 4.65 (d, $J_{b,a}$= 12.3 Hz, 1H, C*H*$_2$Ph), 4.58 (d, $J_{1,2}$ = 7.9 Hz, 1H, H-1), 4.30 (dd, $J_{6a,6b}$ = 12.3, $J_{6a,5}$=4.7 Hz, 1H, H-6a), 4.20 (dd, $J_{6b,6a}$ = 12.3, $J_{6b,5}$= 2.2 Hz, 1H, H-6b), 3.70 (ddd, $J_{5,4}$ = 9.9, $J_{5,6a}$=4.7, $J_{5,6b}$=2.2 Hz, 1H, H-5), 2.14 (s, 3H, acetyl), 2.05 (s, 3H, acetyl), 2.03 (s, 3H, acetyl), 2.03 (s, 3H, acetyl). ^{13}C NMR (150 MHz, $CDCl_3$) δ 170.20, 169.80, 168.91, 168.82 (4 CO acetyl), 136.15 (C*ipso*), 128.29 – 127.07 (5C, Ar), 98.80 (C1), 72.37 (C3), 71.37 (C5), 70.82 (C2), 70.27 (*C*H$_2$Ph), 67.96 (C4), 61.48 (C6), 20.3, 20.2,20,13, 20.11 (4 CH3 acetyl). HRMS Calcd for $C_{21}H_{30}NO_{10}$ (M+NH4): 456.1864 Found: 456.1866, Calcd for $C_{21}H_{26}NaO_{10}$ (M+Na): 461.1418 Found: 461.1432, Calcd for $C_{21}H_{26}KO_{10}$ (M+K): 477.1158 Found: 477.1160.

Benzyl *β*-D-glucopyranoside (36)

Compound **35** (2.3 g, 5.25 mmol) catalytic amount of 1M NaOMe (0.3 mL) and methanol (7 mL) were stirred at room temperature for 1.5 h. The mixture was then acidified with Amberlite IR-120H ion exchange resin to pH = 7. The reaction mixture was filtered and concentrated. The crude product was purified via flash chromatography (MeOH/DCM 0-20%) to give a white solid (1.2 g, 84%).

Benzyl 6-*O*-*p*-toluene-sulfonyl-β-D-glucopyranoside (33)

p-TsCl (2 g, 10.5 mmol) was added to compound **36** (0.95 g, 3.5 mmol) in pyridine (28.5 mL) under N_2. The mixture stirred at room temperature for 1.5 h. Pyridine was removed under vacuum. The residue was dissolved in ethyl acetate (100 mL), extracted with H_2O (50 mL) and the organic phase was dried over anhydrous sodium sulfate and concentrated. The crude product was purified using column chromatography (MeOH/DCM 0-10%) to give a white foam (0.89 g, 60%). ^{1}H NMR (600 MHz, MeOD): δ 7.83 (d, J = 8.3 Hz, 2H, Ar), 7.68 – 7.08 (m, 7H, Ar), 4.77 (d, $J_{a,b}$ = 11.8 Hz, 1H, CH_2Ph), 4.57 (d, $J_{b,a}$ = 11.8 Hz, 1H, CH_2Ph), 4.39 (dd, $J_{6a,6b}$ = 10.8 Hz, $J_{6a,5}$=1.8 Hz, 1H, H-6a), 4.29 (d, $J_{1,2}$ = 7.8 Hz, 1H, H-1), 4.20 (dd, $J_{6b,6a}$ = 10.8 Hz, $J_{6b,5}$=6.2 Hz, 1H, H-6b), 3.42 (ddd, $J_{5,4}$ = 9.7 Hz, $J_{5,6b}$=6.2 Hz, $J_{5,6a}$= 1.8 Hz, 1H, H-5), 3.30 (t, J = 9.1 Hz, 1H, H-3), 3.27 – 3.22 (m, 1H, H-4), 3.20 (dd, $J_{2,3}$ = 9.1 Hz, $J_{2,1}$= 7.8 Hz, 1H, H-2), 2.42 (s, 3H, CH_3). ^{13}C NMR (150 MHz, MeOD) δ 144.57, 136.97, 132.56, 129.13, 129.11, 127.43, 127.40, 127.31, 127.27, 127.20, 127.15, 126.85 (12C, Ar), 101.15 (C1), 75.96 (C3), 73.13 (C5), 73.00 (C2), 69.78 (*C*H_2Ph), 69.30 (C4), 68.96 (C6), 19.66 (CH_3). HRMS Calcd for $C_{20}H_{28}NO_8S$ (M+NH_4): 442.1530 Found: 442.1529, Calcd for $C_{20}H_{24}NaO_8S$ (M+Na): 447.1084 Found: 446.1087, Calcd for $C_{20}H_{24}KO_8S$ (M+K): 463.0823 Found: 463.0820.

First attempted synthesis of compound 22

The tosylate **33** (101 mg, 0.238 mmol) and the thioether **24** (120 mg, 0.286 mmol) were dissolved in HFIP (1.5 mL), containing anhydrous K_2CO_3 (5 mg). The mixture was stirred in a sealed reaction vessel in an oil bath at 70 °C for 4 days. The mixture was cooled, then diluted with EtOAc, and evaporated. The crude product was purified using column chromatography (MeOH/DCM 0-10%) to give a syrupy residue (5 mg, 3%).

1,2,3,4-Tetra-*O*-acetyl-α/β-D-glucopyranose (40)

Anhydrous D-glucose (12.0 g, 67 mmol) and triphenylmethyl chloride (19.3 g 69 mmol) were dissolved in anhydrous pyridine (50 mL) by warming in a 80 ^{o}C water bath over 1.5 h. Acetic anhydride (30 mL) was poured in one portion into the pyridine solution without cooling. The solution was allowed to cool to room temperature and kept at that temperature for an additional 12 h. The above mixture was then introduced into the mixture of ice water (950 mL) and acetic acid (50 mL) while rapidly swirling the container. After 2 h of stirring the precipitate was isolated by filtration. To remove residual pyridine, the gummy filter cake was immediately introduced into fresh ice water (1 L) and the mixture was stirred for an additional 10 min. The resulting white precipitate was isolated by filtration and subsequently washed with copious amounts of fresh water. The above tritylated compound (20.5 g, 34.6 mmol) was dissolved in glacial acetic acid (97 mL) by warming on a water bath. The solution was cooled to 10 °C, then a glacial acetic acid solution of hydrogen bromide (33%, 7.5 mL) was added and the mixture was shaken for 45 s. The liberated triphenylmethyl bromide was immediately removed by suction filtration, and the filtrate was poured into ice water (150 mL) and was extracted with chloroform (4 × 110 mL). The extract was washed with cold water (4 × 50 mL) to remove residual acetic acid and then dried over anhydrous sodium sulfate. The solvent was evaporated. Anhydrous diethyl ether (50 mL) was introduced onto the syrupy residue and the compound recrystalized from ether to give a white solid (9.5 g).^{1}H NMR (For major isomer) (500 MHz, $CDCl_3$): δ 5.73 (d, J = 8.3 Hz, 1H, H-1), 5.36 – 5.24 (m, 1H, H-3), 5.16 – 4.97 (m, 2H, H-2, H-4), 3.78 – 3.68 (m, 1H, H-6b), 3.65 (ddd, J = 10.0, 4.0, 2.2 Hz, 1H, H-5), 3.60 – 3.49 (m, 1H, H-6a), 2.09 (s, 3H, acetyl), 2.05 (s, 3H, acetyl), 2.01 (s, 3H, acetyl), 2.00 (s, 3H, acetyl). ^{13}C NMR (For major isomer) (126 MHz, $CDCl_3$) δ 170.28, 170.09, 169.26, 169.05 (4 *C*O acetyl), 91.72 (C1), 74.90 (C5), 72.61 (C3), 70.40 (C2), 68.17 (C4), 60.83 (C6), 20.82, 20.64, 20.61, 20.57 (4 *C*H_3 acetyl).

1, 2,3,4-tetra-*O*-acetyl-6-*O*-trifluoromethanesulfonyl- α/β -D-glucopyranoside (37)

Under N_2 atmosphere, to a solution of 2,6-lutidine (3.25 mL, 28.2 mmol) in dry dichloromethane (150 mL) was added trifluoromethanesulfonic anhydride (Tf_2O, 4.73 mL, 28.2 mmol) at –20 °C. After 5 min, a solution of compound **40** (6.5 g, 18.7 mmol) in dry dichloromethane (150 mL) was added dropwise to the solution at –20 °C. The resulting

mixture was stirred at –20 °C for 5 min, and then at 0 °C for another 30 min. The mixture was poured into ice-cooled water and extracted with dichloromethane. The extract was condensed under reduced pressure to give a pale yellow oil. After column chromatography (EtOAc/Hex 0-100%), compound **37** was obtained as colorless oil (5.4 g, 60%). ^{1}H NMR (For β isomer) (500 MHz, $CDCl_3$) δ 5.77 (d, $J_{1,2}$ = 8.2 Hz, 1H, H-1), 5.33-5.28 (m, 1H, H-3), 5.20 – 5.08 (m, 2H, H-2, H-4), 4.55 (m, 2H, H-6a, H-6b), 4.02 – 3.95 (m, 1H, H-5), 2.15 (s, 3H, COCH_3), 2.10 (s, 3H, COCH_3), 2.07 (s, 3H, COCH_3), 2.05 (s, 3H, COCH_3). ^{1}H NMR (For α isomer) (500 MHz, $CDCl_3$) δ 6.39 (d, $J_{1,2}$ = 3.7 Hz, 1H, H-1), 5.59 – 5.46 (m, 1H, H-3), 5.25 – 5.04 (m, 2H, H-2, H-4,), 4.62 – 4.47 (m, 2H, H-6a, H-6b), 4.27 – 4.22 (m, 1H, H-5), 2.22 (s, 3H, COCH_3), 2.11 (s, 3H, COCH_3), 2.07 (s, 3H, COCH_3), 2.05 (s, 3H, COCH_3). HRMS Calcd for $C_{15}H_{23}F_3NO_{12}S$ (M+NH_4): 498.0888 Found: 498.0890, Calcd for $C_{15}H_{19}F_3NaO_{12}S$ (M+Na): 503.0442 Found: 503.0448, Calcd for $C_{15}H_{19}F_3KO_{12}S$ (M+K): 519.0181 Found: 519.0183.

(2*S*) 1,3,4-Tri-*O*-benzyl-2-deoxy-2-sulfonium-2-[6-(1,2,3,4-tetra-O-acetyl-6-deoxy-α/β -D-glucopyranose)]-D-arabinitol trifluoromethanesulfonate (41)

Under N_2 atmosphere, to a solution of compound **37** (1.06 g, 2.2 mmol) in THF (12 mL) was added a solution of the thioether **24** (1 g, 2.4 mmol) in THF (12 mL) at room temperature. The resulting mixture was then stirred at room temperature for 50 h. After the total consumption of the triflates, the reaction mixture was condensed under reduced pressure to give a pale yellow oil, which on column chromatography (MeOH/DCM 0-10%) gave the desired product as a white syrup (0.8 g, 48%). ^{1}H NMR (600 MHz, $CDCl_3$) δ 7.44-7.18 (m, 15H, Ar), 5.05 (broad signal, 1H, H-2), 5.04 (d, $J_{1',2'}$=8.28 Hz, 1H, H-1'), 4.95-4.88 (m, 2H, H-2',H-3'), 4.83 (d, J=11.34 Hz, 1H, Ph-CH_2), 4.81-4.77 (m, 2H, H-4 and H-4'), 4.75 (d, J=11.58, 1H, Ph-CH_2), 4.72 (broad s, 1H, H-3), 4.69 (d, J= 11.52, 1H, Ph-CH_2), 4.61 (d, J=10.86, 1H, Ph-CH_2), 4.57 (d, J=11.04, 1H,, Ph-CH_2), 4.54 (d, J=11.28, 1H,, Ph-CH_2), 4.12 (d, J=13.02, 1H, H-6b'), 3.93-3.79 (m, 3H, H-5', H-5a, H-5b), 3.54-3.37 (m, 3H, H-1a, H-1b, H-6a'), 2.11 (s, 3H, COCH_3), 2.06 (s, 3H, COCH_3), 2.01 (s, 3H, COCH_3), 1.98 (s, 3H, COCH_3). ^{13}C NMR (150 MHz, $CDCl_3$) δ 170.58, 169.85, 169.13, 168.86 (4×CO), 137.04, 136.85, 136.63 (3× ipso Ar-C), 128.99-128.39 (15×Ar-C), 123.89, 121.77, 119.65, 117.54 (CF3), 91.64 (C1'), 82.04 (C2), 78.49 (C3), 74.74, 74.19, 73.93 (3×Ph-CH_2), 71.91 (C3'), 70.08 (C4'), 69.87 (C2'), 69.77 (C5'), 66.28 (C5), 64.33 (C4),

46.32 (C6'), 40.73 (C1), 20.83, 20.68, 20.62, 20.58 (4×CO*C*H_3). HRMS Calcd for $C_{40}H_{47}O_{12}S$ (M): 751.2783 Found: 751.2802.

(2*S*) 2-deoxy-2-sulfonium-2-[(2S,3S,4R,5S)-2,3,4,5,6-pentahydroxyhexyl]-D-arabinitol Chloride (22)

Route A: A solution of compound **41** (30 mg, 0.04 mmol) in 4N aq HCl (1 mL) and THF (0.5 mL) was stirred at 50 °C for 4h and then the solvents were evaporated. The compound was dissolved in DCM (2.5 mL), the mixture was cooled to -78 ^{o}C and boron trichloride (1M in CH_2Cl_2, 0.4 mL) was added under N_2. The reaction mixture was stirred at the same temperature for 45 min and then quenched by addition of methanol (2 mL), solvents were removed and the residue was co-evaporated with methanol (2 x 2 mL). The residue was then washed with DCM to give a colorless oil which was treated with Amberlyst A—26 resin (50 mg) in methanol (2 mL) at room temperature for 3h. The resins were filtered and washed with methanol. The filtrate and the washings were combined and condensed to give a colorless oil which was then directly treated with sodium borohydride (7 mg, 0.18 mmol) in H_2O (1 mL) at 0 ^{o}C for 3h. The mixture was acidified to pH<4 by dropewise addition of 2M HCl. The compound was partitioned between H_2O and DCM. Water layer was concentrated to give the crude compound **22** as a white solid (5 mg).

Route B: A solution of compound **41** (650 mg, 0.86 mmol) in 4N aq HCl (15 mL) and THF (10 mL) was stirred at 50 °C for 4h and then the solvents were evaporated. Palladium hydroxide (20% weight on carbon,1.5 g) was added to the solution of the sulfonium salt in 85% AcOH/H_2O (40 mL) and the mixture was stirred under 100 psi H_2 for 24h. The catalyst was removed by filtration through a bed of Celite and then washed with water. Solvents were removed, the residue was then dissolved in H_2O (150 mL) and washed with DCM (2 × 75 mL). Amberlyst A—26 resin (1.9 g) was added and the reaction mixture stirred at room temperature for 3h and then filtered through cotton and concentrated. The crude product was dissolved in H_2O (100 mL) and the solution was stirred at room temperature while sodium borohydride (130 mg, 3.4 mmol) was added. Stirring was continued for 3h and the mixture was acidified to pH < 4 by dropewise addition of 2 M HCl. The solvent was evaporated and the residue was co-evaporated with MeOH (5 × 100 mL) to give the crude compound **22** as a white solid (130 mg).

The crude product was washed with EtOAc and then analytical sample (15 mg) was purified via flash chromatography (ACN/ H_2O 60%). The compound was then passed through P-2 gel column for desalting to get 3 mg of white foam for the inhibition studies against UGM. Compound **22** was assigned to have a trans relationship between C-5 and C-1' on the basis of a H-1'/ H-4 correlation in the NOSEY spectrum. ^{1}H NMR (600 MHz, D_2O): δ 4.89 – 4.83 (m, 1H,H-2), 4.68 (dd, J = 7.6, 4.2 Hz, 1H, H-3), 4.37 – 4.31 (m, 1H, H-4), 4.28 (ddd, J = 10.3, 7.4, 3.0 Hz, 1H, H-2'), 4.23 (dd, $J_{5a,5b}$ = 12.3 Hz, $J_{5a,4}$= 5.0 Hz, 1H, H-5a), 4.07 (dd, $J_{5b,5a}$ = 12.3 Hz, $J_{5b,4}$= 9.6 Hz, 1H, H-5b), 3.86 (dd, J = 6.1, 3.2 Hz, 1H, H-1'a), 3.85 – 3.82 (m, 2H, H-5', H-4'), 3.78 (dd, J = 13.3, 6.7 Hz, 1H, H-1b), 3.75–3.71 (m, 3H, H-1'b, H-6'a, H-3'), 3.69 – 3.65 (m, 1H, H-1a), 3.65 – 3.61 (m, 1H, H-6'b).^{13}C NMR (150 MHz, D_2O) δ 73.61 (C2), 73.33 (C3'), 72.81 (C3), 72.77 (C5'), 69.38 (C4'), 67.37 (C2'), 66.19 (C4), 62.31 (C6'), 58.01 (C5), 48.78 (C1'), 41.33 (C1). HRMS Calcd for $C_{11}H_{23}O_8S$ (M): 315.1108 Found: 315.1112.

D-Ribonolactone (42)

A mixture of D-ribose (30 g, 201 mmol), sodium bicarbonate (33.6 g, 390 mmol) and water (180 mL) was stirred at room temperature for 15 min. The flask was then immersed in an ice-water bath. Bromine (33.6 g, 210 mmol) was added to the vigorously stirred aqueous solution at a rate of about 2 drops/sec. When the addition was complete, the resulting orange solution was stirred for an additional 50 min. Sodium bisulfite (1.95 g, 18.8 mmol) was added in order to completely discharge the orange color. The clear aqueous solution was evaporated until a wet slurry remained. EtOH (120 mL) and toluene (30 mL) were added to give a cloudy suspension and the solvent was removed to provide a damp solid. Absolute EtOH (120 mL) was added and the mixture was heated in a water bath (70 ^{o}C) for 30 min. The hot ethanolic suspension was filtered and the solids were rinsed with hot absolute EtOH (30 mL). The filtrate was cooled to room temperature, and then refrigerated for 16 h. The crystalline product was filtered, rinsed first with cold absolute EtOH (30 mL) then with Ether (30 mL), and dried under vacuum to give the crude D-ribonolactone as a white solid (28.6 g). The crude product was used in the next step without purification.

2,5-Di-*O*-tosyl-ribonolactone (43)

To a solution of compound **42** (3 g, 0.02 mol) in dry pyridine (15 mL) at 0 ^{o}C was added TsCl (8.88 g, 0.047 mol) dissolved in acetone (15 mL) over a period of 10 min. The reaction mixture was then stirred at 0 ^{o}C for 5 h after which it was neutralized with 6 M HCl until pH 1. The compound was extracted using EtOAc (3×15 mL), dried over anhydrous sodium sulfate and concentrated and subjected to column chromatography (EtOAc/Hex 0-100%) to give a white solid (5.4 g).

1-deoxy-4-thio-D-arabino-1,4-lactone (44)

Route A) Ammonium tetrathiomolybdate (58 mg, 0.225 mmol) was added to a solution of benzyl triethylammonium chloride (110 mg, 0.487 mmol) in acetonitrile (1 mL) and the mixture was stirred at room temperature for 1 h. The ditosylate **43** (100 mg, 0.219 mmol) in acetonitrile (1 mL) was added to the resultant red solution and stirred at room temperature for 12h. Ethyl acetate (2 mL) was added and the resultant slurry was filtered through Celite. Acetonitrile (0.5 mL) was added to dissolve partly the remaining black residue in the flask followed by ethyl acetate (4 mL) and the resultant slurry was filtered through the same Celite bed. Extracts were concentrated to dryness. The residue was then dissolved in ethyl acetate (20 mL) and the solution was washed with H_2O to remove residual benzyl triethylammonium chloride. The crude compound was purified via flash chromatography (EtOAc/Hex 0-100%) to give a white solid (20 mg, 63%).

Route B) The ditosylate **43** (500 mg, 1.1 mmol) was dissolved in acetonitrile (12.5 mL) along with $Na_2S.9H2O$ (264 mg, 1.1 mmol). The reaction mixture was stirred at room temperature for 3h and the solvent evaporated. The residue was dissolved in DCM (75 mL) and washed with water (50 mL). The organic layer was dried over anhydrous sodium sulfate and concentrated. The crude compound was purified via flash chromatography (EtOAc/Hex 0-100%) to give a white solid (130 mg, 81%).

^{1}H NMR (600 MHz, CD_3COCD_3): δ 4.91 (s, 1H, H-2), 4.45 (s, 1H, H-3), 3.42 (s, 1H, H-4), 3.35 (dd, $J_{1b,1a}$ = 11.2 Hz, $J_{1b,2}$= 2.0 Hz, 1H, H-1b), 3.00 (dd, $J_{1a,1b}$ = 11.2 Hz, $J_{1a,2}$=1.2 Hz, 1H, H-1a). ^{13}C NMR (150 MHz, CD_3COCD_3) δ 173.15 (C5), 82.42 (C2), 78.76 (C3), 44.91 (C4), 31.85 (C1). HRMS Calcd for $C_5H_7O_3S$ (M+H): 147.0110 Found: 147.0111, Calcd for $C_5H_6NaO_3S$ (M+Na): 168.9930 Found: 168.9939.

(2*R*) 1,3,4-Tri-*O*-benzyl-2-deoxy-2-sulfonium-2-methyl)-D-arabinitol tetrafluoroborate (45)

A mixture of protected thioarabinitol **24** (34 mg, 0.08 mmol) with methyl iodide (0.006 mL, 0.1 mmol) and silver tetrafluoroborate (19 mg, 0.1 mmol) in acetonitrile (1 mL) stirred at 65 ^{o}C for 1 day and concentrated. The crude product (40 mg) was used in the next step without purification.

(2*R*) 2-deoxy-2-sulfonium-2-methyl)-D-arabinitol chloride (46)

Compound **45** (20 mg, 0.046) was dissolved in DCM (2 mL), the mixture was cooled to -78 ^{o}C and BCl_3 (1M solution in DCM, 0.46 mL) was added under N_2. The reaction mixture was stirred at the same temperature for 30 min and then allowed to warm to 5 ^{o}C for 6 h. The reaction was quenched by addition of methanol (1 mL), solvents were removed and the residue was co-evaporated with methanol (5 x 5 mL). The residue was then treated with Amberlyst A-26 resin (10 mg) in methanol (2 mL) at room temperature for 3h. The resins were filtered and solvent was evaporated to give a colorless syrup (7 mg). Analysis by ^{1}H NMR indicated that compound **46** was a mixture of diastereomers (2.3:1 ratio) at the sulfur centre. The major component of the mixture was assigned to be the diastereomer with a trans relationship between C-methyl and C-5 on the basis of NOE observations. Irradiation of the methyl protons of the major isomer at δ = 2.97 ppm enhanced the H-1, H-2, H-3, H-4 signals whereas Irradiation of the methyl protons of the minor isomer at δ = 3.02 ppm enhanced the H-1b and H-5a signals. Data for major diastereomer (trans): ^{1}H NMR (600 MHz, D_2O): δ 4.88 (ddd, J = 9.9, 7.2, 2.9 Hz, 1H, H-2), 4.67 (d, J = 2.6 Hz, 1H, H-3), 4.27 – 4.17 (m, 2H, H-5a, H-4), 4.07 (dd, J = 11.5, 9.4 Hz, 1H, H-5b), 3.66 – 3.55 (m, 2H, H-1a, H-1b), 3.09 (s, 3H, CH_3S). ^{13}C NMR (150 MHz, D_2O) δ 72.92 (C2), 72.42 (C3), 67.23 (C4), 57.56 (C5), 40.75 (C1), 26.35 (CH_3). Data for minor diastereomer (cis): ^{1}H NMR (600 MHz, D_2O) δ 4.65 – 4.58 (m, 1H, H-2), 4.56 (m, 1H, H-3), 4.34 (dd, J = 11.7, 4.8 Hz, 1H, H-5b), 4.27 – 4.16 (m, 2H, H-4, H-5a), 4.06 – 4.01 (m, 1H, H-1a), 3.33 – 3.24 (m, 1H, H-1b), 3.13 (s, 3H, CH_3S). ^{13}C NMR (150 MHz, D_2O) δ 73.44 (C2), 72.37 (C3), 58.44 (C4), 54.65 (C5), 42.73 (C1), 22.18 (CH_3). HRMS Calcd for $C_6H_{13}O_3S$ (M): 160.0580 Found: 160.0586.

2.5. Conclusion

In summary thiosugars **22** and **46** have been synthesized. NOE experiments revealed that compound **46** was a mixture of diastereomers (2.3:1 ratio) at the sulfur center. The major component of the mixture was assigned to be the diastereomer with a trans relationship between C-methyl and C-5. However, due to the bulky group attached to sulfur, compound **22** was not a mixture of diastereomers and it was assigned to have a trans relationship between C-5 and C-1' on the basis of a NOSEY experiment.. Compound **22** was tested as an inhibitor of UGM and the results are discussed in chapter 4.

2.6. Supporting information

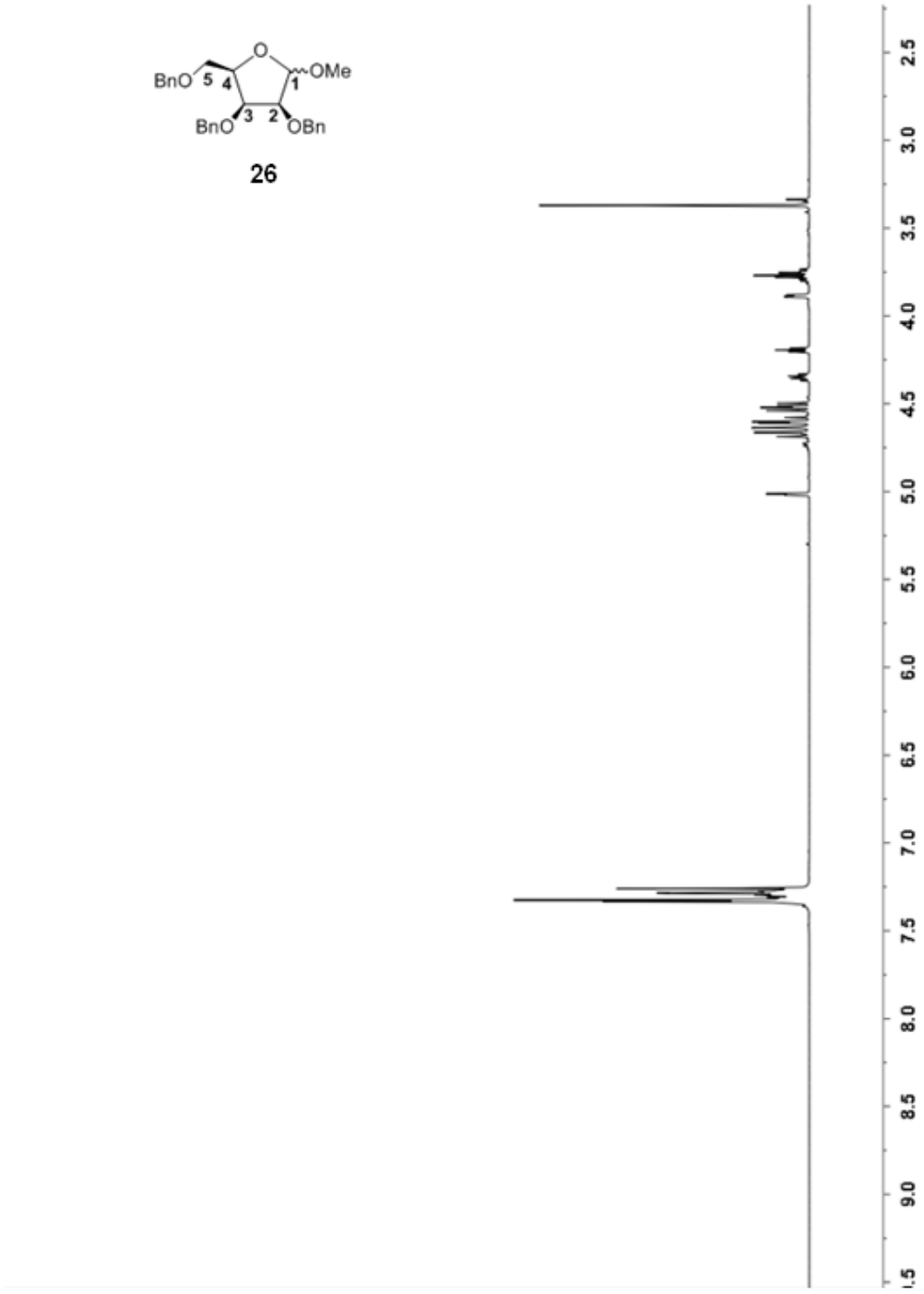

Figure 2-10: ^{1}H NMR of compound 26

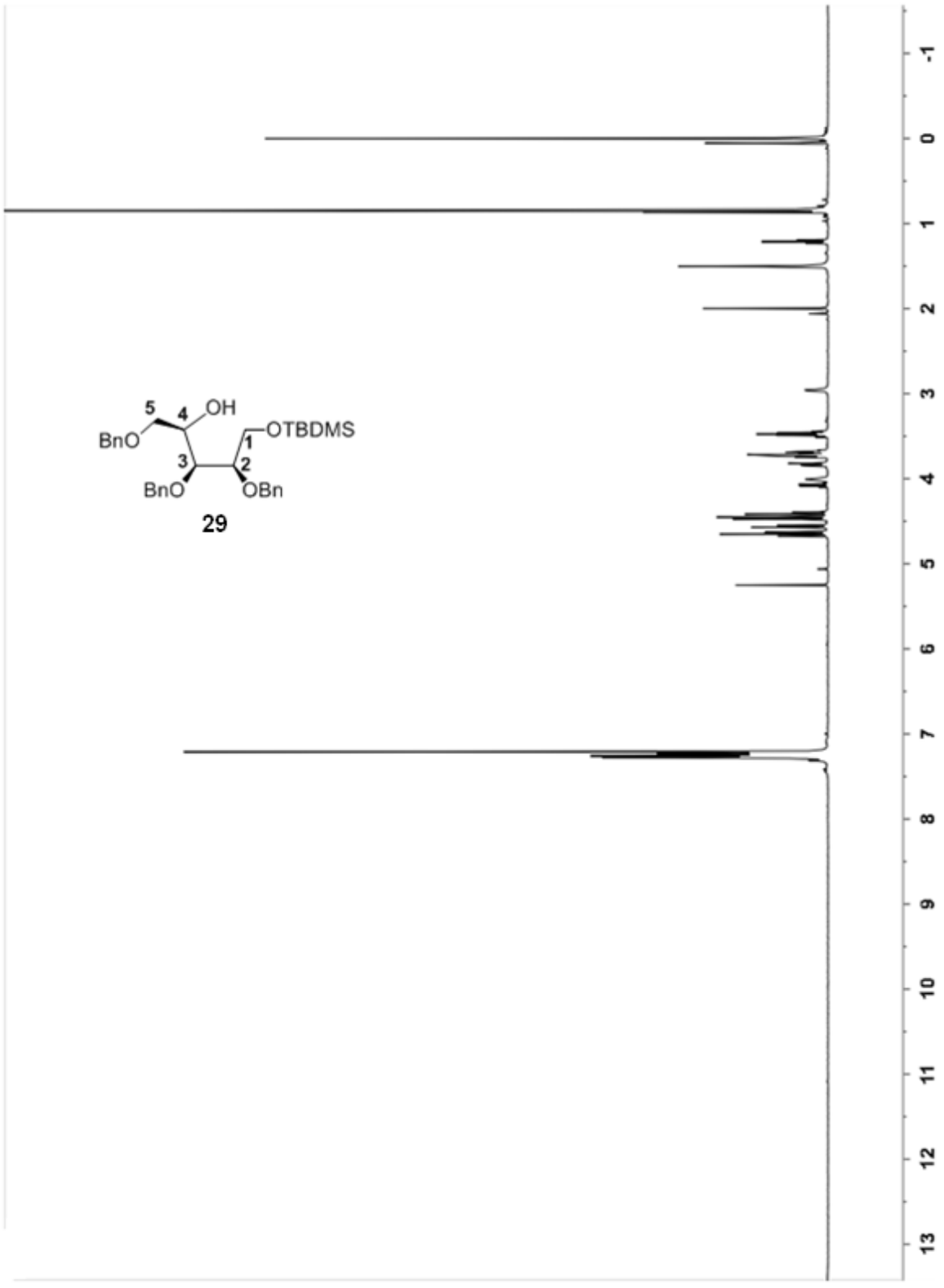

Figure 2-11: ^{1}H NMR of compound 29

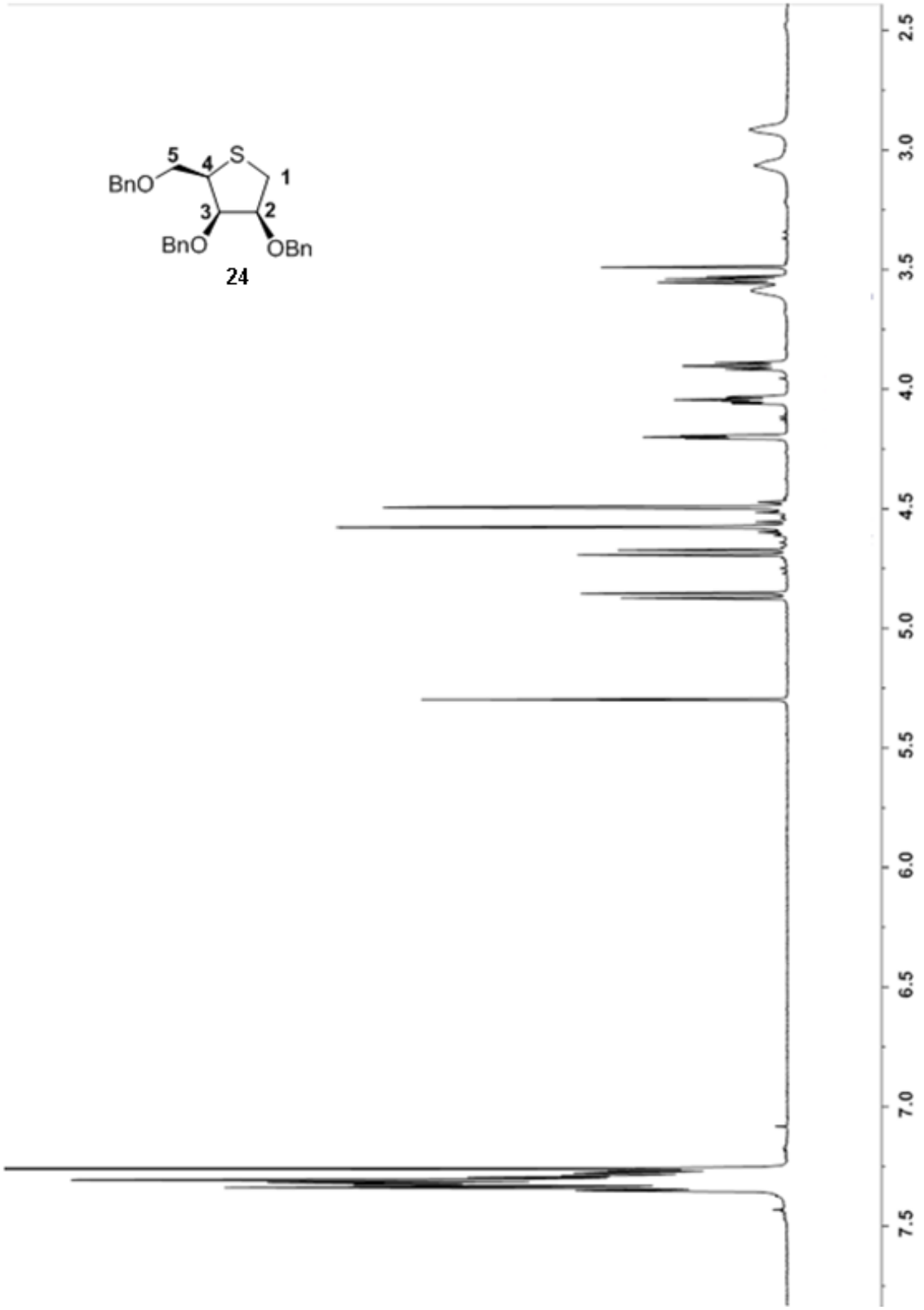

Figure 2-12: ^{1}H NMR of compound 24

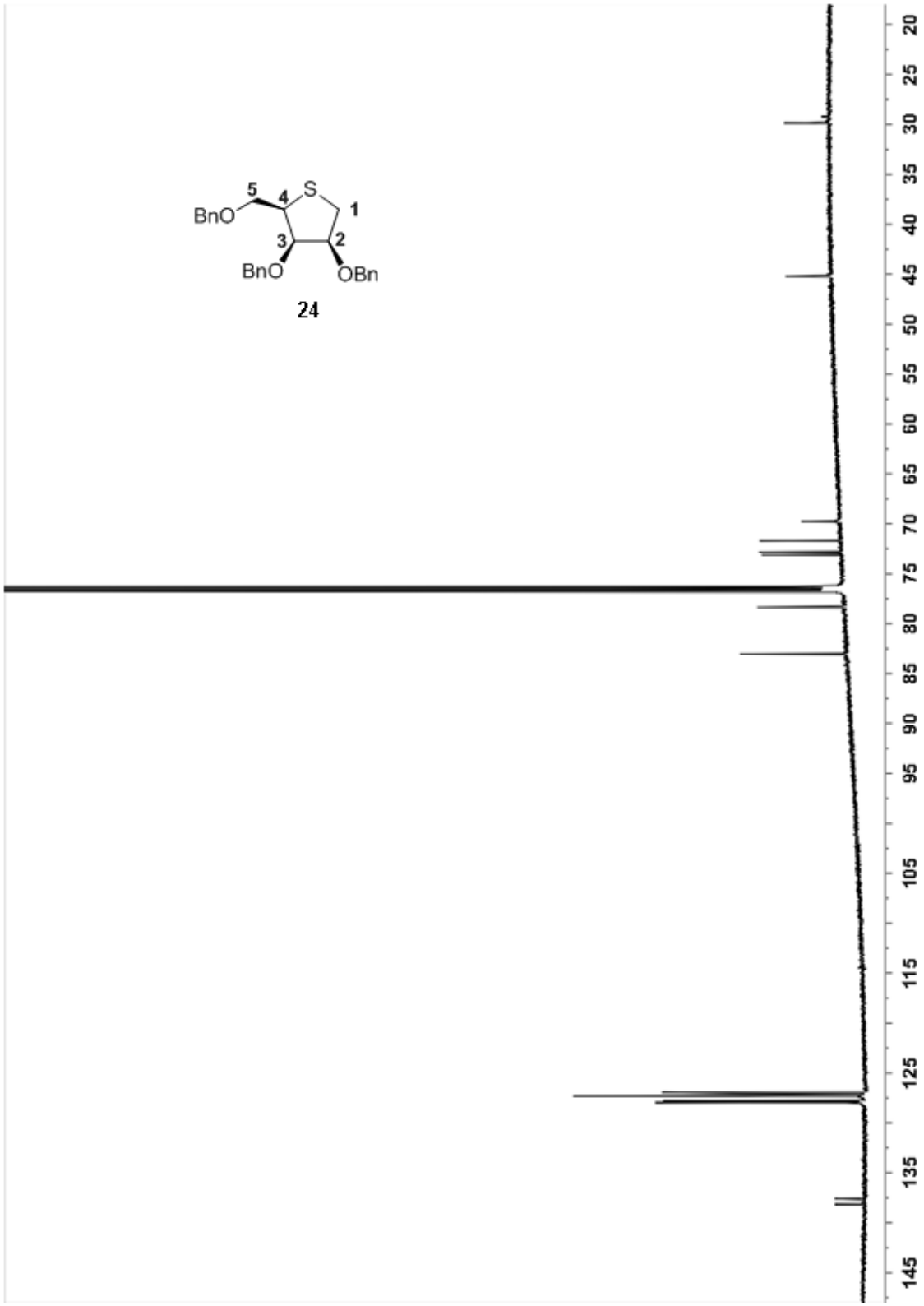

Figure 2-13: ^{13}C NMR of compound 24

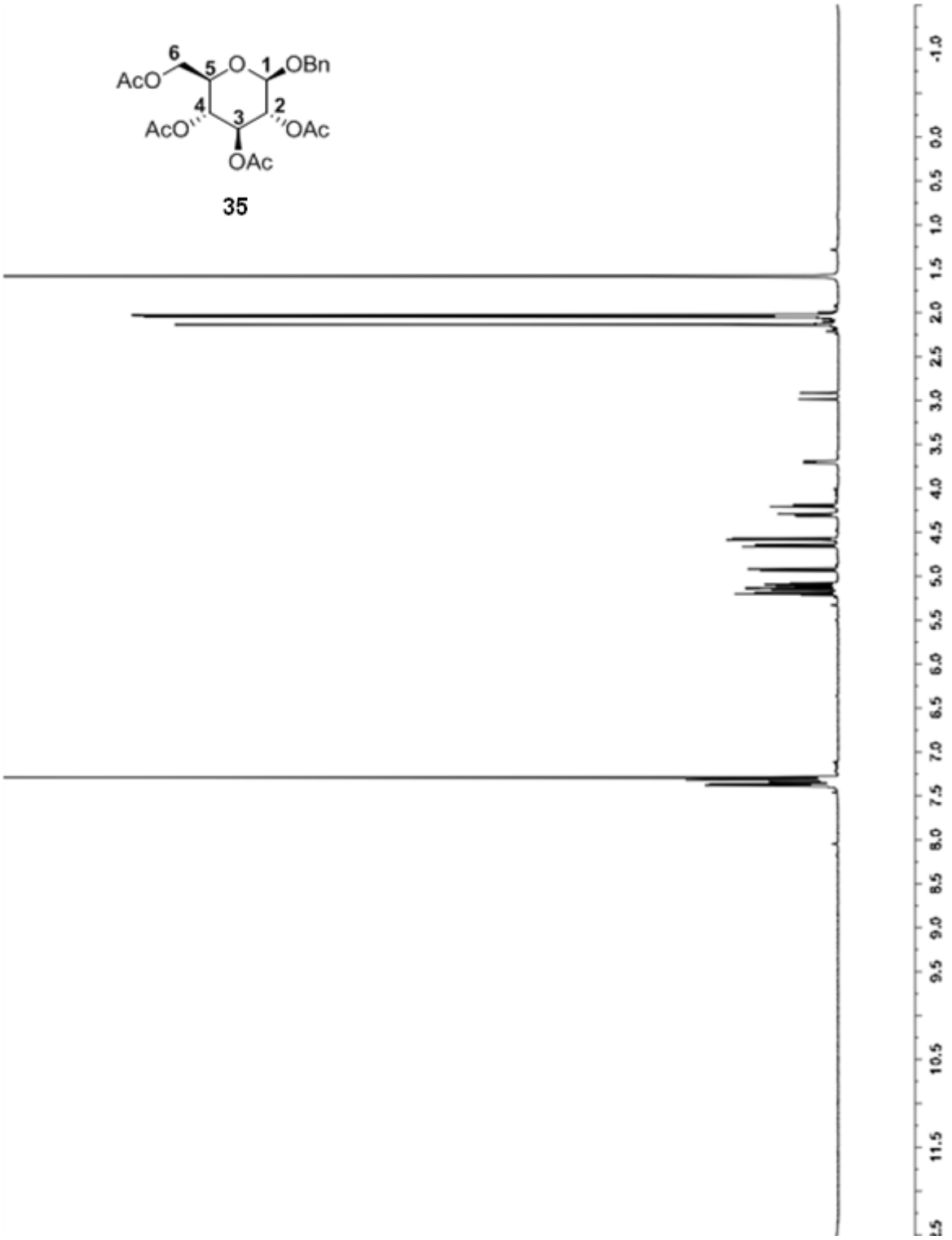

Figure 2-14: ^{1}H NMR of compound 35

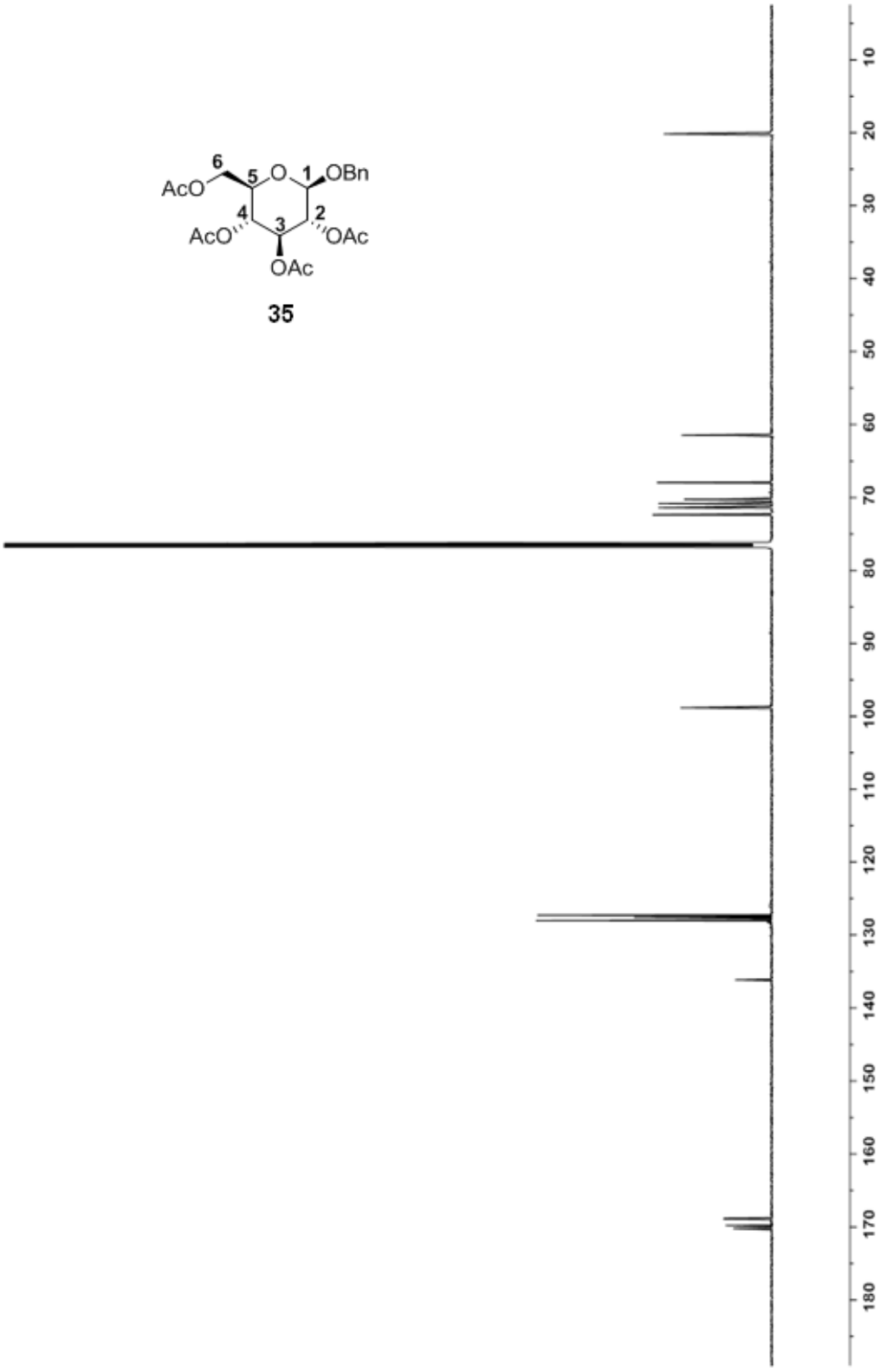

Figure 2-15: ^{13}C NMR of compound 35

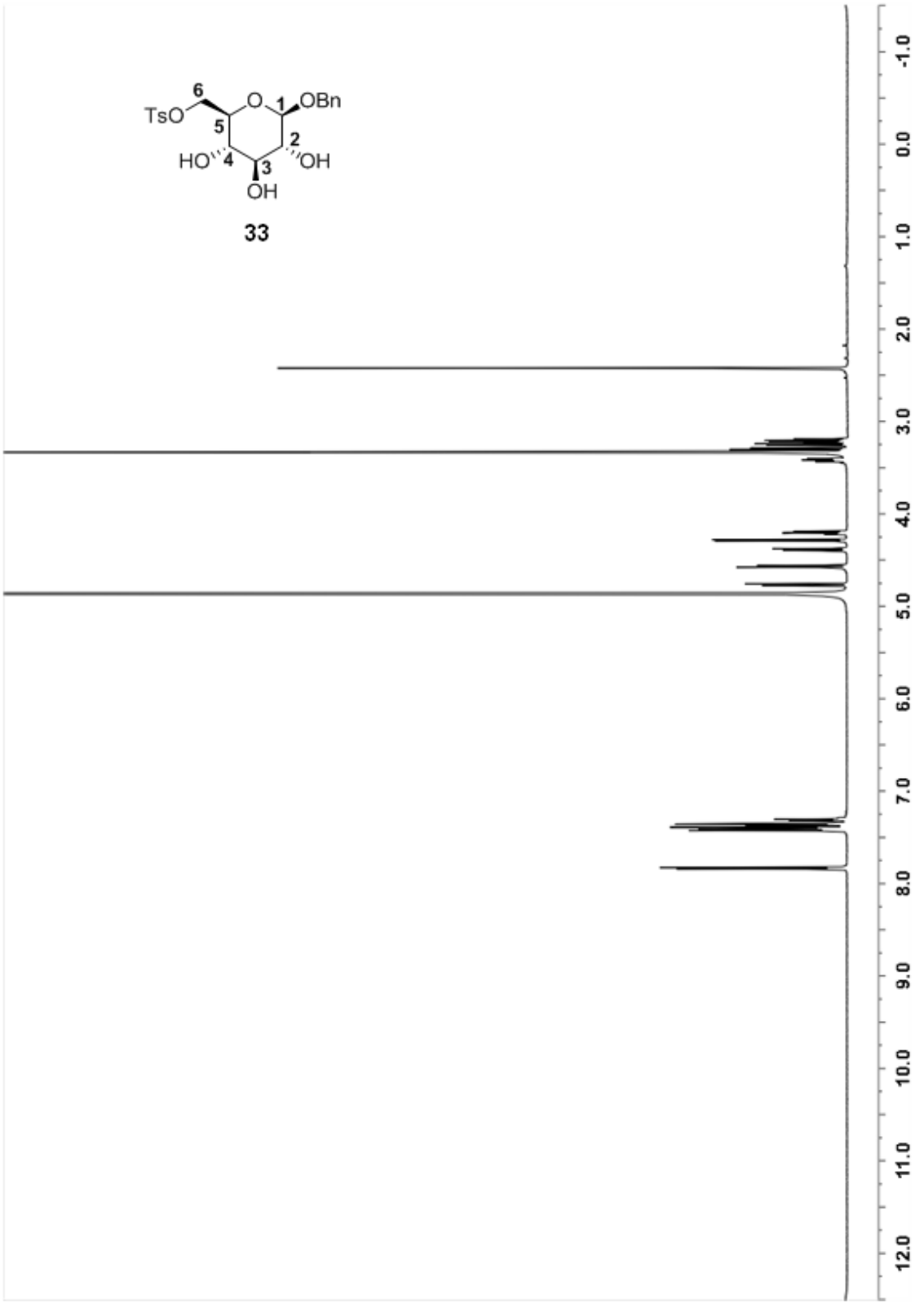

Figure 2-16: ^{1}H NMR of compound 33

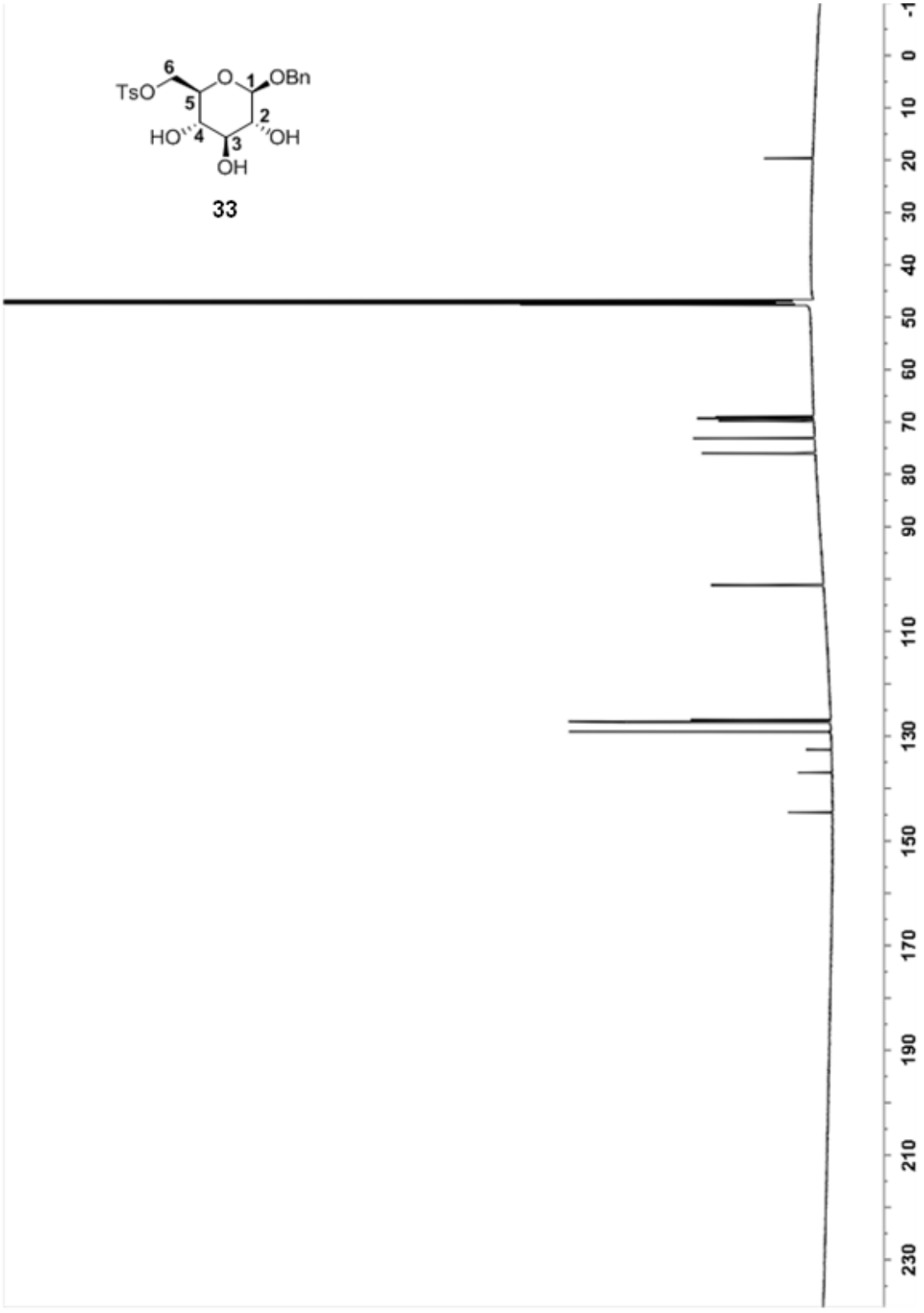

Figure 2-17: ^{13}C NMR of compound 33

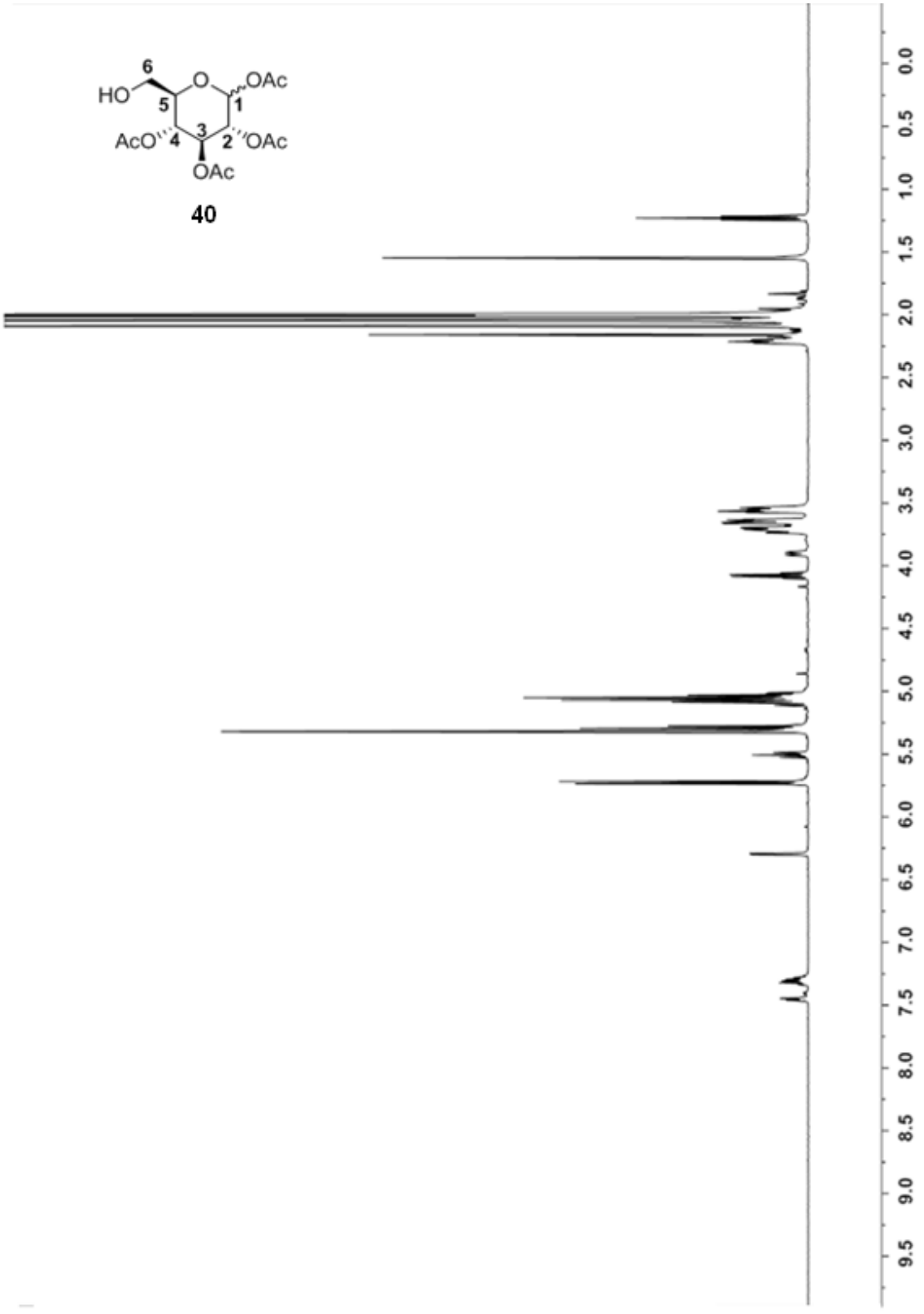

Figure 2-18: ^{1}H NMR of compound 40

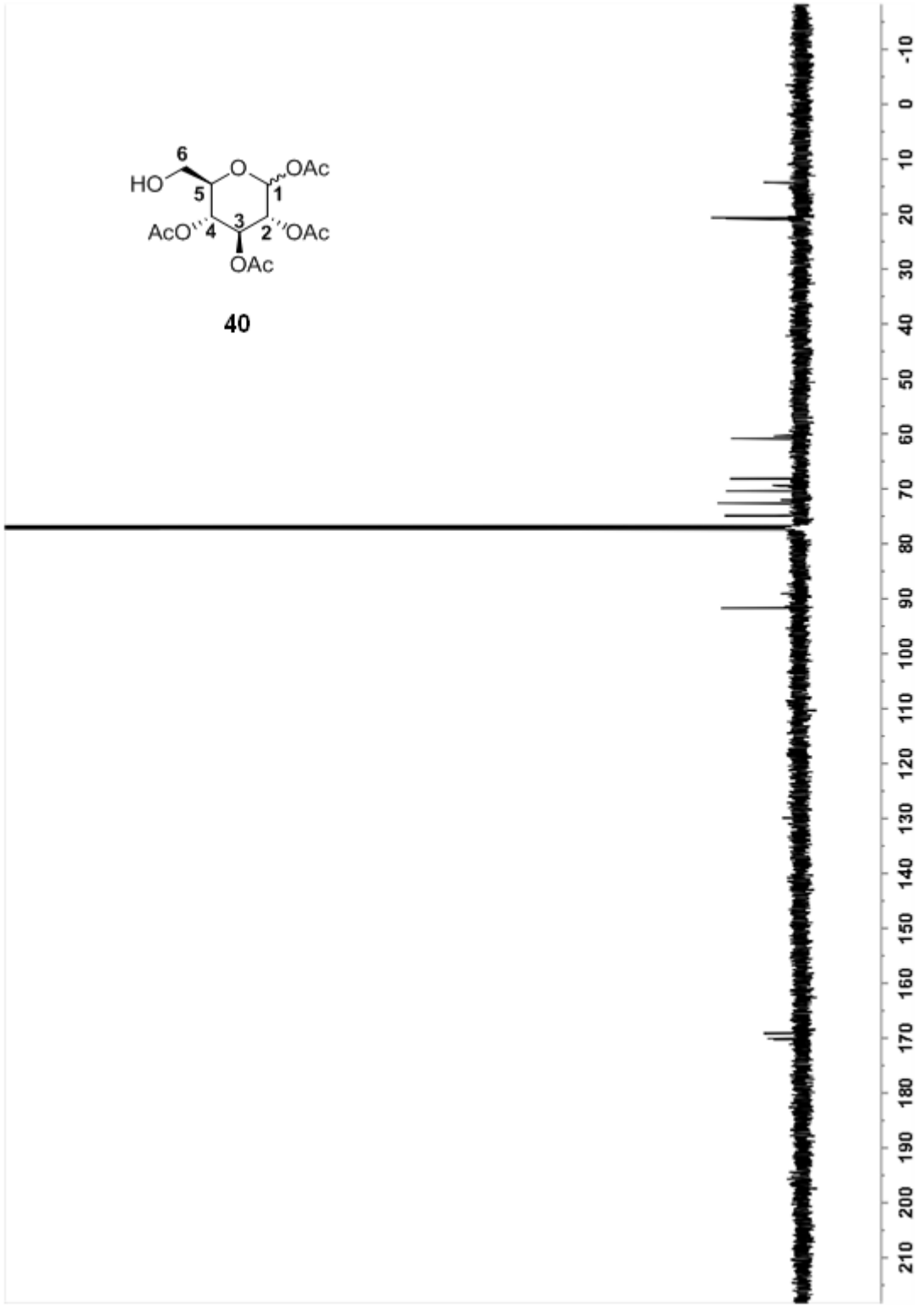

Figure 2-19: ^{13}C NMR of compound 40

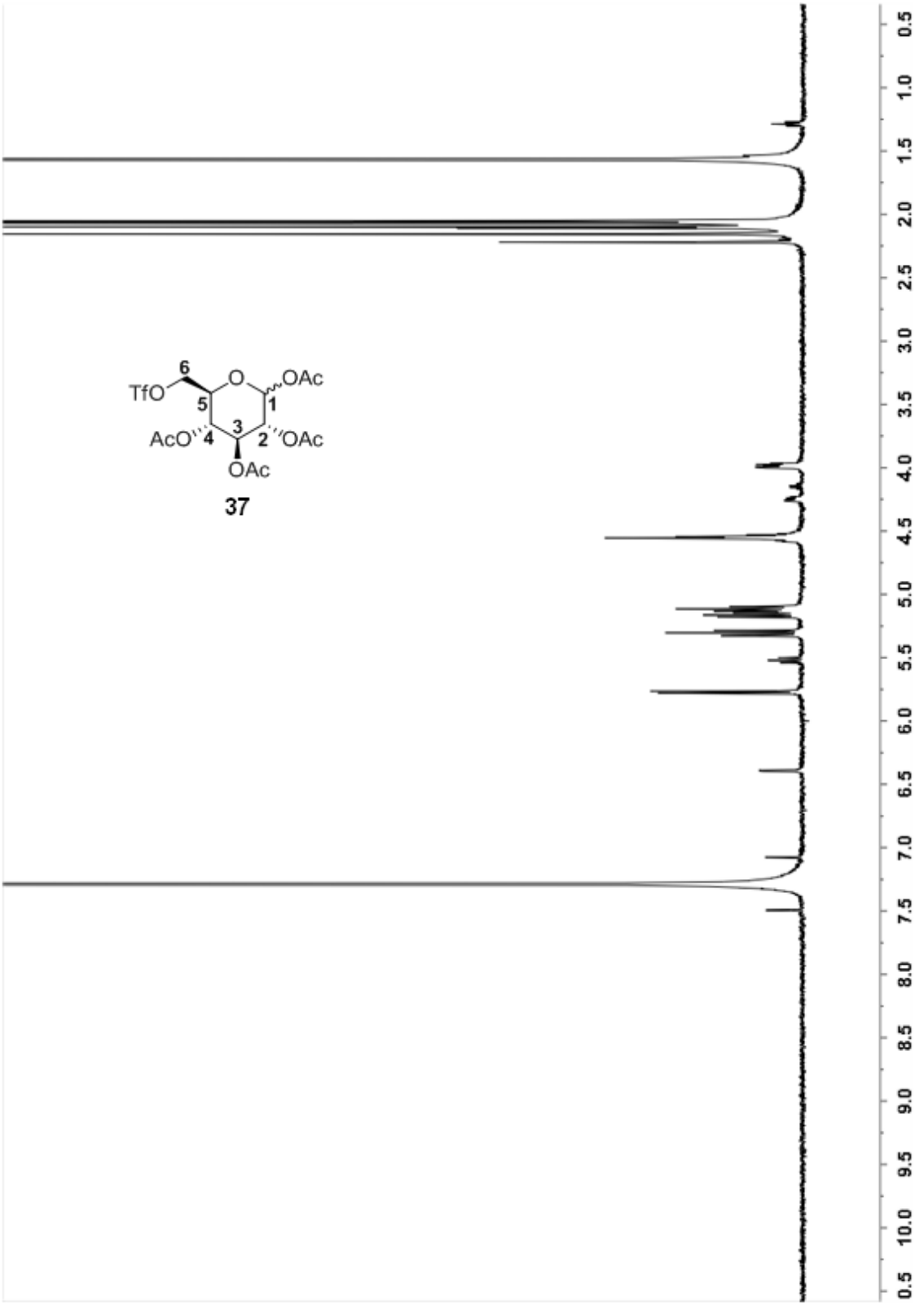

Figure 2-20: ^{1}H NMR of compound 37

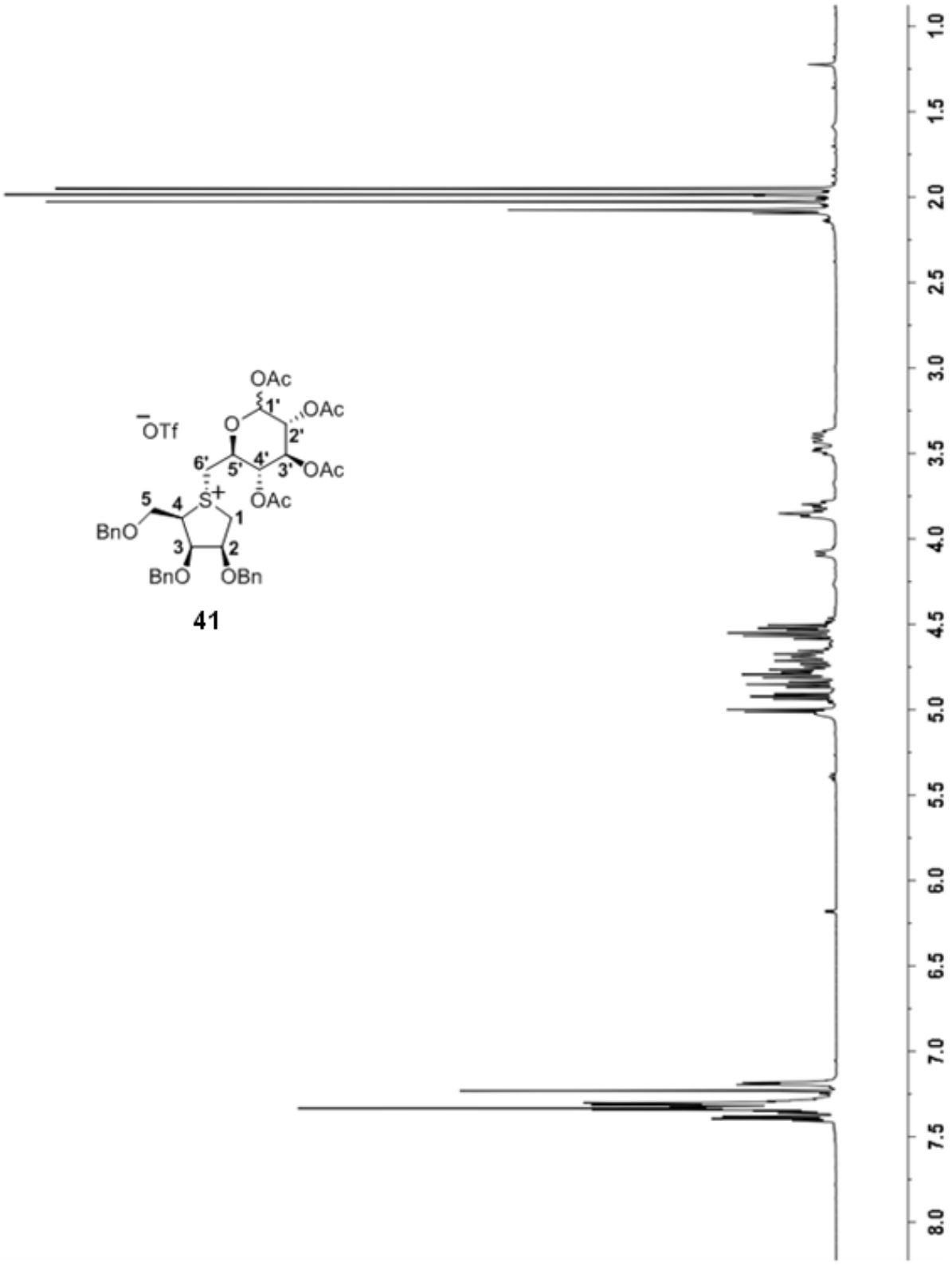

Figure 2-21: ^{1}H NMR of compound 41

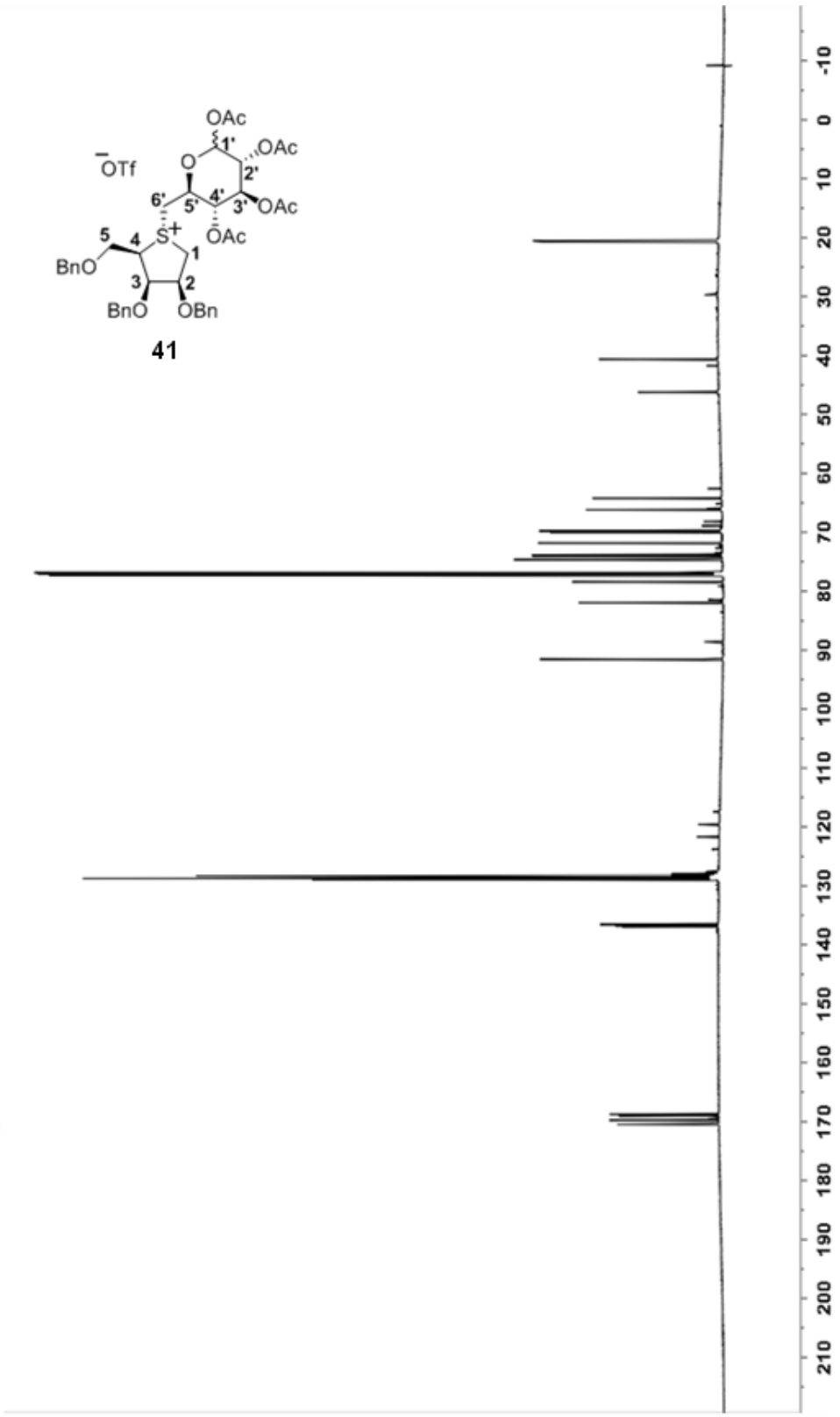

Figure 2-22: ^{13}C NMR of compound 41

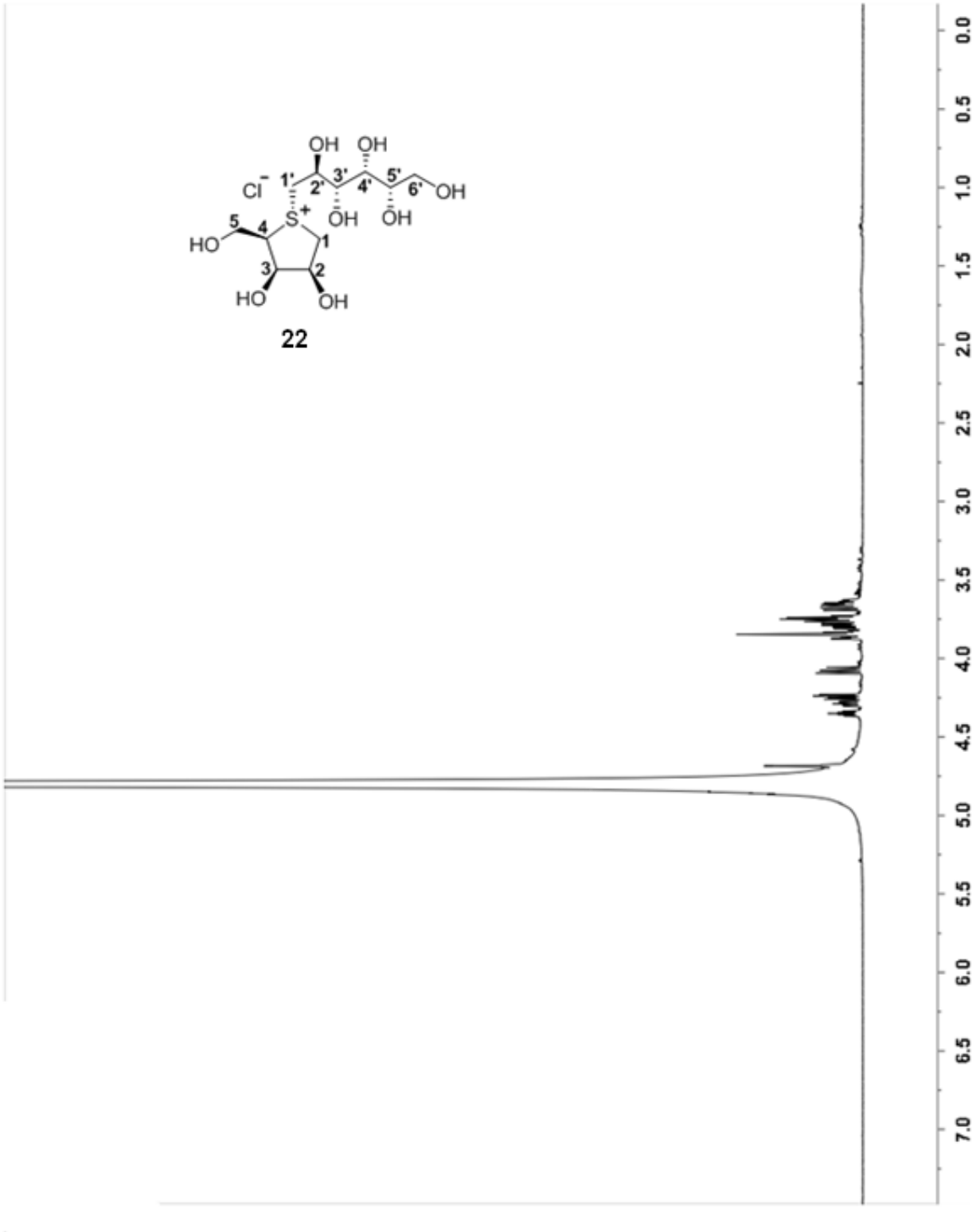

Figure 2-23: ^{1}H NMR of compound 22

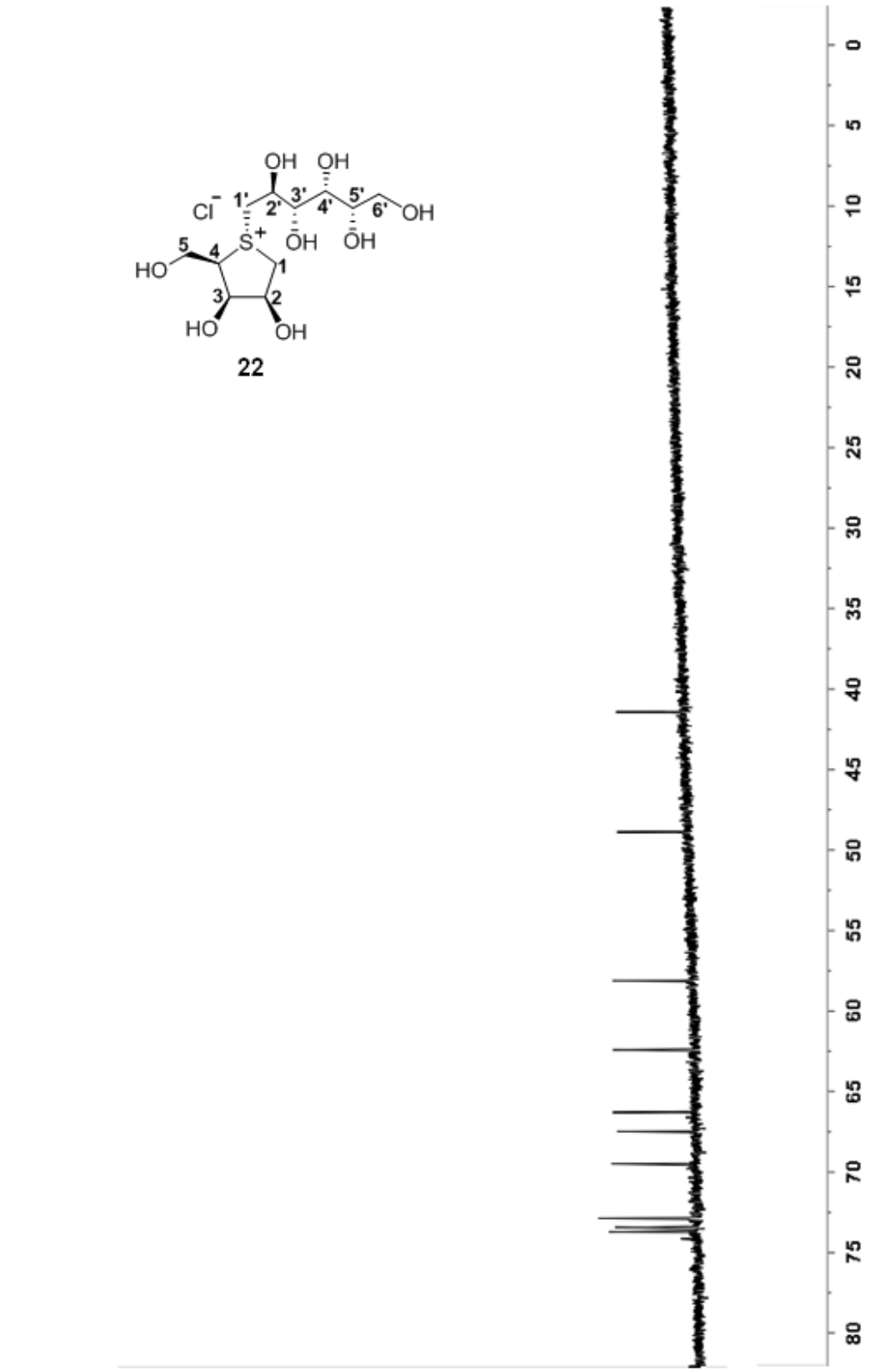

Figure 2-24: ^{13}C NMR of compound 22

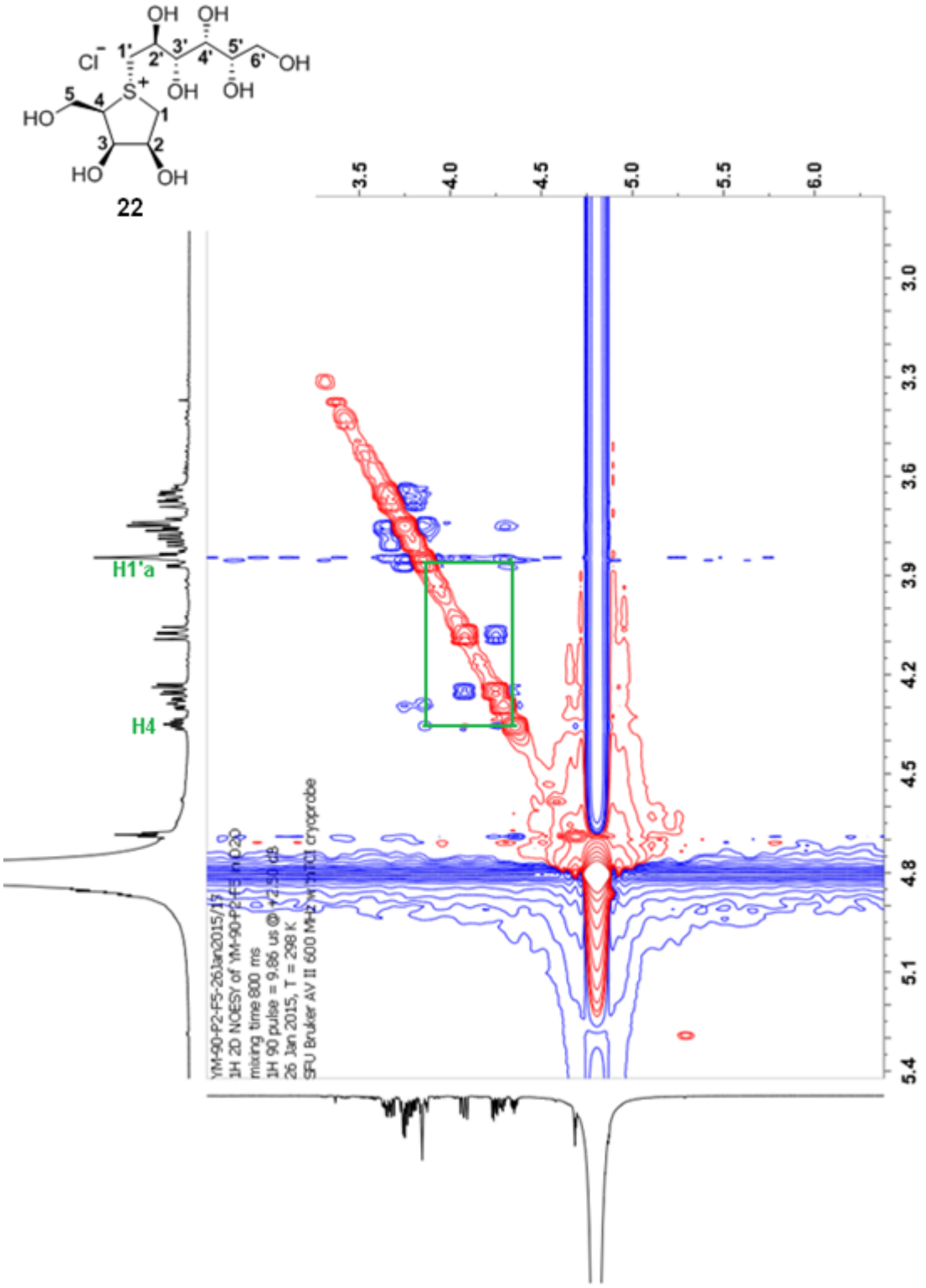

Figure 2-25: ^{1}H 2D NOESY of compound 22

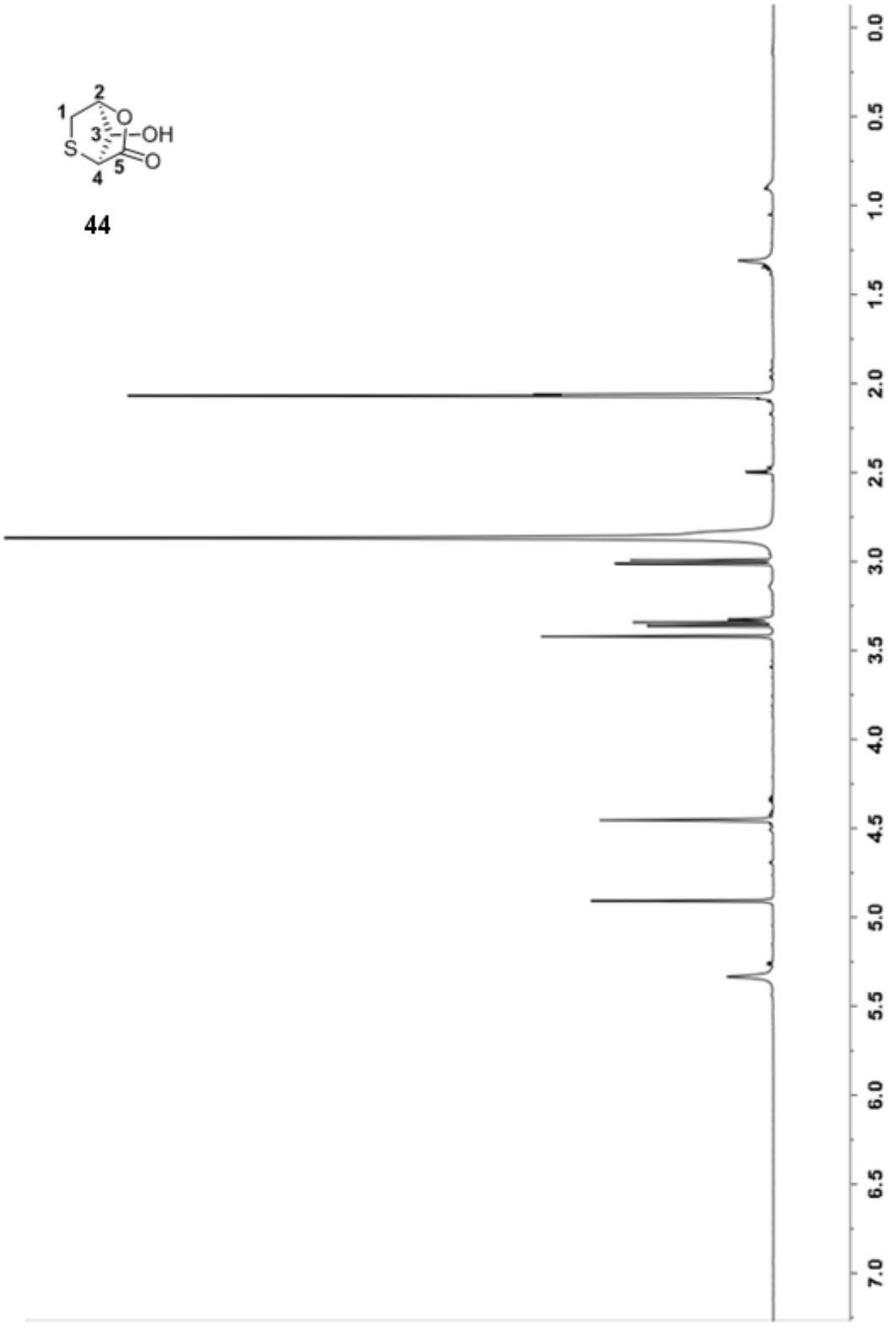

Figure 2-26: ^{1}H NMR of compound 44

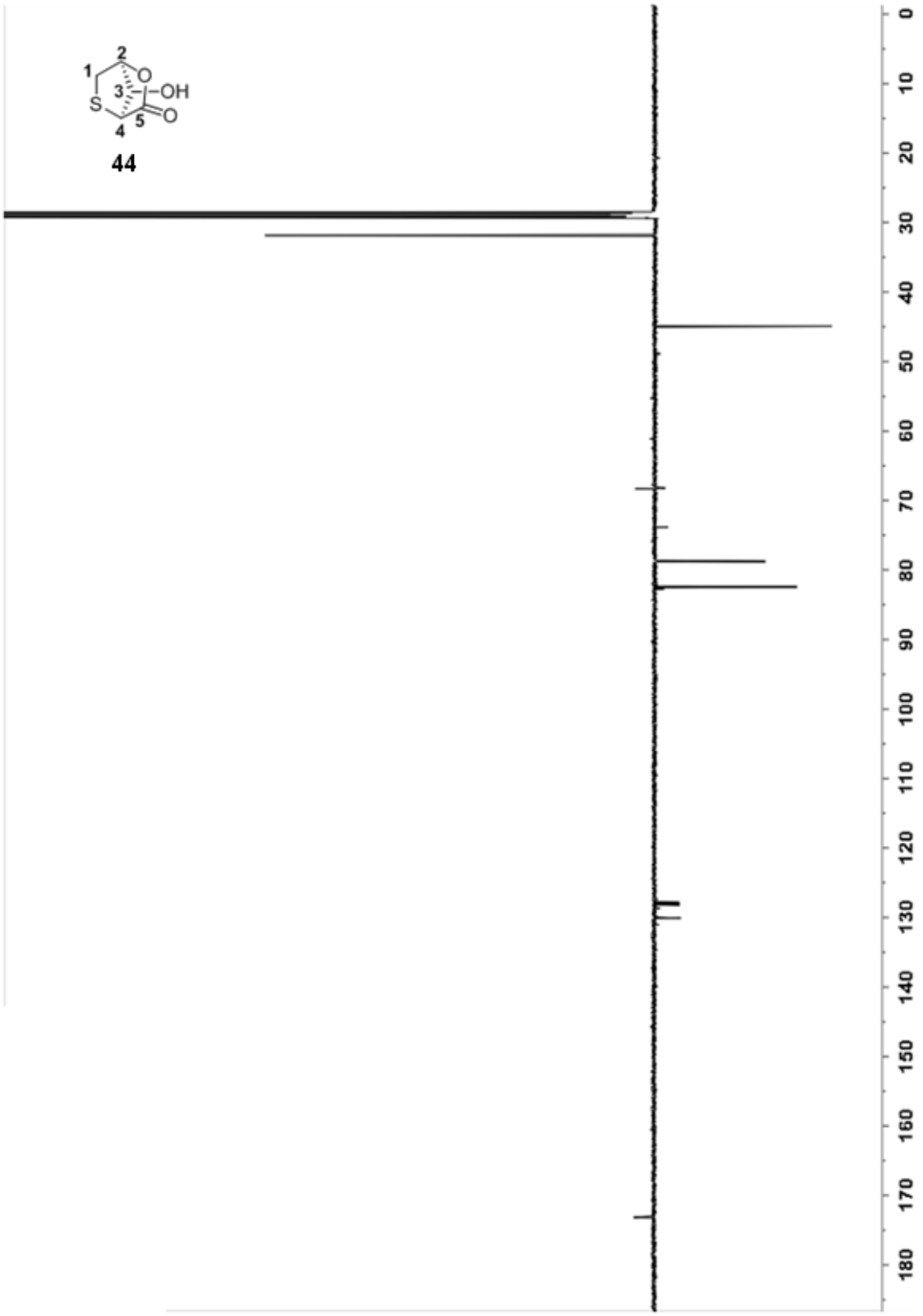

Figure 2-27: ^{13}C NMR of compound 44

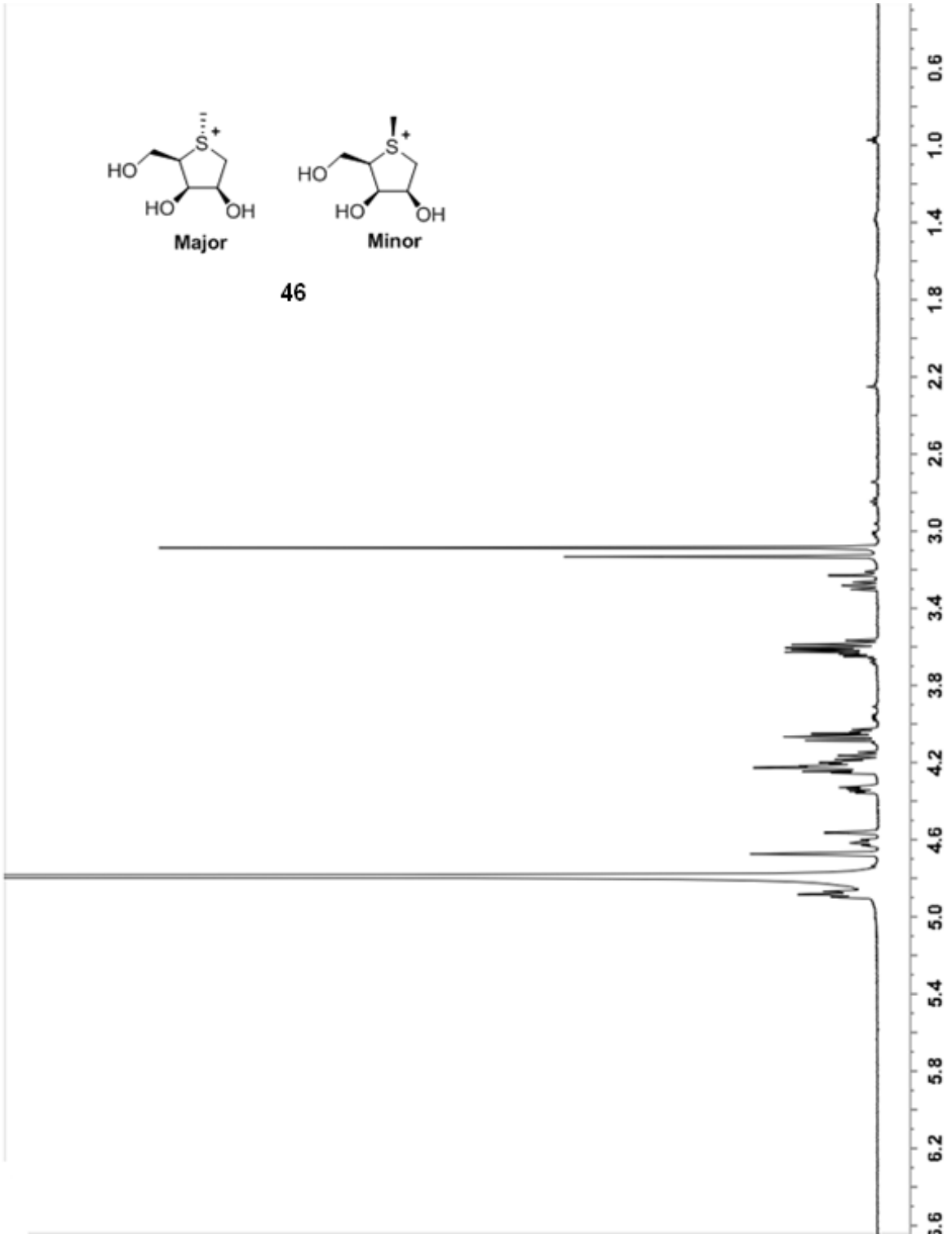

Figure 2-28: ^{1}H NMR of compound 46

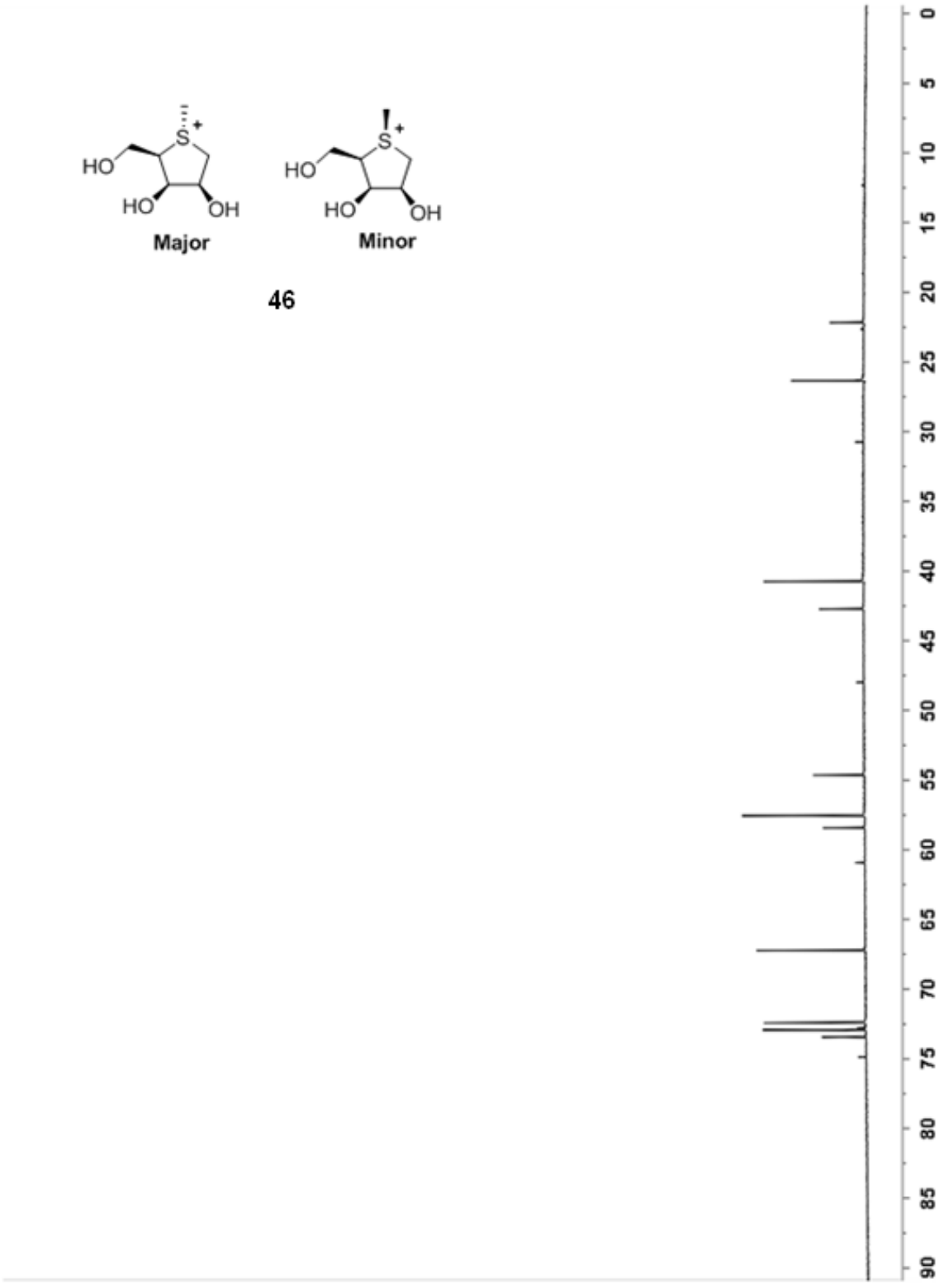

Figure 2-29: ^{13}C NMR of compound 46

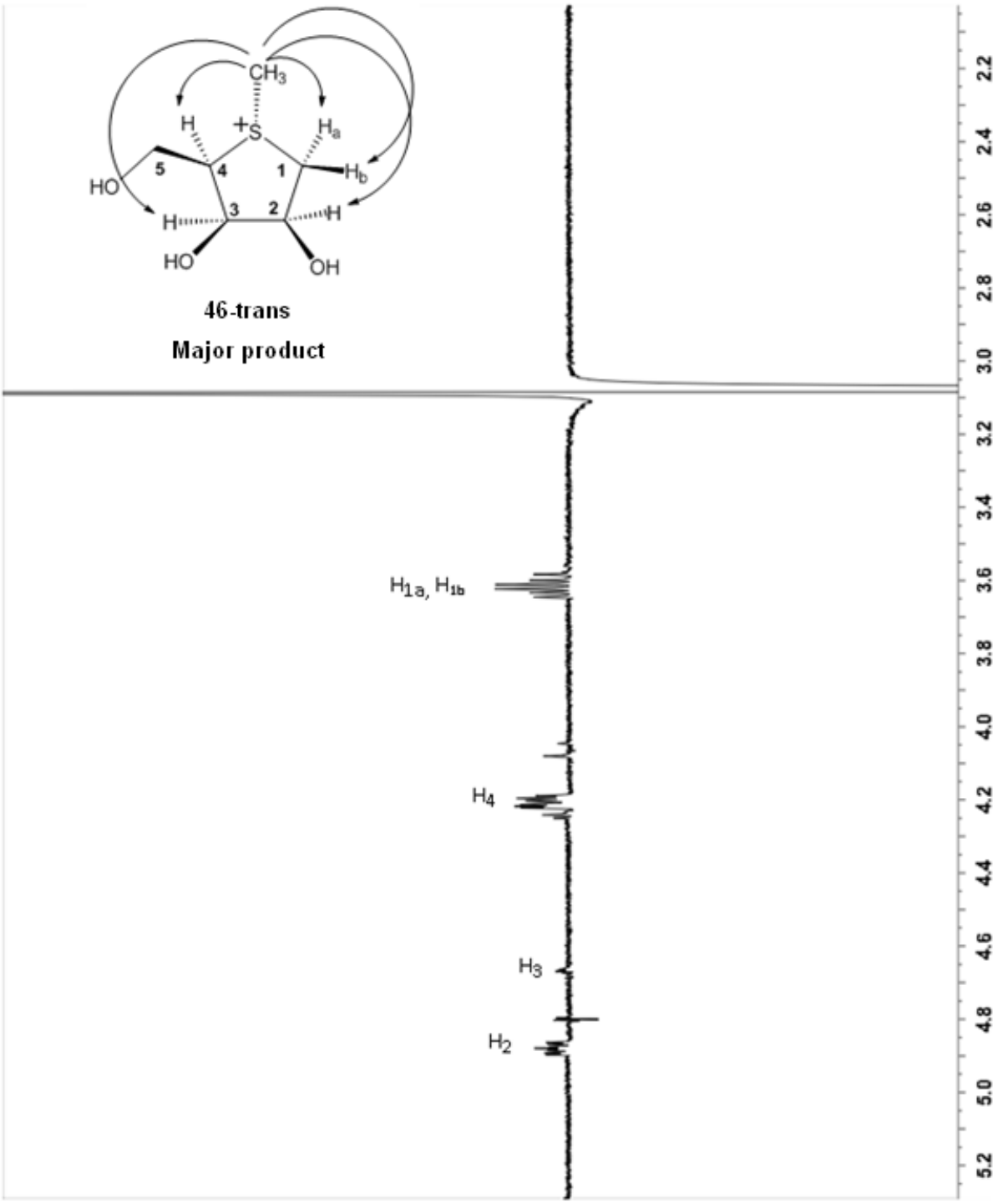

Figure 2-30: NOE spectrum for compound 46 (major product)

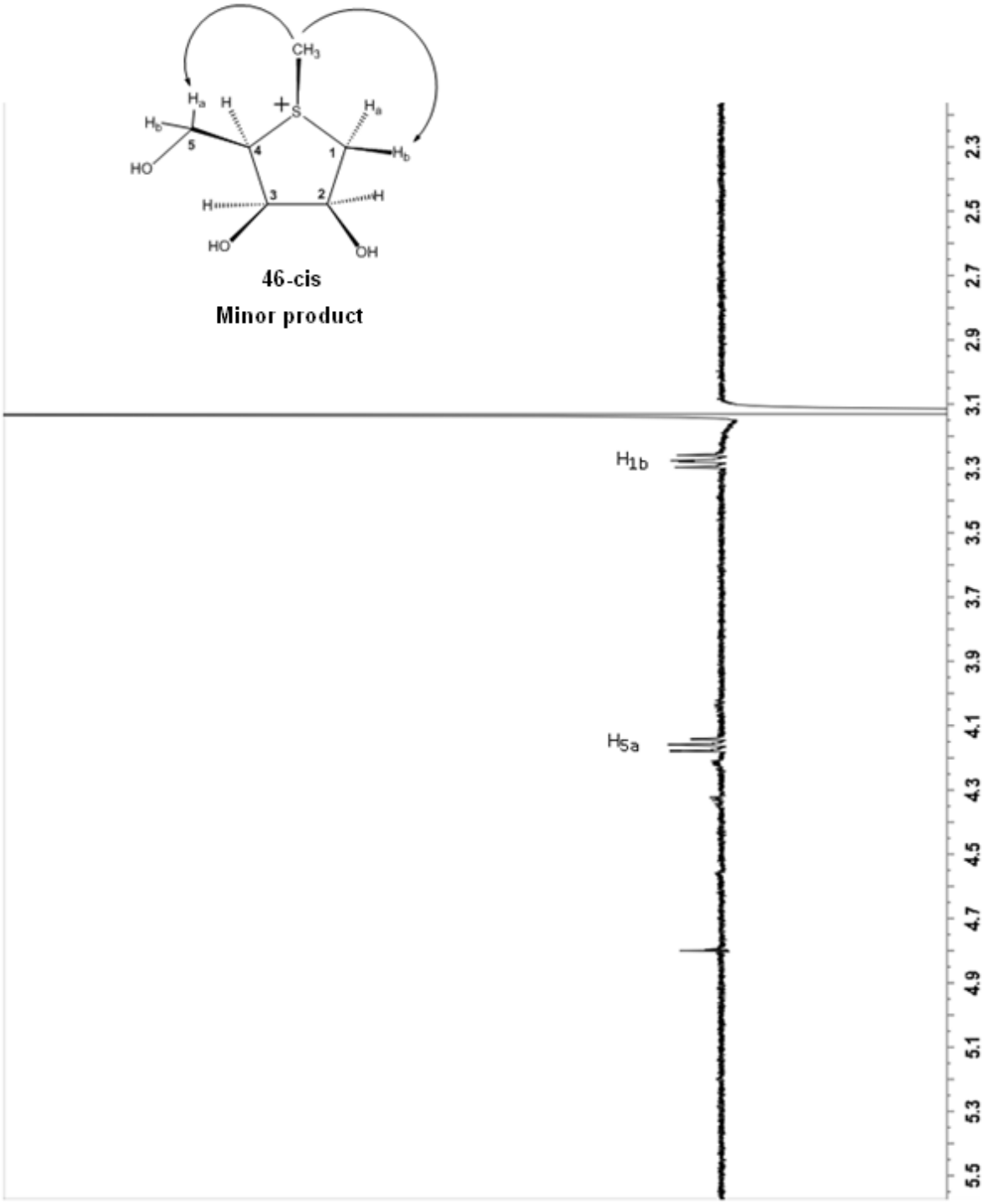

Figure 2-31: NOE spectrum for compound 46 (minor product)

Chapter 3.
Novel Selenonium ion as a potential UGM inhibitor

3.1. Abstract

In this chapter the synthesis of compound **23**, the selenium analogue of compound **22**, as a potential inhibitor of UGM, is described.

3.2. Introduction

Sugars containing heteroatoms like carbon, nitrogen or sulfur in place of the endocyclic oxygen have been studied extensively in the field of synthetic and medicinal chemistry [52], [53], [54]. Selenium belongs with sulfur in group 16 elements and therefore the chemical properties of these two elements are similar; this chemical similarity has led to an interest in studying selenium analogues of sulfur-containing compounds.

Replacement of the ring-sulfur heteroatom by selenium in carbohydrate analogues resulted in compounds with higher or comparable inhibitory activities against various enzymes in several cases. It has been shown that the selenium congener of salacinol, Blintol (Figure 3.1) was a slightly better inhibitor of glucoamylase G2 enzyme in comparison to salacinol. Blintol was also shown to discriminate between certain glycosidase enzymes. Salacinol inhibited barley alpha-amylase (AMY1) and porcine pancreatic alpha-amylase (PPA) with K_i values in μM range but blintol showed no significant inhibition of either AMY1 or PPA. (Table 3-1) [55]. Moreover, salacinol itself is a 4 to 5-fold better inhibitor of C-terminal subunit of sucrose-isomaltase (ctSI) as compared to the N-terminal enzymes and C-terminal subunit of maltase glucoamylase (ctMGAM-N2). Replacement of the ring-sulfur of salacinol by selenium, to make blintol, induces a 10-fold improvement in its inhibition of ctMGAM-N2, while having little effect on the other enzyme units (Table 3-2) [56].

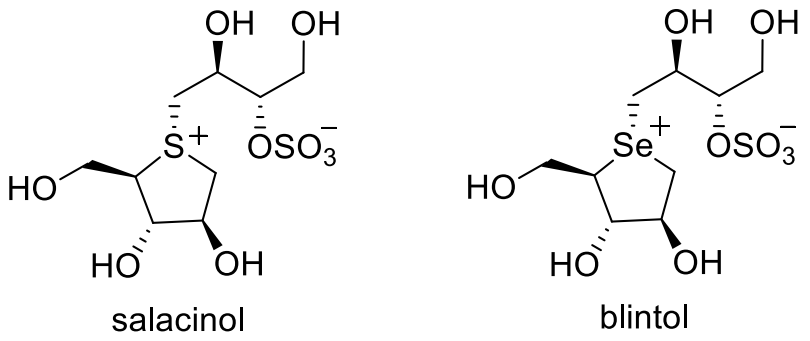

Figure 3-1: Structures of salacinol and its congener blintol

Table 3-1: K_i values for salacinol and blintol with glucoamylase G2, PPA and AMY1 [ref. 55]

	glucoamylase G2	PPA	AMY1
salacinol	1.7 mM	10 ± 2 μM	15 ± 1 μM
blintol	0.72 mM	No inhibition	No inhibition

Table 3-2: K_i values for salacinol and blintol with ntMGAM, ctMGAM, ntSI and ctSI (μM) [ref. 56]

	ctMGAM-N2	ctMGAM-N20	ntMGAM	ctSI	ntSI
salacinol	0.213 ± 0.018	0.058 ± 0.003	0.19 ± 0.02	0.047 ± 0.0077	0.277 ± 0.068
blintol	0.018 ± 0.004	0.013 ± 0.002	0.49 ± 0.05	0.029 ± 0.005	0.16 ± 0.01

Also substitution of ring sulfur atom in glucosidase inhibitors, de-*O*-sulfonated ponkoranol (**47**) and its 5' epimer (**48**), by selenium (Figure 3.2) resulted in an increase in their inhibitory activity against N-terminal and C-terminal subunits of sucrose-isomaltase (ntSI and ctSI) whereas it did not have much effect in the case of N-terminal subunit of maltase glucoamylase (ntMGAM) and C-terminal subunit of maltase glucoamylase (ctMGAM-N20) (Table 3-3) [57].

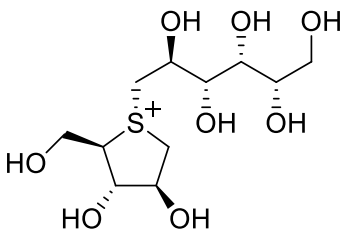

De-*O*-sulfonated ponkoranol
47

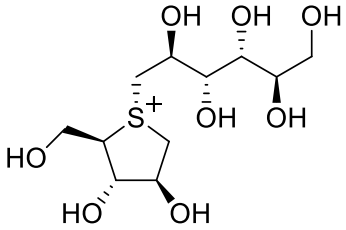

5'-stereoisomer of
de-*O*-sulfonated ponkoranol
48

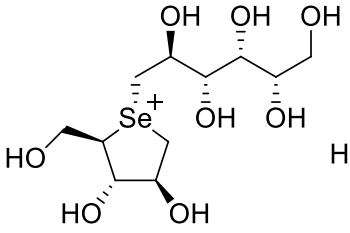

49

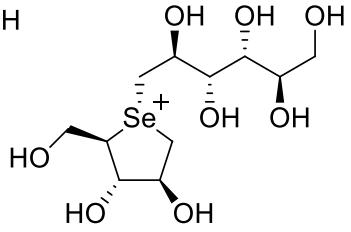

50

Selenium analogues

Figure 3-2: Structures of de-*O*-sulfonated ponkoranol, its 5' epimer and their selenium analogues

Table 3-3: K_i values for inhibitors 47-50 with ntMGAM, ctMGAM, ntSI and ctSI (µM) [ref. 57]

	ctMGAM-N20	ntMGAM	ctSI	ntSI
47	0.096 ± 0.015	0.043 ± 0.001	0.103 ± 0.037	0.302 ± 0.123
48	0.0138 ± 0.068	0.015 ± 0.001	0.132 ± 0.047	0.138 ± 0.012
49	0.047 ± 0.014	0.038 ± 0.008	0.018 ± 0.004	0.013 ± 0.008
50	0.041 ± 0.027	0.025 ± 0.014	0.019 ± 0.010	0.010 ± 0.002

The choice of selenium as a heteroatom in compound **23** was motivated by these encouraging increase in inhibitory activities and selectivities of the selenium compounds against intestinal glucosidases compared to the corresponding sulfur analogues.

3.3. Result and discussion

Compound **23** was synthesized by a pathway similar to the synthesis of compound **22**. The protected seleno D-arabinitol **51** was synthesized by the treatment of dimesylate **32** with selenium metal and sodium borohydride (Scheme 3.1).

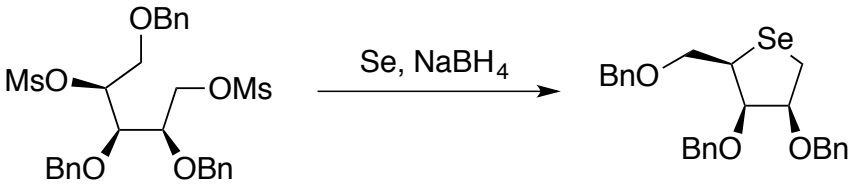

32 **51**

Scheme 3.1: Synthesis of protected seleno D-arabinitol

The coupling reaction between compound **51** and the triflate **37** yielded the selenonium ion **52**. Acetyl and benzyl groups were removed by treatment with 4N aqueous hydrochloric acid at 50 °C and hydrogenolysis, respectively. The product was subsequently treated with Amberlyst A-26 resin (chloride form) to completely exchange the *p*-toluenesulfonate counter ion with chloride ion. Finally, the crude product was reduced with sodium borohydride to provide the desired compound **23** (Scheme 3.2).

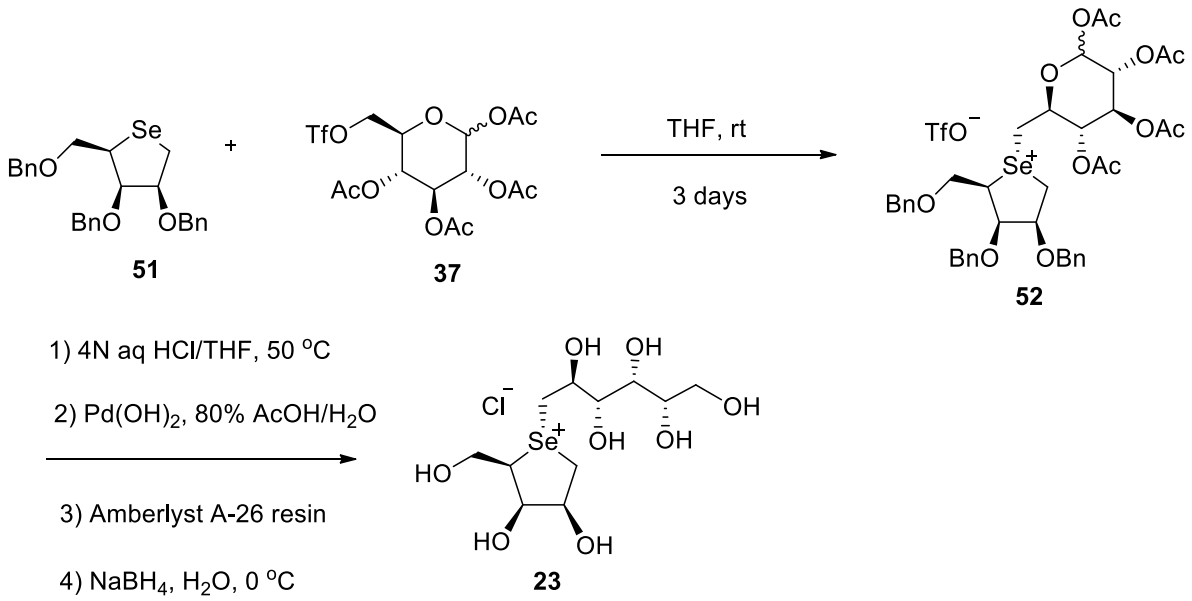

Scheme 3.2: Synthesis of the target compound 23

3.4. Experimental

3.4.1. General methods

Optical rotations were measured at 23 °C. ^{1}H NMR spectra were recorded at 600 MHz. ^{13}C NMR spectra were recorded at 150 MHz. Assignments were confirmed with the aid of attached proton test (^{13}C-APT) and two-dimensional ^{1}H-^{1}H (COSY), ^{1}H-^{13}C (HSQC) and ^{1}H-^{13}C (HMBC) experiments using standard pulse programs. Processing of the spectra was performed with MestReNova software. Analytical thin-layer chromatography (TLC) was performed on aluminum plates pre-coated with silica gel 60F-254 as the adsorbent. The developed plates were air-dried, exposed to UV light and/or sprayed with a solution containing 1% ceric sulfate and 1.5% molybdic acid in 10% aqueous sulfuric acid, and heated. Column chromatography was performed with an automated flash chromatography system. High resolution mass spectra were obtained by the electrospray ionization method, using a TOF LC/MS high resolution magnetic sector mass spectrometer.

3.4.2. Compound synthesis and characterization

2,5-Anhydro-1,3,4-tri-*O*-benzyl-2-deoxy-2-seleno-D-arabinitol (51)

In a round bottom flask, selenium metal (0.57 g, 7.2 mmol) and ethanol (55 mL) were added. Sodium borohydride was then added portionwise at room temperature until the color of the reaction mixture changed from black to white. The dimesylate **32** (2.6 g, 4.5 mmol) dissolved in THF (12 mL) was then added to the reaction and mixture was heated and stirred at 60 ^{o}C for 1 day and concentrated. The crude compound was purified via flash chromatography (EtOAc/Hex 2-10%) to give a yellow oil (1.4 g, 67 %) $[\alpha]_D$= +35 (*c* 0.01, $CHCl_3$). ^{1}H NMR (600 MHz, $CDCl_3$): δ 7.44 – 7.27 (m, 15H, Ar), 4.91 (d, $J_{a,b}$ = 11.8 Hz, 1H, C*H*$_2$Ph), 4.72 (d, $J_{b,a}$ = 11.8 Hz, 1H, C*H*$_2$Ph), 4.62 (d, $J_{a,b}$ = 12.1 Hz, 1H, C*H*$_2$Ph), 4.58 (d, $J_{b,a}$ = 12.1 Hz, 1H, C*H*$_2$Ph), 4.51 (s, 2H, C*H*$_2$Ph), 4.31 (d, $J_{3,2}$ = 2.6 Hz, $J_{3,4}$ = 4.1 Hz, , 1H, H-3), 4.07 – 4.02 (m, 1H, H-2), 4.00 (t, J = 8.5 Hz, 1H, H-5b), 3.77 (dd, J = 11.4, 7.1 Hz, $J_{4,3}$= 4.1 Hz, 1H, H-4), 3.66 – 3.57 (m, 1H, H-5a), 3.13 (t, J = 9.1 Hz, 1H, H-1b), 3.01 (t, J = 9.1 Hz, 1H, H-1a). ^{13}C NMR (150 MHz, $CDCl_3$) δ 138.89, 138.31, 138.28 (3 C*ipso*), 128.86 – 127.16 (15C, Ar), 85.65 (C2), 79.72 (C3), 73.67, 73.38, 72.16 (3*C*H_2Ph), 70.62 (C5), 39.39 (C4), 22.33 (C1). HRMS Calcd for $C_{26}H_{29}O_3Se$ (M+H): 469.1278 Found: 469.1278, Calcd for $C_{26}H_{28}NaO_3Se$ (M+Na): 491.1098 Found: 491.1101, Calcd for $C_{26}H_{28}KO_3Se$ (M+K): 507.0837 Found: 508.0839.

(2*S*) 1,3,4-Tri-*O*-benzyl-2-deoxy-2-selenonium-2-[6-(1,2,3,4-tetra-O-acetyl-6-deoxy-α/β -D-glucopyranose)]-D-arabinitol trifluoromethanesulfonate (52)

Under an N_2 atmosphere, to a solution of compound **37** (0.84 g, 1.75 mmol) in THF (10 mL) was added a solution of selenosugar **51** (0.82 g, 1.75 mmol) in THF (10 mL) at room temperature. The resulted mixture was then stirred at room temperature for 24 h and concentrated. Crude compound on column chromatography (MeOH/DCM 0-10%) gave the desired product as a white solid (1.13 g, 68%). HRMS Calcd for $C_{40}H_{47}O_{12}Se$ (M): 799.2232 Found: 799.2239.

(2*S*) 2-deoxy-2-selenonium-2-[(2S,3S,4R,5S)-2,3,4,5,6-pentahydroxyhexyl]-D-arabinitol chloride (23)

A solution of compound **52** (1.2 g, 1.5 mmol) in 4N aq HCl (30 mL) and THF (15 mL) was stirred at 50 °C for 4h and then the solvents were evaporated. Palladium hydroxide , 20% weight on carbon (2.5 g) was added to the solution of selenium salt in 85% AcOH/H_2O (40 mL) and the mixture was stirred under 100 psi H_2 for 3 days. The catalyst was removed by filtration through a bed of celite and then washed with water. Solvents were removed, the residue was then dissolved in H_2O (150 mL) and washed with DCM (2 × 75 mL). Amberlyst A—26 resin (3.5 g) was added and the reaction mixture stirred at room temperature for 3h and then filtered through cotton and concentrated. The crude product was dissolved in H_2O (200 mL) and the solution was stirred at room temperature while sodium borohydride (230 mg, 6.1 mmol) was added. Stirring was continued for 3h and mixture was acidified to PH<4 by dropewise addition of 2M HCl. The solvent was evaporated and the residue was co-evaporated with MeOH (5 × 200 mL). The crude compound was dissolved in methanol and ethyl acetate was added until a white precipitate formed. The precipitate was then filtered and analytical sample (15 mg) was passed through a P-2 gel column for desalting and 3 mg of white foam was obtained for the inhibition studies against UGM. Analysis by ^{1}H NMR indicated that compound **23** was a mixture of isomers (19:1) at the selenium center. The major component of the mixture was assigned to be the diastereomer with a trans relationship between C-5 and C-1' on the basis of a H-1'/ H-4 correlation in the NOSEY spectrum. ^{1}H NMR (600 MHz, D_2O) δ 4.83 – 4.74 (m, 2H, H-2, H-3), 4.45 – 4.40 (m, 1H, H-4), 4.30 (ddd, J = 8.4, 7.0, 3.8 Hz, 1H, H-2'), 4.23 (dd, J5a,5b = 12.3 Hz, $J_{5a,4}$=5.4 Hz, 1H, H-5a), 4.09 (dd, $J_{5b,5a}$ = 12.3 Hz, J5b,4= 9.4 Hz, 1H, H-5b), 3.90-3.81 (m, 5H, H-1'a, H-4', H-5', H-1'b, H-3'), 3.79 (dd, $J_{1b,1a}$ = 12.0 Hz, $J_{1b,2}$= 5.2 Hz, 1H, H-1b), 3.78-3.75 (m, 1H, H-6'b), 3.68-3.64 (m, 1H, H-6'a), 3.54 (dd, $J_{1a,1b}$ = 12.0 Hz, $J_{1a,2}$ = 9.9 Hz, 1H, H-1a). ^{13}C NMR (150 MHz, D_2O) δ 75.29 (C3), 74.03 (C2), 73.84 (C3'), 72.77 (C5'), 69.62 (C4'), 67.38 (C2'), 65.84 (C4), 62.38 (C6'), 57.99 (C5), 46.00 (C1'), 37.95 (C1). HRMS Calcd for $C_{11}H_{23}O_8Se$ (M): 363.0553 Found: 363.0554.

3.5. Conclusion

In summary, the selenonium ion **23** has been synthesized. Analysis by ^{1}H NMR revealed that compound **23** was a mixture of isomers (19:1) at the selenium center. The major component of the mixture was assigned to be the diastereomer with a trans relationship between C-5 and C-1' on the basis of a H-1'/ H-4 correlation in the NOSEY spectrum. Compound **23** was tested as inhibitor of UGM and the results are discussed in chapter 4.

3.6. Supporting information

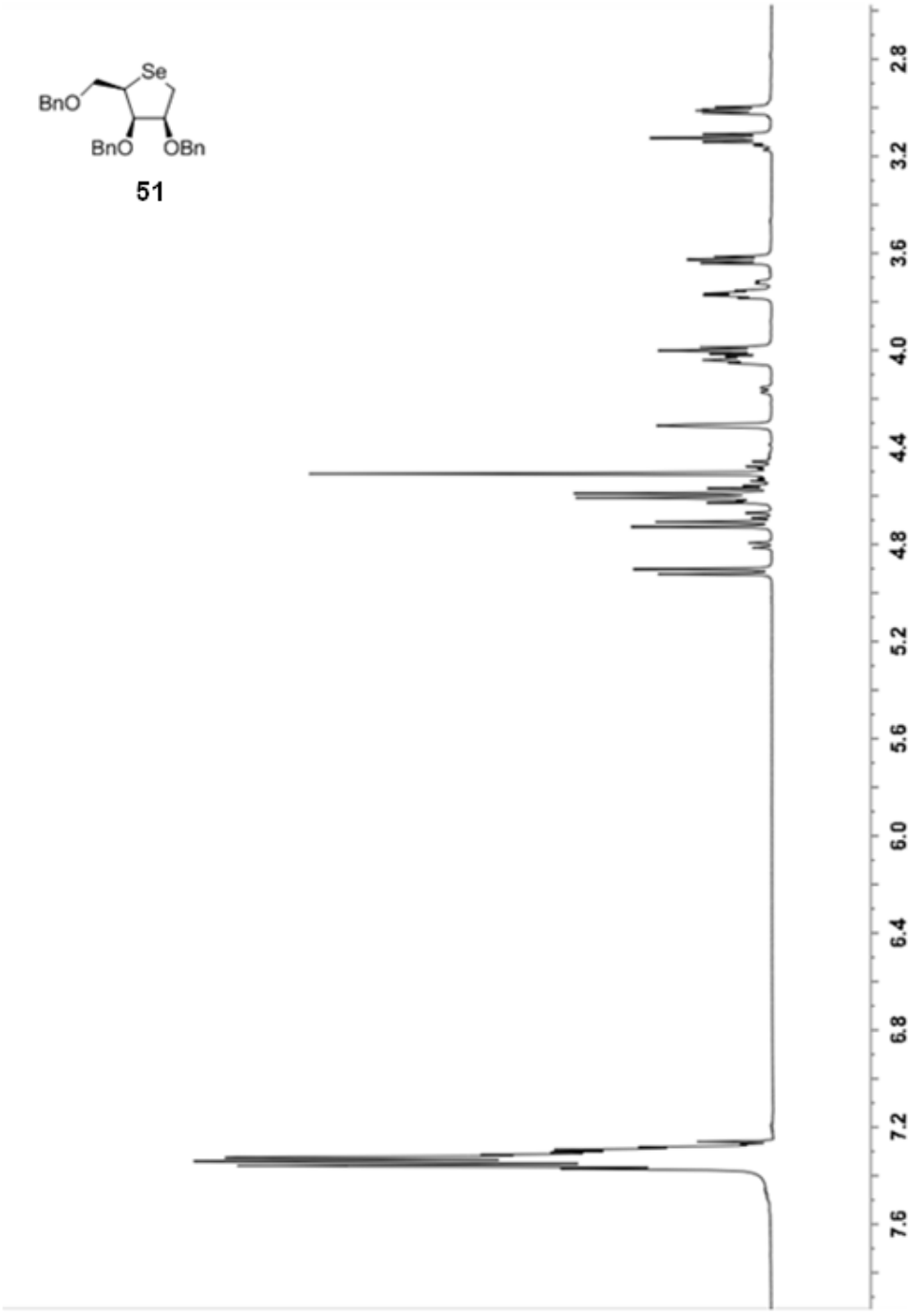

Figure 3-3: ^{1}H NMR of compound 51

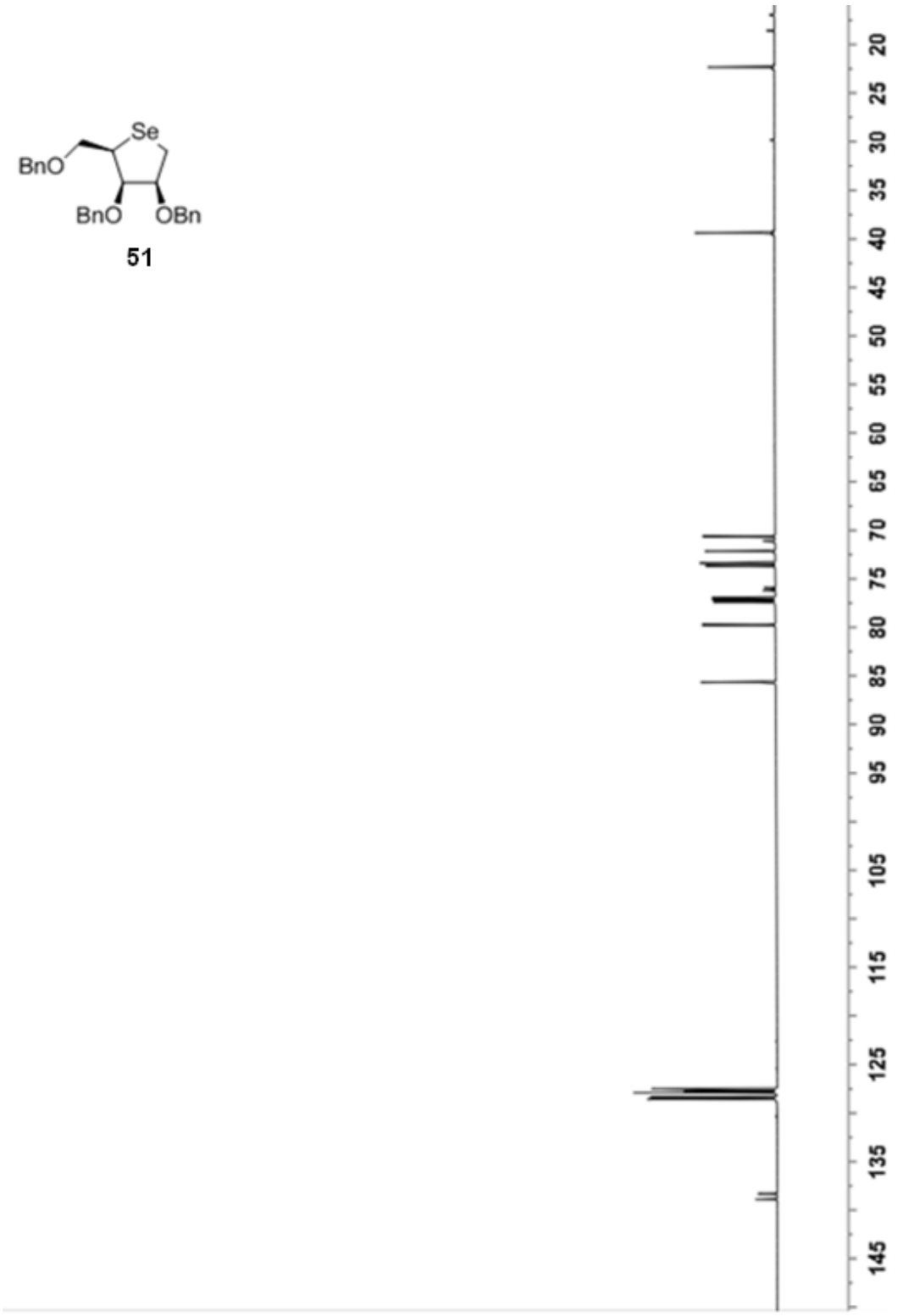

Figure 3-4: ^{13}C NMR of compound 51

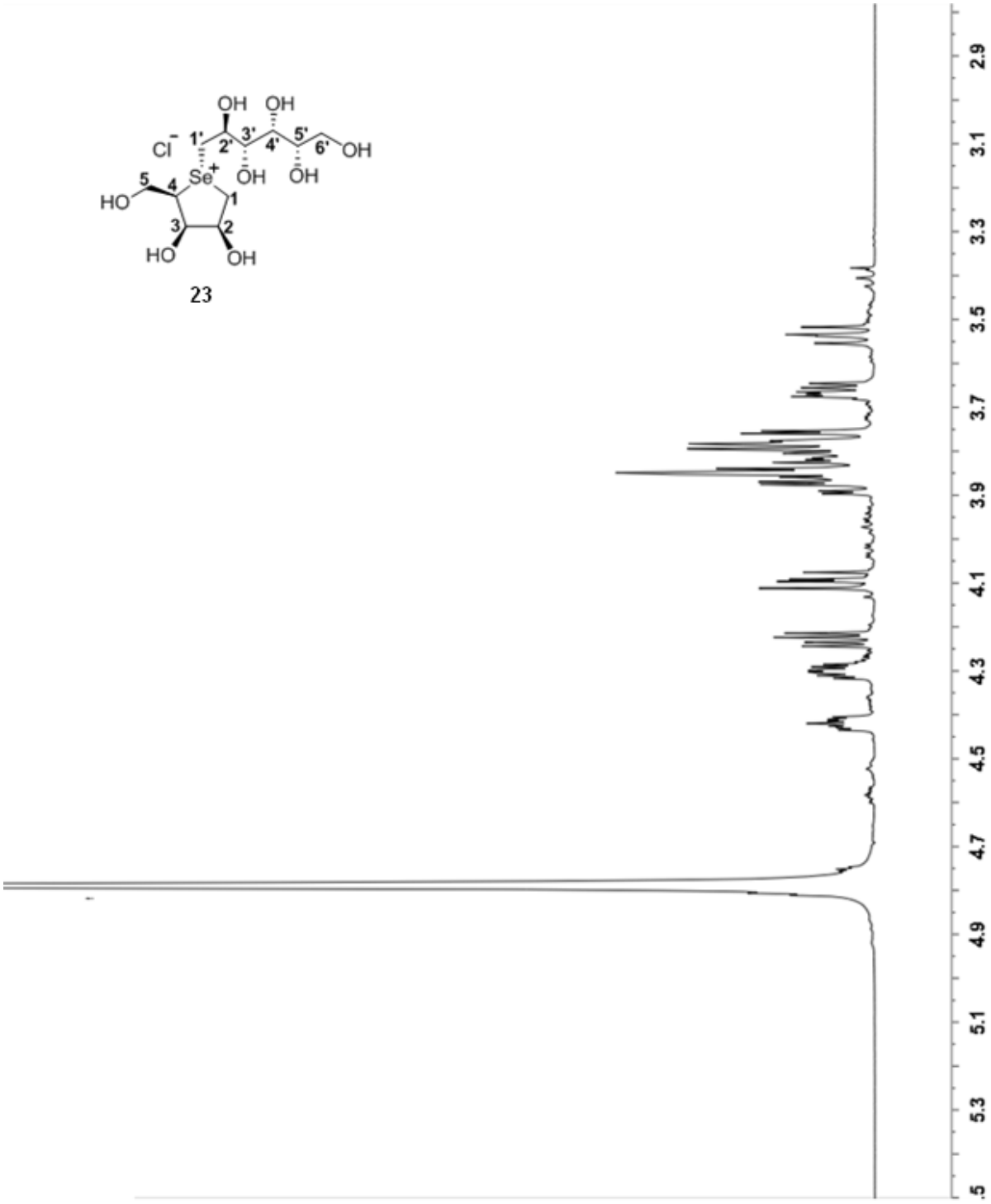

Figure 3-5: ^{1}H NMR of compound 23

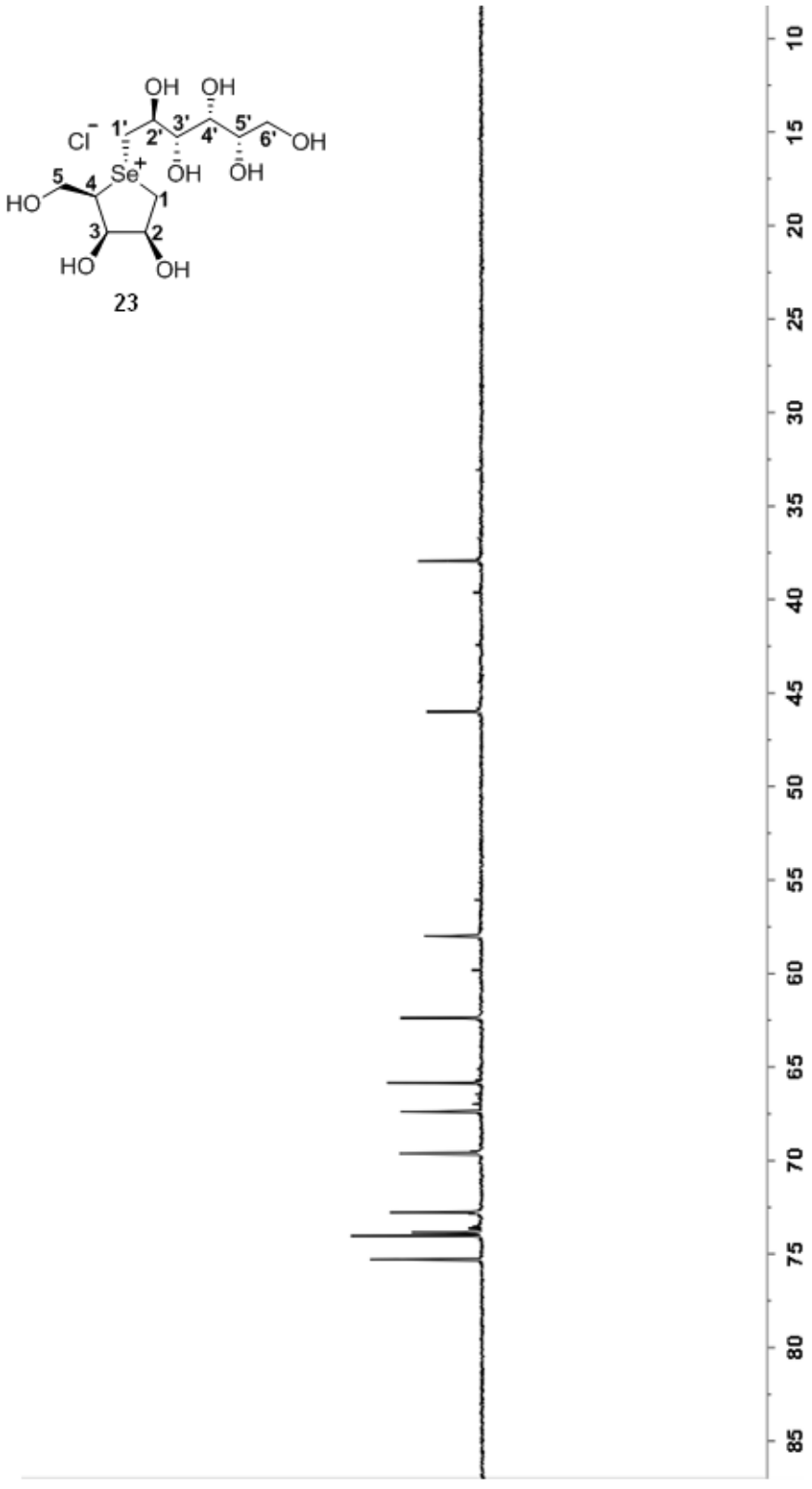

Figure 3-6: ^{13}C NMR of compound 23

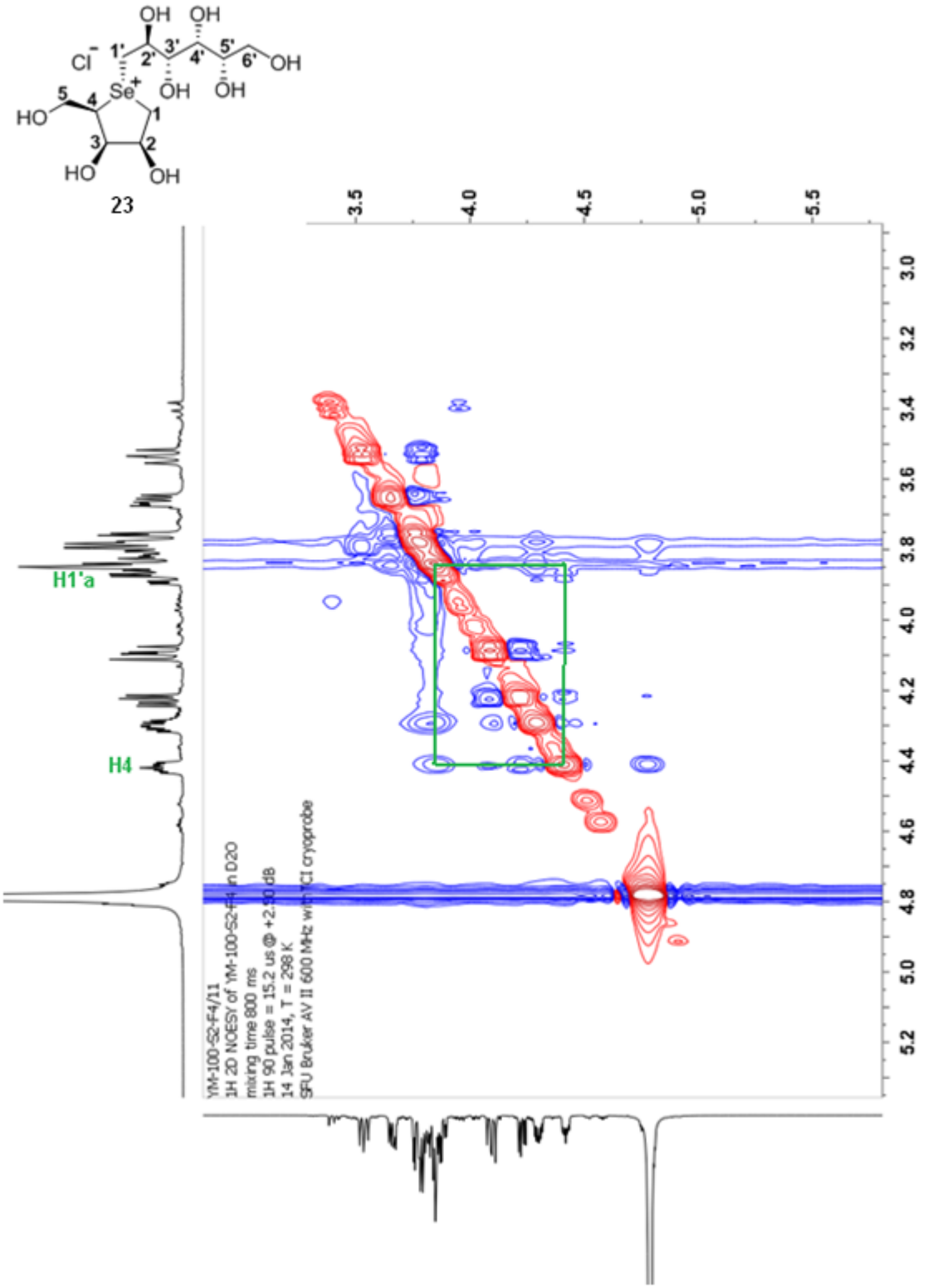

Figure 3-7: ^{1}H 2D NOESY of compound 23

Chapter 4.
Biological assays

4.1. Expression and purification of *Mycobacterium tuberculosis* UDP-galactopyranose mutase

UDP-galactopyranose mutase (UGM) from *M. tuberculosis* was expressed and purified as described earlier [58], the concentrated protein (protein concentration adjusted to 8.67 μM) was frozen in small aliquots and used for the inhibition assay. The enzyme, ready to use, was kindly provided by Dr. David A. R. Sanders, University of Saskatchewan, Saskatoon, Saskatchewan, Canada.

4.2. Enzyme inhibition assay

Enzyme inhibition assays were performed as described earlier [58], [59].The assay determines the conversion of UDP-Gal*f* into UDP-Gal*p* in the presence and in the absence of compound **22** and compound **23** as potential inhibitors of the enzymatic reaction. Briefly, the reactions were carried out in freshly prepared sodium phosphate buffer 50 mM, pH 7.0, containing 87 nM of *M. tuberculosis* UGM which was reduced with 20 mM sodium dithionite. The final volume was 100 μl. This mixture was incubated at room temperature with either compound **22** or compound **23** (concentration tested was 500 μM) for 5 min and then UDP-Gal*f* was added to a final concentration of 20 μM. The reaction was allowed to proceed for ~1.5 min, and the time adjusted to give ~50% conversion from UDP-Gal*f* into UDP-Gal*p* without inhibitors. The reaction mixture was quenched with 100 μl of n-butanol. The extent of inhibition was expressed as % inhibition. Samples (aqueous layer) were analyzed by HPLC (Agilent 1200) on a Agilent Eclipse XDB-C18 5 μm 4.6x150 mm following conditions similar to those described [60], [61] run isocratically with 20 mM triethylammonium acetate buffer (TEAA) then with a linear gradient 0-2% acetonitrile in TEAA buffer over 7 min. The two sugar nucleotides separated with base line resolution, and the extent of conversion was determined by integration of the two peaks

$$\%\ \text{conversion} = \frac{(\text{area of UDP} - \text{Gal}p\ \text{peak})}{(\text{area of UDP} - \text{Gal}p\ \text{peak} + \text{area of UDP} - \text{Gal}f\ \text{peak})} \times 100$$

Percent inhibition was calculated as:

$$\%\ \text{inhibition} = \frac{((\%\ \text{conversion (control)} - \%\ \text{conversion (inhibitor)})}{(\%\ \text{conversion (control)})} \times 100$$

4.3. Results

Compounds **22** and **23** proved to be poor inhibitors of UGM. At the highest concentrations tested (500 μM) the %inhibition was ~25% for each (Table 4-1).

Table 4-1: Inhibition of UDP-galactopyranose mutase

Inhibitor (500 μM final concentration)	% Conversion[a]	% Inhibition[a]
compound **22**	63	23
compound **23**	61	24

[a] Each result was measured in triplicate.

Chapter 5.
Conclusions and future work

5.1. Conclusions

The work described in this thesis focused on the design and syntheses of UGM inhibitors as potential therapeutic agents for the treatment of tuberculosis disease. Syntheses of sulfonium ion **22** and selenonium ion **23** have been completed by the thesis author in Chapters 2 and 3. Biological evaluation of compounds **22** and **23** against UGM enzyme has been described in Chapter 4. Examination of enzyme inhibitory activities showed that these compounds were poor inhibitors of UGM.

5.2. Future work

Poor inhibitory activities of compounds **22** and **23** are possibly due to the lack of uridine portion. We believe that incorporating a nucleotide moiety in these molecules might enhance their inhibitory activities. Hence we propose compounds **A** and **B** as potential inhibitors of UGM to be synthesized in the future.

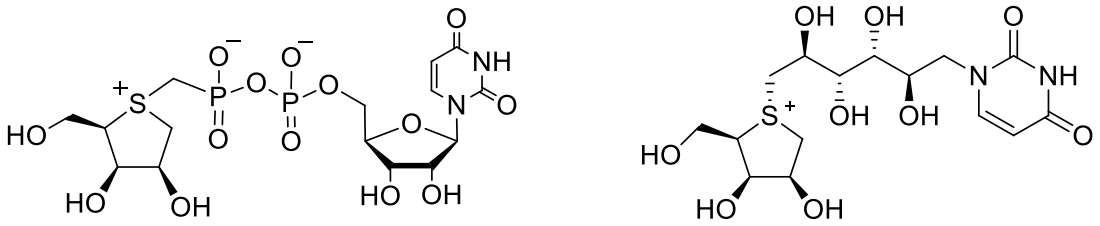

Figure 5-1: Candidates for future synthesis

References

1. Whitfield, C.; *Trends Microbiol.* **1995**, *3*, 178-185
2. Pedersen, L. L.; Turco, S. J. *Cell. Mol. Life Sci*. **2003**, *60*, 259-266.
3. Brennan, P.J.; Nikaido, H. *Annu. Rev. Biochem.* **1995**, *64*, 29-63.
4. World Health Organization, Global tuberculosis report 2014.
5. Crick DC, Brennan PJ. Biosynthesis of the arabinogalactan-peptidoglycan complex of *Mycobacterium tuberculosis*. In: Daffé M, Reyrat J-M, editors. The mycobacterial cell wall. Washington, DC: ASM Press; 2008.
6. Takayama, K.; Kilburn, J. O. *Antimicrob. Agents Chemother.* **1989**, *33*, 1493-1499.
7. Richards, M. R.; Lowary, T.L. *ChemBioChem* **2009**, *10*, 1920-1938.
8. Sanders, D. A. R.; Staines, A. G.; McMohan, S. A.; McNeil, M. R.; Whitfield, C.; Naismith, J. H. *Nat. Struct. Biol.* **2001**, *8*, 858-863.
9. Beis, K.; Srikannathasan, V.; Liu, H.; Fullerton, S. W. B.; Bamford, V. A.; Sanders, D. A. R. Whitfield, C.; McNeil, M. R.; Naismith, J. H. *J. Mol. Biol*. **2005**, *348*, 971-982.
10. Pan, F.; Jackson, M.; Ma, Y.; McNeil, M. *J. Bacteriol*. **2001**, *183*, 3991-3998.
11. Lee, R. E.; Smith, M. D.; Nash, R. J.; Griffiths, R. C.; McNeil, M.; Grewal, R. K.; Yah, W.; Besra, G. S.; Brennan, P. J.; Fleet, G. W. J. *Tetrahedron Lett*., **1997**, *38*, 6733-6736.
12. Veerapen, N.; Yuan, Y.; Sanders, D. A. R.; Pinto, B. M. *Carbohydr. Res.* **2004**, *339*, 2205-2217.
13. Itoh, K.; Huang, Z.; Liu, H.-W. *Org. Lett.* **2007**, *9*, 879–882.
14. Soltero-Higgin, M.; Carlson, E. E.; Philips, J. H.; Kiessling, L.L. *J. Am. Chem. Soc.* **2004**, *126*, 10532-10533.
15. Manetti, F.; Magnani, M.; Castagnolo, D.; Passalacqua, L.; Botta, M.; Corelli, F.; Saddi, M.; Deidda, D.; De Logu, A. *ChemMedChem* **2006**, *1*, 973-989.

16. Castagnolo, D.; De Logu, A.; Radi, M.; Bechi, B.; Manetti, F.; Magnani, M; Supino, S.; Meleddu, R.; Chisu, L.; Botta, M. *Bioorg. Med. Chem.* **2008**, *16* 8587–8591.

17. Borrelli, S.; Zandberg, W. F.; Mohan, S.; Ko, M.; Martinez-Gutierrez, F.; Partha, S. K.; Sanders, D. A. R.; Av-Gay, Y.; Pinto, B. M. *Int. J. Antimicrob. Ag.* **2010**, *36*, 364-368.

18. Barlow, J. N.; Girvin, M. E.; Blanchard, J. S. *J. Am. Chem. Soc.* **1999**, *121*, 6968-6969.

19. Zhang, Q.; Liu, H. *J. Am. Chem. Soc.* **2000**, *122*, 9065-9070.

20. Soltero-Higgin, M.; Carlson, E. E.; Gruber, T. D.; Kiessling, L. L. *Nat. Struct. Mol. Biol.* **2004**, *11* (6), 539-543.

21. Gruber, T. D.; Westler, W. M.; Kiessling, L. L.; Forest, K. T.; *Biochemistry* **2009**, *48*, 9171-9173.

22. Sun, H.; Ruszczycky, M.; Chang, W.; Thibodeaux, C.; Liu, H. *J. Biol. Chem.* **2012**, *287*, 4602-4608 .

23. Pauling, L. *Nature* **1948**, *161*, 707-709

24. Wolfenden, R. *Nature* **1969**, *223*, 704-705.

25. Schramm, V. L. *J. Biol. Chem*. **2007**, *282*, 28297-28300

26. Ho, M. C.; Shi, W.; Matthis, A. R.; Tyler, P. C.; Evans, G. B.; Clinch, K.; Almo, S. C.; Schramm, V. L. *Proc. Natl. Acad. Sci. USA* **2010**, *107*, 4805-4812.

27. Schaefer, K.; Albers. J.; Sindhuwinata, N.; Peters, T.; Meyer, B.; *ChemBioChem* **2012**, *13*, 443-450.

28. Schaefer, K.; Sindhuwinata, N.; Hackl, T.; Kotzler, M. P.; Niemeyer, F. C.; Palcic, M. M.; Peters, T.; Meyer, B.; *J. Med. Chem.* **2013**, *56*, 2150-2154.

29. Yoshikawa, M.; Murakami, T.; Shimada, H.; Matsuda, H.; Yomahara, J.; Tanabe, G.; Muraoka, O. *Tetrahedron Lett.* **1997**, *38*, 8367-8370.

30. Yoshikawa, M.; Murakami, T.; Yashiro, K.; Matsuda, H.; *Chem. Pharm. Bull.* **1998**, *46*, 1339-1340.

31. Yoshikawa, M.; Xu, F. M.; Nakamura, S.; Wang, T.; Matsuda, H.; Tanabe, G.; Muraoka, O. *Heterocycles* **2008**, *75*, 1397-1405.

32. Minami, Y.; Kurlyarna, C.; Ikeda, K.; Kato, A.; Takebayashi, K.; Adachi, I.; Fleet, G. W. J.; Kettawan, A.; Karnoto, T.; Asano, N. *Bioorg. Med. Chem.* **2008**, *16*, 2734-2740.

33. Tanabe, G.; Xie, W. J.; Ogawa, A.; Cao, C. N.; Minematsu, T.; Yoshikawa, M.; Muraoka, O. *Bioorg. Med. Chem. Lett.* **2009**, *19*, 2195-2198.

34. Jayakanthan, K.; Mohan, S.; Pinto, B. M. *J. Am. Chem. Soc.* **2009**, *131*, 5621-5626.

35. Ozaki, S.; Oe, H.; Kitamura, S. *J. Nat. Prod.* **2008**, *71*, 981-984.

36. Muraoka, O.; Xie, W. J.; Tanabe, G.; Amer, M. F. A.; Minematsu, T.; Yoshikawa, M. *Tetrahedron Lett.* **2008**, *49*, 7315-7317.

37. Eskandari, R.; Kuntz, D. A.; Rose, D. R.; Pinto, B. M. *Org. Lett.* **2010**, *12*, 1632-1635.

38. Xie, W. J.; Tanabe, G.; Akaki, J.; Morikawa, T.; Ninomiya, K.; Minematsu, T.; Yoshikawa, M.; Wu, X. M.; Muraoka, O. *Bioorg. Med. Chem.* **2011**, *19*, 2015-2022.

39. Mohan, S.; Pinto, B. M. *Carbohydr. Res.* **2007**, *342*, 1551-1580.

40. Mohan, S.; Pinto, B. M. *Nat. Prod. Rep.* **2010***, 27*, 481-488.

41. Mohan, S.; Pinto, B. M. *Collect. Czech. Chem. Commun.* **2009**, *74*, 1117-1136.

42. Mohan, S.; Eskandari, R.; Pinto, B. M. *Acc. Chem. Res.* **2014**, *47*, 211-225.

43. Sim, L.; Jayakanthan, K.; Mohan, S.; Nasi, R.; Johnston, B.D.; Pinto, B. M.; Rose, D. R. *Biochemistry* **2010**, *49*, 443-451.

44. Mohan, S.; Sim, L.; Rose, D. R.; Pinto, B. M. *Carbohydr. Res.* **2007**, *342*, 901-912.

45. Borrelli, S.; Mohan, S.; Pinto, B. M. unpublished data.

46. Kumar, N. S.; Pinto, B. M. *Carbohydr. Res.* **2005**, *340*, 2612-2619.

47. Smits, E.; Engberts, J. B. F. N.; Kellogg, R. M.; van Doren, H. A. *J. Chem. Soc., Perkin Trans 1*, **1996**, *1*, 2873-2877.

48. Liu, D.; Xie, W.; Liu, L.; Yao, H.; Xu, J.; Tanabe, G.; Muraoka, O.; Wu, X. *Tetrahedron Lett.* **2013**, *54*, 6333-6336.

49. Lee, G. S.; Lee, Y.; Choi, S. Y.; Park, Y. S.; Yoon, K. B. *J. Am. Chem. Soc*. **2000**, *122*, 12151-12157.

50. Gunasundari, T.; Chandrasekaran, S. *Carbohydr. Res.* **2013**, *382*, 30-35

51. Williams, J. D.; Kamath, V. P.; Morris, P. E.; Townsend, L. B. *Org. Synth.* **2005**, *82*, 75-79.

52. Asano, N.; Nash, R. J.; Molyneux, R. J.; Fleet, G. W. J. *Tetrahedron: Asymmetry*, **2000**, *11*, 1645-1680.

53. Legler, G. *Adv. Carbohydr. Chem. Biochem.* **1990**, *48*, 319-384.

54. Suami, T.; Ogawa, S. *Adv. Carbohydr. Chem. Biochem.* **1990**, *48*, 21-90.

55. Johnston, B. D.; Ghavami, A.; Jensen, M. T.; Svensson, B.; Pinto, B. M. *J. Am. Chem. Soc*. **2002**, *124*, 8245-8250.

56. Jones, K.; Sim, L.; Mohan, S.; Kumarasamy, J.; Liu, H.; Avery, S.; Naim, H. Y.; Quezada-Calvillo, R.; Nichols, B. L.; Pinto, B. M.; Rose, D. R. *Bioorg. Med. Chem.* **2011**, *19*, 3929-3934.

57. Eskandari, R.; Jones, K.; Rose, D. R.; Pinto, B. M. *Chem. Commun.* **2011**, *47*, 9134-9136.

58. Partha, S. K.; Sadeghi-Khomami, A.; Slowski, K.; Kotake, T.; Thomas, N. R.; Jakeman, D. L.; Sanders, D. A. R. *J. Mol. Biol.* **2010**, *403*, 578-590.

59. Partha, S. K.; van Straaten, K. E.; Sanders, D. A. R. *J. Mol. Biol.* **2009**, *394*, 864-877.

60. Poulin, M. B.; Nothaft, H.; Hug, I.; Feldman, M. F.; Szymanski, C. M.; Lowary, T. L. *J. Biol. Chem.* **2010**, *285*, 493-501.

61. Rabina, J.; Maki, M.; Savilahti, E. M.; Jarvinen, N.; Penttila, L.; Renkonen, R. *Glycoconj. J.* **2001**, *18*, 799-805.